Cobalt(III) Complexes of α-ω-Diaminocarboxylic Acids and Chloroquine

By

Kuvasani Govender (BSc. Honours)

Submitted to the Faculty of Science and Agriculture in partial fulfilment of the requirements for the degree of Master of Science in the Department of Chemistry at the University of Zululand

Supervisors: Professor G.A. Kolawole
Professor P. O' Brien

January 2001

DECLARATION

The work described in this thesis was carried out in the Department of Chemistry at the University of Zululand, South Africa and the University of Manchester, United Kingdom. All the work is my own unless otherwise stated to the contrary and has not been submitted previously for a degree at this or any other University.

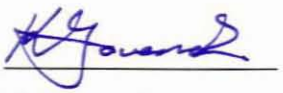

K. Govender

TABLE OF CONTENTS

Section B

Chapter 4

LIST OF TABLES

LIST OF FIGURES

:

LIST OF ABBREVIATIONS AND SYMBOLS

DAPH	-	Diaminopropionic Acid
en	-	Ethylenediamine
AA	-	Amino acid
Lys	-	Lysine
Asp	-	Aspartic Acid
Glu	-	Glutamic Acid
Ser	-	Serine
Cys	-	Cysteine
Tyr	-	Tyrosine
His	-	Histidine
OECys-		Cysteine Ethyl Ester
SMCys	-	S-Methyl-L-Cysteine
ORD	-	Optical Rotatory Dispersion
CD	-	Circular Dichroism
NMR	-	Nuclear Magnetic Resonance
IR	-	Infrared
MS	-	Mass Spectroscopy
UV	-	Ultraviolet
CQ	-	Chloroquine

ν	-	frequency
α_m	-	optically rotatory power
α	-	observed angle of rotation
ε	-	extinction coefficient
δ	-	chemical shift

ACKNOWLEDGEMENTS

I am indebted to:

Professor Gabriel. A. Kolawole (University of Zululand, South Africa) and Professor Paul O'Brien (University of Manchester, United Kingdom) for the opportunity to carry out research in the UK and for the helpful discussions and constructive criticisms.

The technical staff both at the University of Zululand and the University of Manchester for all services rendered.

Dr. Iain O'Hare, Dr. Georgios Rafeletos and Dr. T. Radhakrishnan for proof-reading the thesis.

My friends in Zululand, London and Manchester for being unfailingly positive and for keeping spirits high.

My family for their love and support.

National Research Foundation (NRF), South Africa and The Royal Society, United Kingdom for financial support.

To My Mother

SECTION A

Cobalt(III) Complexes of α-ω-Diaminocarboxylic Acids

ABSTRACT

α-ω-Diaminocarboxylic acids, such as lysine and 2,3-diaminopropionic acid (2,3-DAPH), are trifunctional, and thus, when only two sites are available for coordination, an interesting question is posed as to which functional groups are utilised in chelation. A series of cobalt(III) complexes of the formulation $[Co(en)_2AA]^{2+}$, where en is ethylenediamine and AA represents lysine and DL-2,3-DAP, were prepared. In addition, complexes of the type $[Co(AA)(AAH)Cl_2]$ and $[Co(AA)_2]^+$, where AA is DL-2,3-DAP, have been synthesised. The compounds were characterised using elemental analysis, NMR, IR and electronic spectroscopy and mass spectrometry. The reaction of *cis*-$[Co(en)_2Cl_2]Cl$ with lysine yielded two products notably, $[Co(en)_2(lys)]^{2+}$, within which lysine coordinates via the α-nitrogen and oxygen donor atoms, and $[Co(en)_3]^{3+}$. The reaction of *cis*-$[Co(en)_2Cl_2]Cl$ with DL-2,3-DAPH, however, yielded three products, viz. $[Co(en)_2(2,3\text{-}DAP)]^{2+}$, in which the glycinate portion of 2,3-DAP is involved in chelation, $[Co(2,3\text{-}DAP)_2]^+$ where 2,3-DAP acted as a tridentate ligand, and $[Co(en)_3]^{3+}$. In $[Co(2,3\text{-}DAP)(2,3\text{-}DAPH)Cl_2]$, one of the 2,3-DAP ligands coordinated via the two amino groups leaving the carboxylic acid group free whilst the second ligand coordinated via the glycinate portion leaving the terminal amino group free.

CHAPTER ONE

Introduction

1.1 INTRODUCTION

The most common oxidation state for cobalt is that of +3, which gives rise to a wide variety of kinetically inert complexes. Virtually all of these are low spin in nature and exhibit octahedral coordination, a major stabilising influence being the high crystal field stabilisation energy associated with the t_{2g}^6 configuration. The paucity of simple salts of cobalt(III) contrasts sharply with the great abundance of its complexes, especially in coordination with N-donor ligands. Since complexes of cobalt are kinetically inert indirect methods of preparation are required.

The usual methods for the preparation of Co(III) complexes may be classified into two categories, viz. the oxidation from Co(II) to Co(III), and the substitution between a cobalt (III) complex and a ligand. Oxidation may be successfully carried out either by air, or with an oxidising agent such as hydrogen peroxide or occasionally in the presence of a catalyst such as decolourising charcoal or lead oxide. The technique of aeration is applicable to the oxidation of a cobalt(II) salt in a basic aqueous solution containing either an amine or ammonia and a salt of the amine or ammonia, e.g.

$$Co^{2+}\ (aq) + 3\ H_2NCH_2CH_2NH_2 \xrightarrow{O_2} [Co(H_2NCH_2CH_2NH_2)_3]^{3+}\ (aq)$$

$$4\ Co(NO_3)_2 + 16\ NH_3 + 4\ (NH_4)_2CO_3 \xrightarrow{O_2} 4\ [Co(CO_3)(NH_3)_5]NO_3 + 4\ NH_4NO_3 + 2\ H_2O$$

The cobaltammines, whose number is legion, were amongst the first coordination compounds to be studied in great detail and represent the most extensively investigated class of cobalt(III) complexes. Compounds analogous to cobaltammines may be obtained using chelating amines such as ethylenediamine and 2,2'-bipyridyl. These complexes have played important roles within a number of stereochemical investigations.

Complexes of amino acids with transition metals are often cited as models for metal ion coordination in biological systems. Simple amino acids exist as zwitterions,

LH (**2**), in the solid state, but almost invariably coordinate as the anionic species, L^- (**1**), where L represents a given amino acid (Figure 1.1).

(1) **(2)**

Figure 1.1 : Anionic (1) and Zwitterionic (2) Forms of Amino Acids

There are numerous examples of the *in vivo* interaction of transition metal ions with amino acids and peptides. These interactions are of considerable biological significance, as in the example of the biosynthesis of methionine from methylcobalamin and homocysteine[1], or in the alleviation of the symptoms of Wilson's disease by the administration of L-penicillamine[1], which assists in the removal of copper.

Bis(ethylenediamine)cobalt(III) complexes containing amino acids have been used to study both the stereochemistry and reactions of amino acids bound to metal ions[2-6]. Complexes of the type $[Co(en)_2AA]^{2+}$ containing an amino acid anion were first prepared by Meisenheimer[7] in 1924 by the reaction of *trans*-dichlorobis(ethylenediamine)cobalt(III) chloride with amino acids such as glycine and sarcosine in aqueous solution. Subsequently, a variety of aminoacidobis(ethylenediamine)cobalt(III) complexes have been prepared and studied[8-10]. These early studies were concerned only with amino acids containing nitrogen- and oxygen- based functional groups. The mode of coordination in most of these complexes involves bidentate chelation via the amino and carboxylate groups.

Alexander and Busch[11], however, have prepared and characterised complexes containing both monodentate glycine and glycine esters. The glycine esters are found to coordinate via the amino group only. Such complexes were found to undergo hydrolysis in strongly acidic aqueous solution.

Complexes of the amino acids serine and threonine, which contain weakly coordinating hydroxyl groups, have also been examined[6]. In this instance also, only the glycine units of the amino acids are incorporated within the complex to form a five-membered system.

Moreover, trifunctional amino acids, such as those listed in Table 1.1, pose an additional question in relation to the utilisation of functional groups in chelation. These amino acids are of particular interest, since only two of the three functional groups present may bind under circumstances within which two ligation sites are available, such as in the cases of the $[Co(en)_2Cl_2]Cl$ and $[Co(en)_2CO_3]Cl$ complexes.

Table 1.1: Review of Potentially Tridentate Amino Acids

Amino acid	Structural Formula	Abbreviation	Origin
Arginine[a,b]	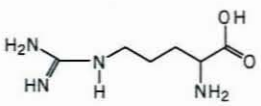	ArgH	Hydrolysis of caseine[12]; first synthesised by Schulze and Winterstein[13].
Aspartic Acid[c]	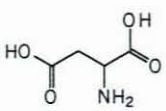	$AspH_2$	First prepared by Dessaignes[14]; derived from asparagine.
Asparagine	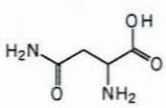	AsaH	Isolated from juice of asparagus plant[15].
Glutamic Acid[c]	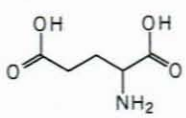	$GluH_2$	Hydrolysis of gliadin[16]; synthesised by Wolff.
Histidine[b,d]	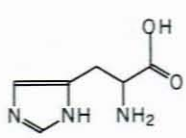	HisH	Extracted from salmon sperm[17] or ovalbumin; synthesised by Pyman[18].
Lysine[b,d]	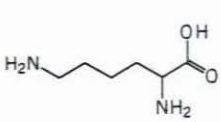	LysH	Hydrolysis of caseine[19]; synthesised by Fischer and Weigart[20].

Ornithine	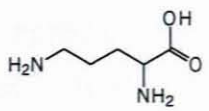	OrnH	Occurs in nature as constituent of certain antibiotics[21]; synthesised by Fischer[22].
Serine	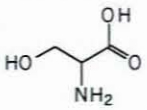	SerH	Hydrolysis of silk[23]; first synthesised in 1902[24].
Threonine	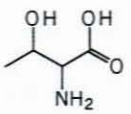	ThrH	Synthesised by Burch[25].
Tryptophan[d]	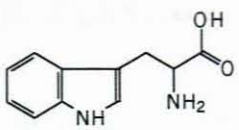	TryH	Isolated by Hopkins and Cole[26]; synthesised by Ellingert and Flamand[27].
Tyrosine	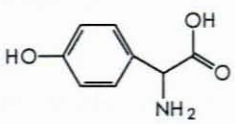	TyrH	Isolated from casein[28]; synthesised in 1882[29].
2,3-Diaminopropionic acid[b]	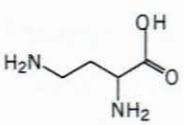	DapH	Found in hydrolysates of antibiotic viomycin[30]; synthesised by Klebs[31].
2,4-Diaminobutyric acid[b]	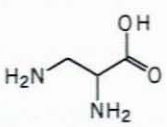	DabH	First synthesised by Fischer[32].

a: Strongly basic, because of guanido group

b: In solid state zwitterionic form, the proton does not reside on the α-amino group

c: Aqueous solutions are acidic because of additional carboxylic acid group

d: Basic amino acids

A series of cobalt(III) complexes of the formulation $[Co(en)_2AA]^{n+}$ where AA is L-cysteine, S-methyl-L-cysteine and L-cysteine ethyl ester hydrochloride have been prepared and characterised[32]. In contrast to the previously mentioned examples, the coordination of cysteine in $[Co(en)_2Cys]^+$ occurs through the amino and mercaptide groups. The carboxylate group of cysteine in this complex is not coordinated; it undergoes protonation upon treatment with acid. The ethyl cysteinate ligand, within the complex $[Co(en)_2OECys]^{+2}$, is also coordinated through the amino and mercaptide groups. S-methyl-L-cysteine, however, is coordinated through the amino and carboxylate groups in $[Co(en)_2SMCys]^{+2}$.

In 1966, Gillard *et al.* synthesised the complex d(+)-$[Co(en)_2(l\text{-glu})]ClO_4$, the crystal structure of which revealed the five-membered glycinate ring was formed by the glutamic acid whilst the dangling γ-carboxylate group was hydrogen bonded to the amine protons of one of the ethylenediamine molecules[33].

The third functional group of an amino acid primarily contributes to two simple effects on the stability of the α-amino acid chelation[1] notably competition with the α-amino acid chelating system for coordination sites and electron inductive effects.

It was found that of the diaminocarboxylic acids, the complexes of 2,3-diaminopropionic acid and 2,4-diaminobutyric acid retain the highest stability constants (Table 1.2)[34] and this appears to indicate chelation through both the nitrogen atoms of these ligands[1]. Lysine, on the other hand, has stability constants resembling those of glycine and β-alanine thus leading to the conclusion that the terminal amino acid group does not coordinate to the central metal ion[1]. At low pH, protonation of the terminal amine group reduces the stability of chelation, whilst at higher pH values(~10), coordination involving the terminal amine group becomes favourable. It should be noted that, in compiling the table, certain conditions were applied in order to standardise the data. Such conditions are outlined as follows: -

Temperature:	20 °C
Method:	Glass Electrode
Ionic Strength:	0.005 M – 0.03 M

Table 1.2 : Stability Constants (log K) of Potentially Tridentate Amino Acid Complexes with Transition Metals

	Co^{2+}	Cu^{2+}	Fe^{2+}	Ni^{2+}	Zn^{2+}
2,3-Diaminopropionic acid	11.80	20.34	5.00	15.20	11.50
2,4-Diaminobutyric acid	12.80	19.48		16.40	12.80
Ornithine		13.00			6.90
Lysine	6.80	13.70		8.80	7.60
Glycine	8.90	15.40	7.80	11.00	14.50
β-Alanine	7.00	12.90	4.00		

In this investigation, the synthesis of bis(ethylenediamine)cobalt(III) complexes of 2,3-diaminopropionic acid and lysine, together with that of the dichlorobis(diaminopropionato)cobalt(III) complexes, is reported. Such amino acids were of interest to us since relatively few reports exist within the literature regarding bidentate chelation in complexes of α-ω-diaminocarboxylic acids, in particular with the cobalt(III) ion.

1.2 α-ω-DIAMINOCARBOXYLIC ACIDS

1.2.1 2,3-Diaminopropionic Acid

2,3-Diaminopropionic acid or β-alanine represents the lowest member of a series of homologous α-ω-diaminocarboxylic acids, of which ornithine and lysine are higher members. 2,3-Diaminopropionic acid is a non-protein amino acid, which may be isolated from the plants *Mimosa palmeri* and *Acacia* and which is also found in the hydrolysates of the antibiotic *viomycin*[30]. This non-protein amino acid is the direct precursor of the neurotoxin, 3-N-oxalyl-L-2,3-diaminopropionic acid (β-ODAP), which can be isolated from the legumes of the plant *Lathyrus sativus*. Excessive ingestion of the legumes can lead to a disease known as neurolathyrism.

2,3-Diaminopropionic acid contains an asymmetric carbon and therefore exists in the enantiomeric forms as illustrated in Figure 1.2.

(a) *(b)*

Figure 1.2: ***(a)*** **L-2,3-diaminopropionic acid and** ***(b)*** **D-2,3-diaminopropionic acid**

When DL-2,3-diaminopropionic acid reacts with the tris(carbonato)cobaltate(III) ion, it behaves as a tridentate ligand. The bis(2,3-diaminopropionato)cobalt(III) ion has five possible geometric isomers[35].

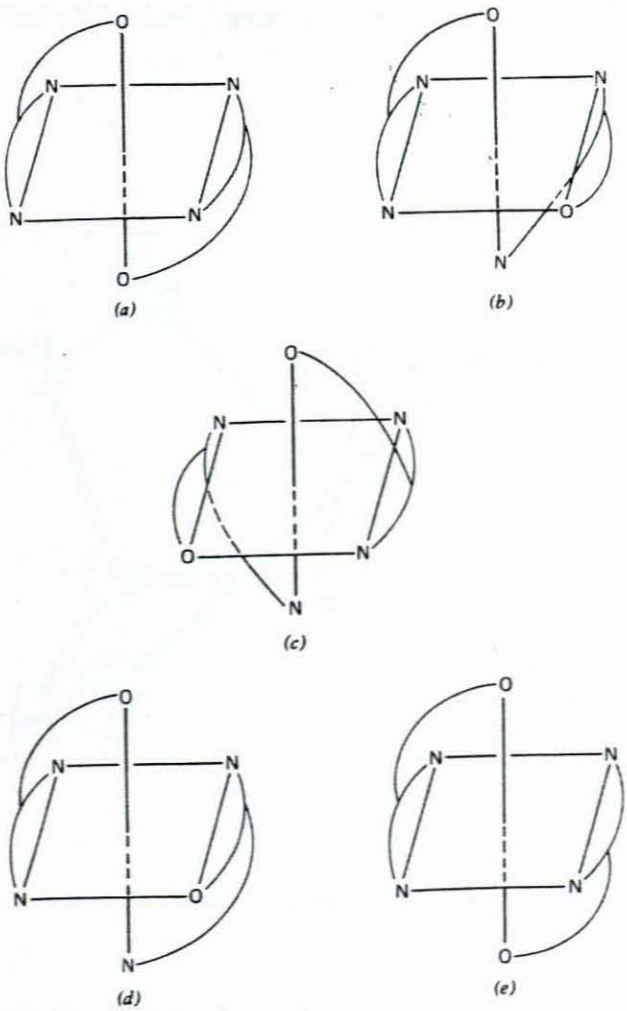

Figure 1.3: Geometrical isomers of bis(2,3-diaminopropionato)cobalt(III) ion:
(a) *trans,cis,cis;* ***(b)*** *cis,cis,trans;* ***(c)*** *cis,trans,cis;* ***(d)*** *cis,cis,cis;* ***(e)*** *trans,trans,trans*

Each of the isomers is labelled according to the convention that the carboxyl groups are designated first, followed by the α-amino group and finally the β-amino group. As a consequence, the five isomers may be designated as a) *trans, cis, cis;* b) *cis, cis, trans;* c) *cis, trans, cis;* d) *cis, cis, cis; and* e) *trans, trans, trans*. Isomers a, b and c require two ligands of the same absolute configuration. The other two geometries (d and e) require the two ligands to be enantiomeric. It is worth noting that only with DL-2,3-diaminopropionic acid, can all five possible geometrical isomers form. All the isomers have been previously isolated. Their configurations were assigned on the basis of absorption, circular dichroism and optically rotatory dispersion spectra as well as by classical methods of analysis. Unambiguous differentiation of isomers b and c proved to be impossible. The structure of the red crystalline product, (-)546-$[Co(C_3H_7N_2O_2)_2]Br$, has been determined[36]. Such a structure represents that of the S-*cis,trans,cis* isomer.

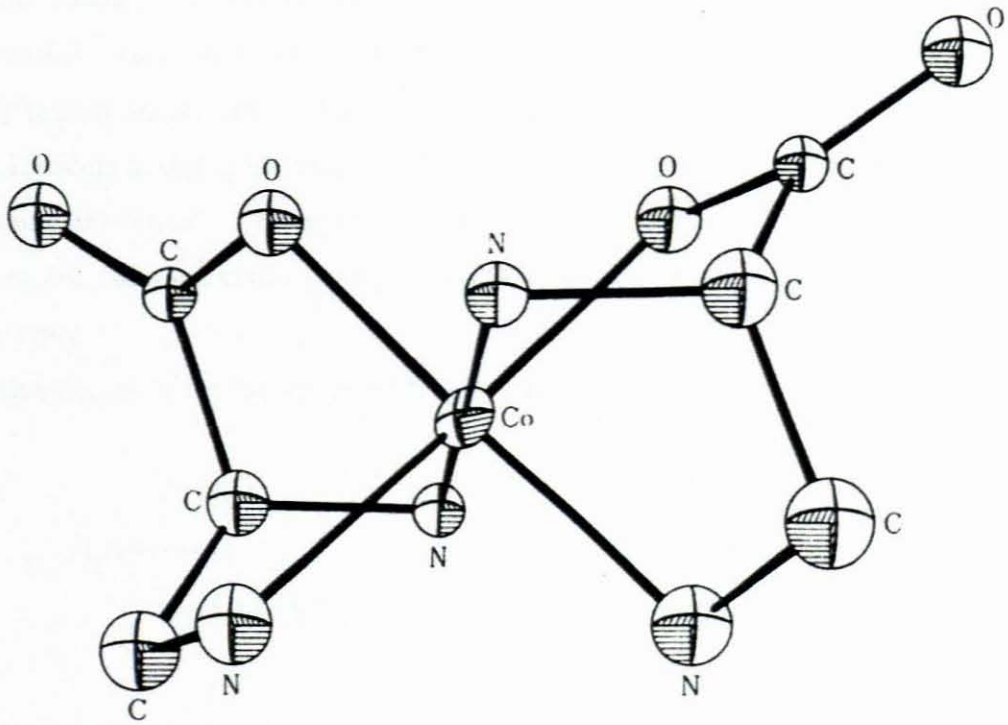

Figure 1.4: The S-*cis,trans,cis* isomer (-)546-$[Co(C_3H_7N_2O_2)_2]Br$

The two ligand molecules coordinate to the central metal atom through four amino nitrogen atoms and two carboxyl oxygen atoms in order to produce a distorted octahedral geometry. As such the ligand molecule acts as a terdentate species and

forms a rigid fused-ring chelate system in which the configuration of the ligand uniquely determines the absolute configuration of the complex.

1.2.2 Lysine

Lysine is an essential amino acid required both for growth and to maintain nitrogen balance in the body. It is incorporated within proteins and also enables the body to absorb and in turn to conserve calcium. Lysine interferes with replication of the *Herpes* virus and is therefore often prescribed by doctors to patients suffering from cold sores and genital herpes.

Moreover, lysine has also been shown to be useful in the prevention of arteriosclerosis, a hardening of the arterial walls resulting from the deposits of lipoproteins. Such treatment reduces the susceptibility of an individual to hypertension.

More recently it was demonstrated that cobalt complexes of the type $[Co^{III}(acacen)L_2]^{+2}$ (acacen = bisacetylacetonatoethylenediimine; L = NH_3, 2-Me-imidazole), exhibit potent antiviral activity against a number of *Herpes* viruses by binding to histidine and to a lesser extent to cysteine within the viral active enzyme, thus inhibiting the virus[37]. It appears be reasonable to assume therefore, that a cobalt(III) lysine complex could possibly exhibit enhanced antiviral activity against the *Herpes* virus.

Lysine occurs in the two enantiomeric forms:

(a) *(b)*

Figure 1. 5: Enantiomeric forms of lysine. *(a)* L-lysine and *(b)* D-lysine

Copper(II) complexes of lysine have been prepared[38,39] and characterised[39] using ultraviolet charge-transfer spectroscopy, visible circular dichroism and absorption spectroscopy, titrimetric analysis and the measurement of formation constants in order to ascertain the mode of coordination of the trifunctional amino acid. It has been established that copper(II) complexes of lysine are bound through

the carboxylate oxygen and α-amino acid groups whilst the terminal amino group remains unbound.

Cobalt(II) lysine complexes have been used as so-called 'tracers' or staining agents in visualisation of neuronal alterations in larvae of the moth, *Manduca Sexta*[40], as such creatures undergo changes during metamorphosis and in viewing both organisations of the spinal cord[41] and retinal projections[42] within frogs.

1.3 STEREOSELECTIVITY IN COMPLEXES

The phenomenon of stereoselectivity has been observed in the study of optically active chelate compounds. In general, the enantiomorphic ligands may give rise to a series of complexes of the general formula ML_mD_{n-m}. The preference of one isomer over the other may be due to conformational effects, steric hindrance factors, or in certain circumstances, lattice-energy effects associated with the solid complexes.

In the case of mixed diamine-α-amino acid-cobalt (III) species, such as bis(ethylenediamine) series, the tendency towards stereoselective reaction is relatively small since the chelated α-amino ring is nearly planar and is the only group containing a bulky substituent. It is reasonable to expect that any stereoselective effects might be most significant when the size of the side chain is greatest such as in the case of leucine or phenyalanine. Compounds of this type, using both the D- and L-isomers of -α-alanine, leucine and phenyalanine have been isolated by Liu and Douglas[4], who concluded, from the magnitude of the Cotton effects, that even in the case of L-phenyalanine, the preparative mixture of the unresolved complex (±)-$[Co(en)_2(L\text{-phenylalanine})]^{+2}$ contains both diastereoisomers in equal proportion.

In 1970 Gillard and co-workers[13] observed that when L-glutamic acid reacts with (±)-$[Co(en)_2CO_3]^+$, there is stereoselective formation of the (+)-$[Co(en)_2(L\text{-glutamate})]^+$ and then the (-)-$[Co(en)_2(L\text{-glutamate})]^+$ in equal amounts. This was in direct contrast with previous analogous reactions with α-alanine, leucine and phenylalanine. The observed stereoselectivity with L-glutamic acid appears to result from the three-point attachment of the ligand involving a hydrogen bonding between the dangling γ-carboxylate group and a diamine-ring nitrogen. Molecular models indicate that such three-point attachment with L-glutamate is sterically favourable only for the D- isomer and not for the L-configuration.

1.4 TECHNIQUES USED TO CHARACTERISE THE COMPLEXES

1.4.1 Nuclear Magnetic Resonance (NMR) Spectroscopy

Many diagmagnetic inorganic compounds yield uncomplicated NMR spectra. Cobalt(III) coordination compounds are particularly suited to such studies since they are relatively inert and the absorptions observed are uncomplicated by ligand exchange. Several NMR studies of Co(III) complexes have previously been reported in which certain conclusions regarding chelate ring conformations have been drawn. For instance, Powell and Sheppard[43], in 1959, were able to distinguish between the 'envelope' and 'gauche' structures of the cobalt-ethylenediamine ring of the $[Co(en)_3]^{+3}$ ion, using ^1H NMR spectroscopy.

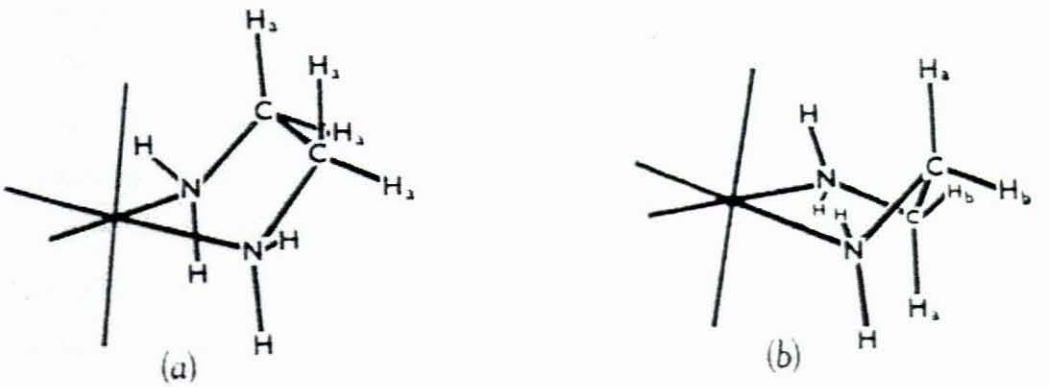

Figure 1.6: The *(a)* 'envelope' and *(b)* gauche structure of the cobalt-ethylenediamine ring within $[Co(en)_3]^{+3}$

The *cis* and *trans* isomers of the type $[Co(en)_2X_2]^{2+}$ have different symmetry properties and this factor appears to govern the difference in the NMR spectra.

When a metal ion is added to an aqueous solution of an α-amino acid, the resonances of the α-CH proton rapidly broaden and are shifted to a lower field relative to an internal (or external) reference[1]. The broadening effect is generally more pronounced for the proton at which the unpaired spin density is greatest, that is, those with the greatest shifts. The resonances for protons, which are more than one carbon atom away from the carboxyl group, usually do not show significant shifts and broaden much less than the resonance of the α-proton.

NMR spectra of amino acid complexes of the type $[Co(en)_2AA]^{2+}$, in which the amino acids were glycine, alanine, leucine, isoleucine, valine and phenyalanine proved to be quite useful in characterising the complexes[5]. The diastereoisomeric pairs of a racemate have different chemical shifts. Thus the ^1H NMR for a racemate shows a more complex pattern than that of an optically pure diastereoisomer.

The suitability of NMR techniques to determine the variation in coordination sites in some potentially tridentate amino acids were carried out by Erickson and co-workers[44,45]. The results of these investigations showed that nickel(II) complexes of both aspartic acid and glutamic acid show considerable differences in their respective NMR spectra. The larger α-proton shift exhibited by the aspartate complex in comparison to the slight shift in the glutamate complex was the most striking difference. Moreover, the CH_2 signal for aspartate is shifted slightly upfield whilst the CH_2 signals of glutamate is shifted slightly downfield. These data are consistent with tridentate coordination for aspartate and bidentate (amino-α-carboxylato) coordination of glutamate.

It was found that the spectrum of the Ni(II)-2,3-diaminopropionic acid system is very sensitive to pH. At high pH, the spectrum shows coordination of both amino groups whilst at lower pH values the β-NH_2 group is protonated and the carboxyl group becomes axially coordinated[1].

Besides yielding conclusive information on the binding variations of tridentate amino acids, NMR data also provide significant information relating to the conformation of these complexes. Erickson *et al.*[45] have shown that the most likely conformation of the coordinated glutamate, aspartate and 2,3-diaminopropionate is one in which the bulky carboxyl groups are in the equatorial positions.

1.4.2 Infrared (IR) Spectroscopy

Infrared spectroscopy is a widely used technique in the elucidation of structures of metal-amino acid complexes. This is due to the fact that the stretching modes of the amino and carboxylate groups are sensitive to coordination. It was observed that the stretching mode of the free carboxylic acid group within the ligand occurs at a lower wavenumber than the corresponding coordinated group[46-48] and coordination of the amino group causes a shift of the stretching bands associated with such a group to lower energy[1]. For a multidentate ligand, IR data are frequently useful in determining

the number of functional groups involved in the coordination. For instance, in the complex $[Co(en)_2Cys]I$, it was deduced from the IR spectra that the mercaptide group was definitely coordinated at one of the two sites, such that either the amino or carboxylate group may thus occupy the other site. An intense carbonyl stretching band occurs at 1616 cm^{-1} in the IR spectrum of $[Co(en)_2Cys]I$, a value that is consistent with the presence of a free carboxylate ion. Consequently, it is reasonable to suggest that the amino group occupies the other site.

1.4.3 Ultraviolet-Visible (UV-Vis)/Electronic Spectroscopy

The electronic spectra of transition metal complexes can be interpreted with the aid of the ligand field theory. Detailed examination of visible spectra retains considerable diagnostic value with respect to structural elucidation. It is possible to observe spin allowed, d-d bands in the visible region of the spectra of low-spin cobalt(III) complexes because of the small value of 10Dq (Δ), which is allowed to induce spin pairing in the cobalt(III) ion[49]. This means that the low-spin configuration occurs in complexes with ligands which do not give rise to the low-energy charge transfer bands which so often dominate the spectra of low spin complexes. In practice the two bands observed are assigned to the following transitions[49]:

$\nu_1 = A_{1g} \rightarrow {}^1T_{1g}$

$\nu_2 = A_{1g} \rightarrow {}^1T_{2g}$

These transitions correspond to the electronic promotion $t_{2g}^6 \rightarrow t_{2g}^5 e_g^1$, the electron maintaining an unaltered spin state. The orbital multiplicity of the $t_{2g}^5 e_g^1$ configuration is six and corresponds to the two orbital triplet terms ${}^1T_{1g}$ and ${}^1T_{2g}$. If the promoted electron changes its spin, the two T terms become triplets ${}^3T_{1g}$ and ${}^3T_{2g}$

.

An intriguing application of d-d absorption spectra has been centred around the process of distinguishing between pairs of geometrical isomers of Co(III) complexes. Based upon the crystal field considerations the *trans*-O and *cis*-O isomers of $Co(III)N_4O_2$, chromophores ought to exhibit distinctively different spectra. In general, the *cis* isomer, having lower symmetry, exhibits a sharp intense absorption band in the visible region, whilst the *trans* isomer, with higher symmetry exhibits a

rather broad low intensity, frequently split band in the same region. Moreover, in the case of the CoN_3O_3 system, the visible spectra enable one to distinguish between meridional and facial isomers. The band at the longer wavelength is due to the transition $A_{1g} \rightarrow {}^1T_{1g}(O_h)$ and the other at the shorter wavelength corresponds to the transition $A_{1g} \rightarrow {}^1T_{2g}$ (O_h). The meridional geometry is lower in symmetry than the facial isomer. The loss of symmetry from the facial to meridional causes splitting or broadening of the $A_{1g} \rightarrow {}^1T_{1g}$ first absorption band for the meridional isomer. Thus the visible absorption peaks of the facial isomers are generally sharp and symmetrical whilst those of the meridional are broadened.

For complexes of the type $[Co(en)_2AA]^{2+}$, the absorption spectra show two symmetrical peaks which indicate the octahedral (O_h) symmetry i.e. splitting of the $A_{1g} \rightarrow {}^1T_{1g}$ and $A_{1g} \rightarrow {}^1T_{2g}$ bands[4].

1.4.4 Optical Rotatory Dispersion (ORD) and Circular Dichroism(CD)

An optical isomer may be distinguished from its mirror image on the basis of the fact that a pair of diastereoisomers rotate polarised light in opposite directions. Optical activity measurements are concerned with the ability of optically active substances to rotate the plane of polarisation of plane polarised light. Its specific optically rotatory power α_m is given by $\alpha_m = \frac{\alpha V}{ml}$,

where

α= Observed angle of rotation

V = Volume

m = Mass

l = Path length

The reason for this phenomenon rests with the fact that plane polarised light is made up of left and right circularly polarised components and the nature of an optically active substance is such that in passing through it, one component passes through greater electron density than does the other. Thus one component is slowed down relative to the other and the two components emerge out-of-phase i.e. the plane of polarisation of the light has been rotated. If the wavelength of the plane of polarised light is varied and α_m then plotted against wavelength, the curve is known as

the optically rotatory dispersion (ORD) curve. For those wavelengths at which the substance is transparent, α_m is constant and the ORD curve is flat (Figure. 1.7).

In the process of light absorption, the molecules of a substance undergo electronic transitions which involve the displacement of electronic charge. As a consequence of their differing routes through the molecules, the two circularly polarised components of the light produce these excitations to different extents and are consequently absorbed to different extents. The difference in the extinction coefficients ε_{left}-ε_{right} can be measured as the circular dichroism (CD). If CD is plotted against wavelength, it is zero where there is no absorption but passes through a maximum or a minimum where absorption occurs.

ORD is, in effect, a first derivative of CD, passing through zero at the absorption maximum.

The behaviour of CD and ORD curves in the vicinity of an absorption band is known as the Cotton effect. Molecules with the same absolute configuration will exhibit the same Cotton Effect for the same d-d absorption.

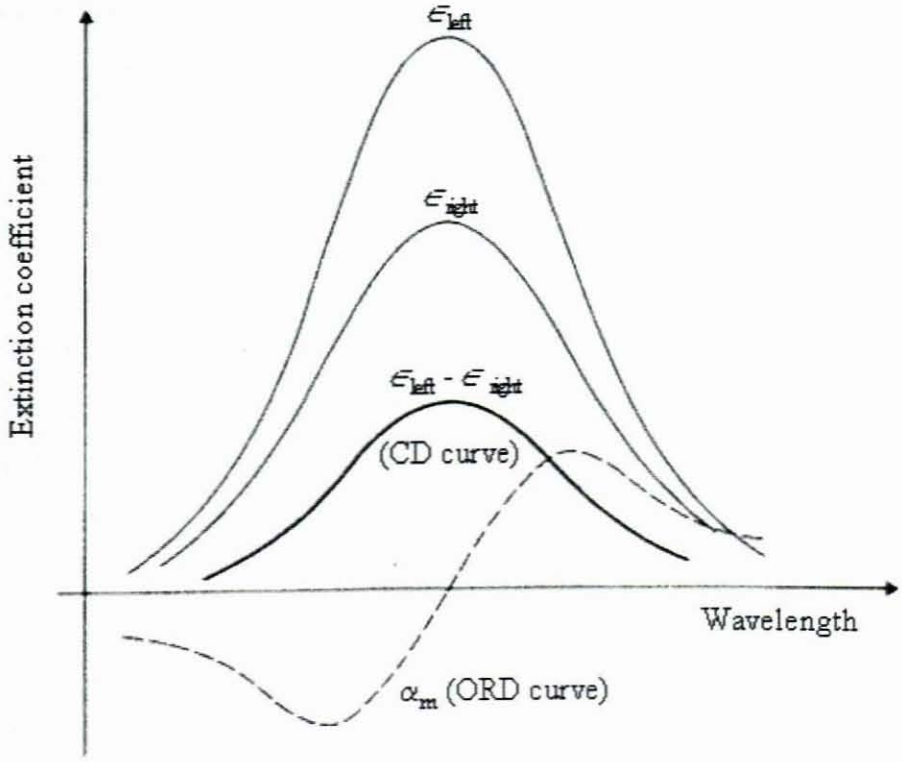

Figure 1.7: Diagrammatic representation of the 'positive' Cotton effect. The 'negative' effect occurs when the CD curve shows a minimum and the ORD curve is the reverse of the above[49].

It was found that ORD and CD are extremely sensitive to molecular geometry and to the interactions of the various groups of the chromophores in the metal complexes. Cobalt, it was found, is by far the most extensively studied metal.

In 1937 Pfeiffer[50] reported the usefulness of ORD as a means of determining the configuration of amino acids in bis(optically active aminoacidato)copper(II) complexes. He demonstrated that the Cu(II) complexes of D-amino acids have a positive Cotton effect whilst the L-amino acid complexes have a negative Cotton effect.

For complexes of optically active amino acids of the type $[Co(en)_2AA]^{2+}$, the optical activity of the complex arises from the dissymmetric arrangement and the vicinal effect of the optically active ligand. The contributions from the effects are additive. It was found that CD curves are much more easily resolved and reveal more splitting of bands than can be observed from absorption and ORD curves.

A third functional group, if not coordinated, was found not to affect the observed CD spectra greatly, if at all.

1.4.5 X-ray crystallographic studies

Single crystal X-ray diffraction provides a unique insight into the overall assembly of the atoms within a complex. The success of this technique is totally dependent upon the growth of single crystals of suitable quality.

The technique is also useful in determining the absolute configuration of complexes of optically active ligands.

For complexes of the type $[Co(en)_2AA]^{2+}$, the crystal structure of (+)-[L-Glutamatobis(ethylenediamine)cobalt(III)] perchlorate has been reported[13].

Table 1.3[1] lists crystallographic data relating to the structures of complexes of metals with potentially tridentate amino acids.

Table 1.3: Crystallographic Data of Metal-Amino Acid Complexes

Complex	Space Group	Unit Cell	Cell Dimension	Structure	Ref.
$Ni(L\text{-}His)_2 \cdot H2O$	C_2	Monoclinic		Octahedral	51
$Ni(DL\text{-}His)_2 \cdot H_2O$	Aba2	Orthorhombic	$a = 15.18$ Å $b = 13.05$ Å $c = 7.72$ Å $z = 4$	Octahedral	52
$Co(L\text{-}His)_2 \cdot H_2O$	C_2	Monoclinic	$a = 29.44$ Å $b = 8.32$ Å $c = 6.35$ Å $\beta = 90°$ $z = 4$	Octahedral	53
$Co(L\text{-}His)(D\text{-}His) \cdot 2H_2O$	$P2_1/c$	Monoclinic	$a = 10.04$ Å $b = 11.10$ Å $c = 15.31$ Å $\beta = 111.6°$ $z = 4$	Octahedral	54
$Zn(L\text{-}His)_2 \cdot 2H_2O$	C_2	Tetragonal	$a = 7.53$ Å $b = 7.53$ Å $c = 30.41$ Å $\beta = 30.41°$ $z = 4$	Tetragonally Octahedral	55
$Zn(DL\text{-}His)_2 \cdot 5H_2O$	C_2	Monoclinic	$a = 16.41$ Å $b = 14.76$ Å $c = 10.99$ Å $\beta = 129.6°$ $z = 4$	Tetragonally Octahedral	56
$Cu(L\text{-}HisH)_2(NO_3)_2 \cdot 2H_2O$	C_2	Triclinic	$a = 5.47$ Å $b = 7.13$ Å $c = 13.84$ Å $\alpha = 97°$ $\beta = 90°$ $\gamma = 102.7°$ $z = 1$	Tetragonal-distorted-rotahedral	57
$Cu(L\text{-}His)(L\text{-}Thr) \cdot H_2O$	$P2_1$	Monoclinic	$a = 5.843$ Å $b = 12.249$ Å $c = 11.049$ Å $\beta = 102.7°$ $z = 2$	Tetragonal-distorted-octahedral	58
$Cu(Glu) \cdot H_2O$	$P2_12_12_1$	Orthorhombic	$a = 11.084$ Å $b = 10.350$ Å $c = 7.238$ Å $z = 4$	Distorted Octahedral	59

Complex	Space Group	Unit Cell	Cell Dimension	Structure	Ref.
$Co(Asp)\cdot 3H_2O$	$P2_12_12_1$	Orthorhombic	$a = 9.39$Å $b = 7.85$ Å $c = 11.37$ Å $z = 4$	Octahedral	60
$Ni(Asp)\cdot 3H_2O$	$P2_12_12_1$	Orthorhombic	$a = 9.40$Å $b = 7.83$ Å $c = 11.35$ Å $z = 2$	Octahedral	60
$Zn(Asp)\cdot 3H_2O$	$P2_12_12_1$	Orthorhombic	$a = 9.38$Å $b = 9.72$ Å $c = 11.53$ Å $z = 2$	Octahedral	60
$Cu(L\text{-}Ser)_2$	$P2_1$	Monoclinic	$a = 9.924$ Å $b = 8.413$ Å $c = 5.651$ Å $\beta = 90.6°$ $z = 2$	Square	61
$Ni(L\text{-}Ser).2H_2O$	C2	Monoclinic	$a = 7.776$ Å $b = 8.546$ Å $c = 8.834$ Å $\beta = 101.5°$ $z = 2$	Octahedral	62
$Zn(L\text{-}Ser)_2$	$P2_1$	Monoclinic	$a = 9.542$ Å $b = 8.818$ Å $c = 5.666$ Å $\beta = 96.7°$ $z = 2$	Square Pyramidal	63
$Cu(L\text{-}Tyr)_2$	$P2_12_12_1$	Orthorhombic	$a = 13.049$ Å $b = 22.227$ Å $c = 6.078$ Å $z = 2$	Square Pyramidal	64
$Cu(LyH)_2Cl_2.2H_2O$	$P2_1$	Monoclinic	$a = 11.48$ Å $b = 16.83$ Å $c = 5.21$ Å $\beta = 93.5°$ $z = 2$	Tetragonal-distorted-octahedral	65
$[Co(2,3\text{-}DAP)_2]Br$	$P2_12_12_1$	Orthorhombic	$a = 11.76$ Å $b = 7.49$ Å $c = 5.91$ Å $z = 2$	Octahedral	37

CHAPTER TWO

Experimental

2.1 MATERIALS

All reagents, amino acids and Sephadex C-25 cation exchange resin were purchased from The Aldrich Chemical Company, United Kingdom and were used without further purification.

2.2 INSTRUMENTATION

2.2.1 Elemental Analysis

Elemental analysis of *trans*- and *cis*- dichlorobis(ethylenediamine)cobalt(III) chloride was carried out at the microanalytical laboratory of South African Bureau of Standards (SABS) in Richards Bay, South Africa. Elemental analysis of *cis*-carbonatobis(ethylenediamine)cobalt(III) chloride and all products was performed at the Chemistry Department at the University of Manchester, United Kingdom.

2.2.2 NMR Spectroscopy

^{1}H and ^{13}C NMR spectra were obtained using a Varian Inova 300 MHz NMR spectrometer and a Varian Unity 500 MHz NMR spectrometer.

2.2.3 IR Spectroscopy

Infrared spectroscopy was carried out using cesium iodide (CsI) discs on an ATI Mattson Genesis Series FTIR spectrometer (300 – 4000 cm^{-1}).

2.2.4 Electronic(UV-Visible) Spectroscopy

Electronic (UV-visible) spectra were measured, using water as a solvent, with a Hewlett Packard 8452A Diode Array Spectrophotometer (200 – 820 nm).

2.2.5 Mass Spectrometry

Mass spectra were done using an Electrospray instrument at the University of Manchester,UK

2.3 METHODS

2.3.1 Preparation of *trans*- and *cis*- dichlorobis(ethylenediamine)cobalt(III) chloride and *cis*-carbanatobis(ethylenediamine)cobalt(III) chloride

The *trans* and *cis* isomers of $[Co(en)_2Cl_2]Cl$ were prepared using published procedures[66].

Yield for *trans*-$[Co(en)_2Cl_2]Cl$ (based on ethylenediamine) : 53 %.

Elemental Analysis:

Calculated: 16.83 % C, 5.65 % H, 19.63 % N

Found: 16.85 % C, 5.69 % H, 19.68 % N

Yield for *cis*-$[Co(en)_2Cl_2]Cl.H_2O$ (based on *trans* isomer) : 60 %.

Elemental Analysis:

Calculated: 15.82 % C, 5.98 % H, 18.46 % N

Found: 16.11 % C, 6.01 % H, 18.74 % N

The *cis* isomer of $[Co(en)_2CO_3]Cl$, which may be used as an alternative starting material for the preparation of the amino acid complexes, was also prepared in accordance with published procedures[67].

Yield for *cis*-$[Co(en)_2CO_3]Cl$ (based on ethylenediamine) : 73 %.

Elemental Analysis:

Calculated: 21.87 % C, 5.87 % H, 20.40 % N, 12.92 % Cl

Found: 22.04 % C, 6.04 % H, 19.96 % N, 12.91 % Cl

2.3.2 Reaction of cis-$[Co(en)_2Cl_2]Cl$ with L-lysine monohydrochloride

A solution of L-lysine monohydrochloride (3.66 g, 0.02 mol) in water (20 ml) was added with stirring to a solution of *cis*-$[Co(en)_2Cl_2]Cl$ (5.72 g ,0.02 mol) in water (25 ml). The pH of the solution was adjusted to 8 with 1 M NaOH. Activated charcoal (0.5 g) was added and the solution stirred at 60 °C for three hours. The solution changed colour from purple to orange during the reaction. The charcoal was removed by filtration and the solution concentrated to a volume of 20 ml. After cooling to room temperature the solution was loaded onto a Sephadex C-25 column and eluted with 0.5 M NaCl (fraction 1) and with 1 M NaCl (fractions 2 and 3). Fraction 1 was pink, fraction 2 was orange and fraction three was yellow. Electronic (UV-visible) spectra of the solutions were recorded. Fraction 1 was found to be excess starting material. An excess of NaI was added to fraction 2 and the solution was placed in the refrigerator. An orange precipitate was subsequently obtained which was filtered and washed with methanol and diethyl ether. Fraction 3 was evaporated to near dryness on a rotary evaporator and cooled. The yellow powder that was obtained was recrystallised from water to yield a dark yellow crystalline product.

Complex 1 – $[Co(en)_2(lys)]I_2$

Yield : 33 %

Elemental Analysis

Calculated: 20.78 % C, 5.06 % H, 14.54 % N, 43.90 % I

Found: 20.01 % C, 4.98 % H, 14.21 % N, 43.43 % I

IR (CsI)

1657 cm^{-1} (C=O str)

3100-3200 cm^{-1} (NH_2 str)

^1H NMR (D_2O):

δ 3.51 and 3.65 ppm (dd, 1H, J = 3.75 and 3.86, J = 3.71 and J = 3.85 respectively, CH of lys),

δ (2.93 - 3.05 ppm) (t, 2H, J = 7.15 and 7.32, CH_2 attached to the ω-NH_2 group of lys)

δ (2.58 – 2.88 ppm) (m, 8H, CH_2 of en)

δ (1.44 – 1.98 ppm) (m, 6H, 3 X CH_2 of lysine adjacent to CH)

^{13}C NMR (D_2O):

δ ~185 ppm (1 pair), ~57 ppm (1 pair), ~ 45-43 ppm (4 pairs), ~39 ppm (1 pair), ~31 ppm (1 pair), ~26 ppm (1 pair), ~22 ppm (1 pair)

UV-Vis (H_2O)

λ_{max} 348 nm (ε = 105.59 $mol^{-1}dm^3cm^{-1}$) 488 nm (ε = 68.97 $mol^{-1}dm^3cm^{-1}$)

MS (Electrospray)

m/z = 264 $[Co(en)lys]^+$

2.3.2.1 Resolution of $[Co(en)_2(lys)]I_2$

An attempt was made to resolve product 1 into the optically active isomers using antimony(III)potassium oxide (+) tartrate 0.5 hydrate. A very slight excess of the resolving agent was added to a solution of the complex, which was in the form of the iodide salt. The KI was removed by filtration. Ethanol was added slowly to the filtrate until the first turbidity remained after complete mixing. Sufficient water was added to clear the solution. On slow cooling, an orange precipitate was formed which was isolated by filtration. A further quantity of ethanol was added to the filtrate in order to precipitate out the more soluble diastereiosomer. The first diastereoisomer was dissolved in a minimum amount of water and treated with KNO_3 to precipitate the resolving agent, which was subsequently removed by filtration. This was followed by the addition of an excess of NaI in order to precipitate the diastereoisomer as the iodide salt. However, the product remained in solution. The second diastereoisomer also remained in solution.

Complex 2 – $[Co(en)_3]Cl_3$

Yield : 12 %

Elemental Analysis

Calculated: 20.85 % C, 7.00 % H, 24.32 % N, 30.78 % Cl

Found: 20.65 % C, 6.98 % H, 24.03 % N, 29.99 % Cl

IR (CsI)

3100-3330 cm^{-1} (NH str)

1624cm^{-1} (NH bending)

1466 cm^{-1} (CH_2 bend)

1365 cm^{-1} (CH_2 wag)

~900 cm^{-1} (CH_2 rock)

^{1}H NMR (D_2O)

δ (2.58 – 2.98 ppm)(1 broad peak, 12H, CH_2 of en)

^{13}C NMR (D_2O)

δ 44 ppm

UV-Vis (H_2O)

λ_{max} 338 nm (ε = 66.06 $mol^{-1}dm^3cm^{-1}$) 466nm (ε = 59.71 $mol^{-1}dm^3cm^{-1}$)

MS (Electrospray)

m/z = 177 $[Co(en)_2]^+$

2.3.3 Reaction of *cis*-$[Co(en)_2Cl_2]Cl$ with DL-2,3-diaminopropionic acid monohydrochloride

A solution of DL-2,3-diaminopropionic acid monohydrochloride(2.82 g, 0.02 mol) in water (15 ml) was added with stirring to a solution of *cis*-$[Co(en)_2Cl_2]Cl$ (5.72 g ,0.02 mol) in water (25 ml). The pH of the solution was adjusted to 8 with 1 M NaOH. Activated charcoal (0.5 g) was added and the solution was stirred at 60 °C for three hours. The solution changed colour from purple to orange during the reaction. The charcoal was removed by filtration and the solution concentrated to a volume of 20 ml. After cooling to room temperature the solution was loaded onto a Sephadex C-25 column and eluted with 0.4 M NaCl (band 1) and with 0.6 M NaCl (band 2-4). Band 1 was pink, band 2 was orange, band 3 was yellow and band 4 was yellowish orange. Electronic spectra of the solutions were recorded and fraction 1 (pink band) was found to be excess starting material. Excess NaI was added to

fractions 2-4 after removing most of the solvent by using a rotary evaporator. The concentrated fractions were placed in a refrigerator at 5 °C. A pink precipitate was obtained from fraction 2, a yellow powder from fraction 3 and an orange crystalline product from fraction 4. The products were filtered and washed with methanol and diethyl ether. The yellow and orange products were recrystallised by dissolving in a minimum amount of warm water, adding NaI and cooling.

Complex 1 – $[Co(2,3\text{-}DAP)_2]I$

Yield :11 %

Elemental Analysis

Calculated: 18.38 % C, 3.60 % H, 14.29 % N, 32.37 % I

Found: 18.39 % C, 3.81 % H, 14.00 % N, 31.69 % I

IR (CsI)

1666 cm^{-1} (C=O str)

3100 – 3200 cm^{-1} (NH str)

362 cm^{-1} (Co-O str)

^1H NMR (D_2O):

δ 2.84 ppm and 2.97 ppm (dd, 1H, J = 3.28 and 4.12 , CH of 2,3-DAP),

δ 3.15 and 3.24 ppm (dd, 1H, J = 3.57, CH of 2,3-DAP)

δ 3.24 and 3.34 ppm (dd, 1H, J = 3.57, CH of 2,3-DAP)

~δ 3.70 ppm (d, 2H, J = 3.43, CH_2 of 2,3-DAP)

~ δ 3.79 ppm. (d, 2H, J = 3.43, CH_2 of 2,3-DAP)

UV-Vis (H_2O)

λ_{max} 348 nm ($\varepsilon = 41.50\ mol^{-1}dm^3cm^{-1}$) 498 nm ($\varepsilon = 66.01\ mol^{-1}dm^3cm^{-1}$)

MS (Electrospray)

m/z = 265 $[Co(2,3\text{-}DAP)_2]^+$

Complex 2 – $[Co(en)_2(2,3\text{-}DAP)_2]I_2$

Yield : 24 %

Elemental Analysis

Calculated: 15.68 % C, 4.32 % H, 15.68 % N, 47.35 % I

Found: 15.69 % C, 4.14 % H, 15.14 % N, 47.27 % I

IR (CsI)

1638 cm^{-1} (C=O str)

3100-3200 cm^{-1} (NH str)

385 cm^{-1} (Co-O str)

454 cm^{-1} (Co-N str)

^1H NMR (D_2O)

δ 2.6-2.9 (m, 8H, CH_2 of en)

δ 3.5-3.7 (m, 1H, CH of 2,3-DAP)

δ 2.98 (m, 2H, CH2 of 2,3-DAP)

^{13}C NMR (D_2O):

δ ~215 ppm, ~173ppm, ~59 ppm (1 pair), ~47 ppm (1 pair), ~44 ppm (2 pairs)

UV-Vis (H_2O)

λ_{max} 338 nm ($\varepsilon = 77.30\ mol^{-1}dm^3cm^{-1}$) 468nm ($\varepsilon = 77.00\ mol^{-1}dm^3cm^{-1}$)

MS (Electrospray)

m/z = 177 $[Co(en)_2]^+$

m/z = 222 $[Co(en)(2,3\text{-}DAP)]^+$

m/z = 281 $[Co(en)_2(2,3\text{-}DAP)]^+$

Complex 3 – $[Co(en)_3]I_3$

Yield : 22 %

Elemental Analysis

Calculated: 11.62 % C, 3.90 % H, 13.56 % N, 61.41 % I

Found: 11.56 % C, 3.97 % H, 12.98 % N, 60.27 % I

IR (CsI)

3100-3400 cm^{-1} (NH str)

1624 cm^{-1} (NH def)

1465 cm^{-1} (CH_2 bend)

1327 cm^{-1} (CH_2 wag)

895 cm^{-1} (CH_2 rock)

^{1}H NMR (D_2O):

δ (2.58 – 2.98 ppm)(1 broad peak, 12H, CH_2 of en)

^{13}C NMR (D_2O):

δ ~44 ppm

UV-Vis (H_2O)

λ_{max} 334 nm (ε = 89.60 $mol^{-1}dm^3cm^{-1}$) 466nm (ε = 79.13 $mol^{-1}dm^3cm^{-1}$)

MS (Electrospray)

m/z = 179 $[Co(en)_2]^+$

2.3.4 Preparation of $[Co(2,3\text{-}DAP)_2]Cl$

DL-2,3-diaminopropionic acid (DL-2,3-DAPH) monohydrochloride(1.41 g, 0.01mol) was added with stirring to a solution of cobalt(II)chloride hexahydrate (1.19 g; 0.005 mol) in water (25 ml). The pH of the solution was adjusted to 11.5 with 1 M NaOH. The colour of the solution changed from pink to yellowish brown when the pH of the solution was changed. A vigorous stream of air was bubbled through the solution for two hours. Concentrated hydrochloric acid was added to the oxidation

product until a final pH of 7 was attained. The solution changed from brown to dark pink after the pH 7 was obtained. The reaction mixture was concentrated using a rotary evaporator and cooled. A dark pink precipitate was formed, which was filtered and washed with ice cold water and diethyl ether.

Yield : 34 %

Elemental Analysis

Calculated: 23.98 % C, 4.69 % H, 18.64 % N, 11.79 % Cl

Found: 24.02 % C, 4.81 % H, 18.01 % N, 12.03 % Cl

IR (CsI)

1666 cm^{-1} (C=O str)

3100–3200 cm^{-1} (NH str)

362 cm^{-1} (Co-O str)

^{1}H NMR (D_2O):

δ 3.75 ppm (d, 2H, J = 3.02, CH_2 of 2,3-DAP),

δ 3.52 ppm (d, 2H, J = 3.30 , CH_2 of 2,3-DAP),

δ 2.69 ppm (d, 2H, J = 3.04, CH_2 of 2,3-DAP),

δ 2.90 ppm (dd, 1H, J = 4.12 and 3.99 , CH of 2,3-DAP),

δ 3.27 ppm (dd, 1H, J = 3.44 and 3.57, CH of 2,3-DAP),

^{13}C NMR (D_2O):

δ ~180 ppm (3 peaks), ~44 ppm(3 peaks), and ~62 ppm(3 peaks)

UV-Vis (H_2O)

λ_{max} 348 nm (ε = 42.90 $mol^{-1}dm^3cm^{-1}$) 498 nm (ε =67.03 $mol^{-1}dm^3cm^{-1}$)

MS (Electrospray)

m/z = 265 $[Co(2,3\text{-}DAP)_2]^+$

2.3.5 Preparation of [Co(2,3-DAP)(2,3-DAPH)Cl_2]

DL-2,3-diaminopropionic acid (DL-2,3-DAPH) monohydrochloride (1.41 g, 0.01mol) was added with stirring to a solution of cobalt(II)chloride hexahydrate (1.19 g; 0.005 mol) in water (25 ml). The pH of the solution was adjusted to 10.5 with 1 M NaOH. The solution changed from pink to yellowish brown when the pH of the solution was changed. A vigorous stream of air was bubbled through the solution for six hours. Concentrated hydrochloric acid (3.75 ml) was added to the oxidation product and the reaction mixture was concentrated on a steam bath. The colour changed to a dark bluish-green solution and a dark green precipitate appeared. The precipitate was filtered and washed with ice cold water, ethanol and diethyl ether. A further quantity of the green product was obtained from the filtrate upon prolonged standing.

Yield : 40 %

Elemental Analysis

Calculated: 21.38 % C, 4.48 % H, 16.62 % N, 21.03 % Cl

Found: 20.38 % C, 4.49 % H, 15.69 % N, 20.98 % Cl

IR (CsI)

~1720-1707 cm^{-1} (C=O str. - uncoordinated and non-ionised COOH).

1655 cm^{-1} (C=O str. - coordinated COO^-)

3200 cm^{-1} (N-H str)

1584 cm^{-1} (N-H bending)

1426 cm^{-1} (CH_2 bend)

1354 cm^{-1} (CH_2 wag)

944 cm^{-1} (CH_2 rock)

1080 cm^{-1} (C-N str.).

^{13}C NMR (D_2O)

δ 170 ppm, δ 59 ppm, δ 54 ppm

UV-Vis (H_2O)

λ_{max} 400 nm, 460 nm and 610nm

CHAPTER THREE

Results and Discussion

3.1 PREPARATION OF *CIS*- AND *TRANS*- ISOMERS OF DICHLOROBIS(ETHYLENEDIAMINE)COBALT(III) CHLORIDE

The *trans*- and *cis*-$[Co(en)_2Cl_2]Cl$ isomers, which were prepared and characterised, have been used as the starting materials for the preparation of the amino acid complexes.

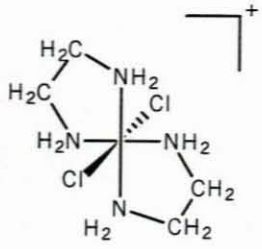

(a) *trans*-$[Co(en)_2Cl_2]Cl$

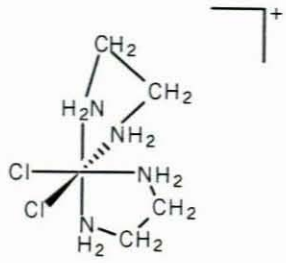

(b) *cis*-$[Co(en)_2Cl_2]Cl$

Figure 3.1: Geometric Isomers of $[Co(en)_2Cl_2]Cl$

3.1.1 Infrared Spectroscopy

The differences in the infrared spectra of the *cis*- and *trans*-$[Co(en)_2Cl_2]Cl$ isomers (Figure 3.1) in the ~1600 cm^{-1} N-H asymmetric deformation region are distinct. In the trans isomer, a single sharp band occurs at 1580 cm^{-1} (Figure. 3.2), whereas in the cis complex they occur over a wider range ~1634-1527cm^{-1} and are more complex (Figure 3.3).

Chamberlain and Bailar[68] suggested that the region 1120-1050 cm^{-1} could be used to distinguish *cis*- and *trans*- bis(ethylenediamine) isomers. The *trans*-compounds show two sharp peaks in the ranges 1050-1120 cm^{-1}, whilst the cis compounds show a group of four bands.

The most consistent variations between the spectra of the *cis* and *trans*-isomers have been found in the CH_2 rocking region, i.e. 870-900 cm^{-1} [69]. In this case, complexes with a *cis* configuration exhibit two bands whilst those of the *trans* form show only one.

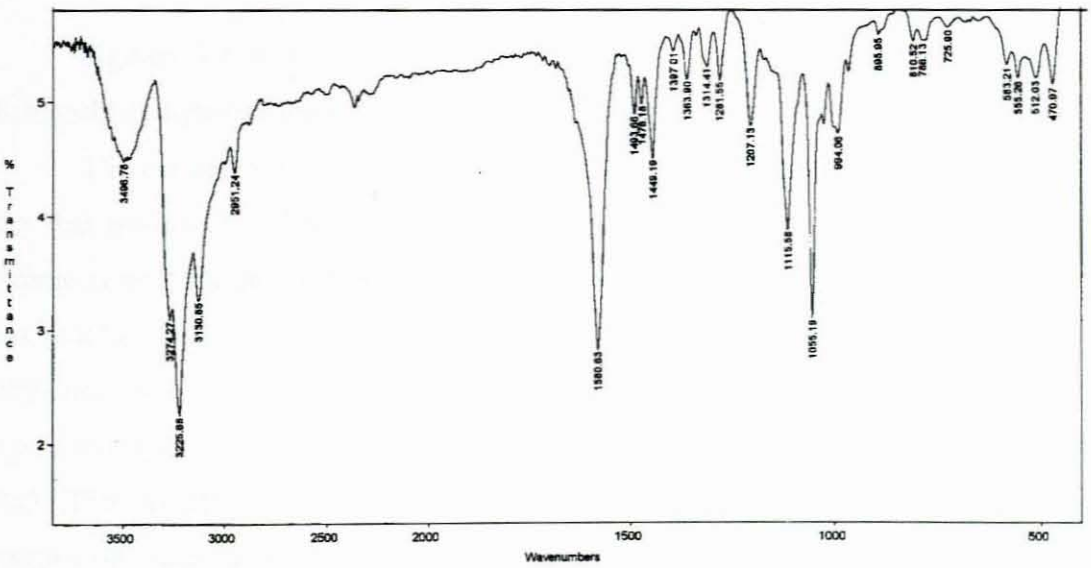

Figure 3.2: IR Spectrum of *trans*-$[Co(en)_2Cl_2]Cl$

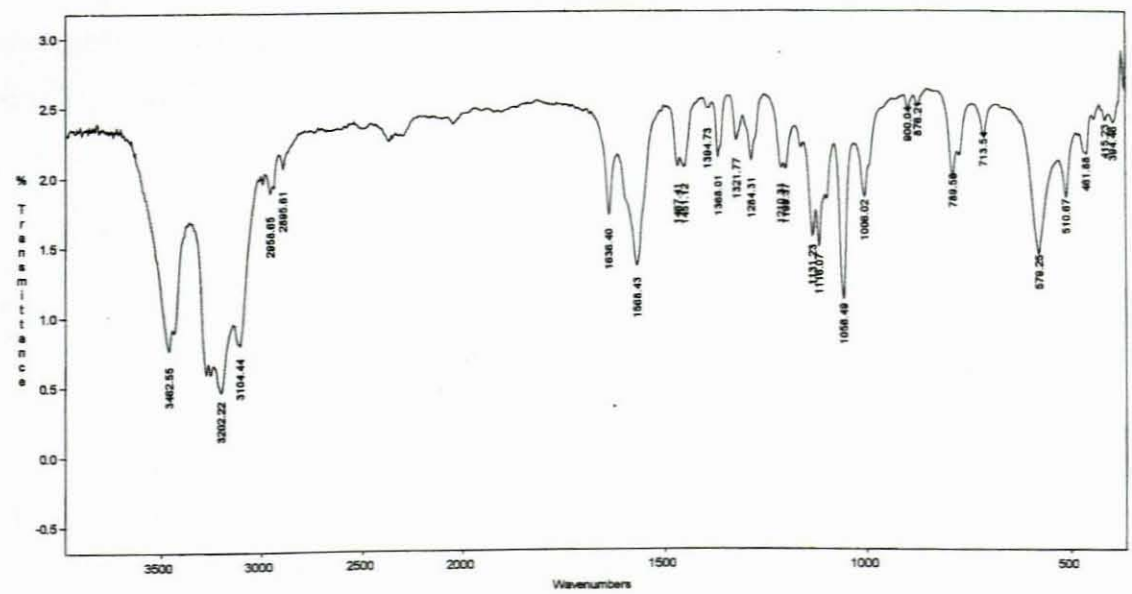

Figure 3.3: IR Spectrum of *cis*-$[Co(en)_2Cl_2]Cl$

3.1.2 NMR Spectroscopy

Figures 3.4 and 3.5 represent the ^1H NMR spectra of the *cis* and *trans*-dichlorobis(ethylenediamine)cobalt(III) chloride complexes.

The *cis* and *trans* isomers retain different symmetry properties and it is this fact that governs the difference in the NMR spectra. The *cis* isomer exhibits C_{2v} symmetry with the two-fold axis in the plane of the cobalt and the two Cl groups and this factor makes the $-CH_2-CH_2-$ groups equivalent provided the cobalt-ethylenediamine rings have the same conformation. If the conformers were relatively rigid (inversion rate < 10 s^{-1}), then an ABCD pattern would be expected to emerge in D_2O. If an average conformer is observed, an A_2B_2 system should appear, since the protons on either side of each cobalt-ethylenediamine ring would entertain different fields[9].

The *trans* isomer, however, with D_{4h} symmetry have each side of the cobalt-ethylenediamine rings in identical fields. If the conformer interchange is fast a singlet should appear and conversely if the interchange is slow, an A_2B_2 system could be observed.

The proton spectra for the *cis* complex gives varying results in the $-CH_2CH_2-$ region. Some show considerable splitting whilst others give a broad resonance band. The *cis*-$[Co(en)_2(D_2O)]Cl$ complex exhibits an A_2B_2 system. Thus it appears reasonable to suggest the splitting results from $-CH_2CH_2-$ coupling and not from $-NH_2CH_2-$ coupling

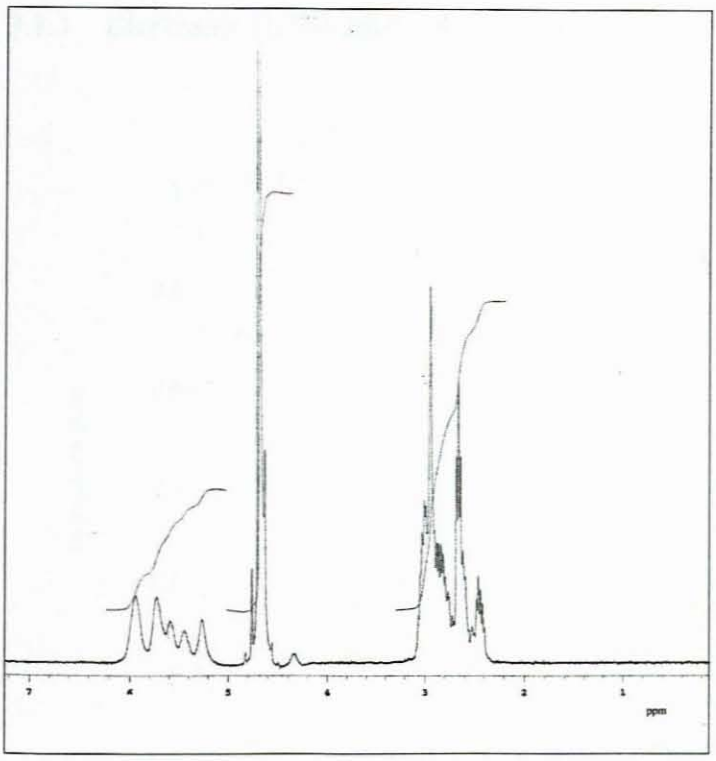

Figure 3.4: ^{1}H NMR Spectrum of *cis*-$[Co(en)_2Cl_2]Cl$

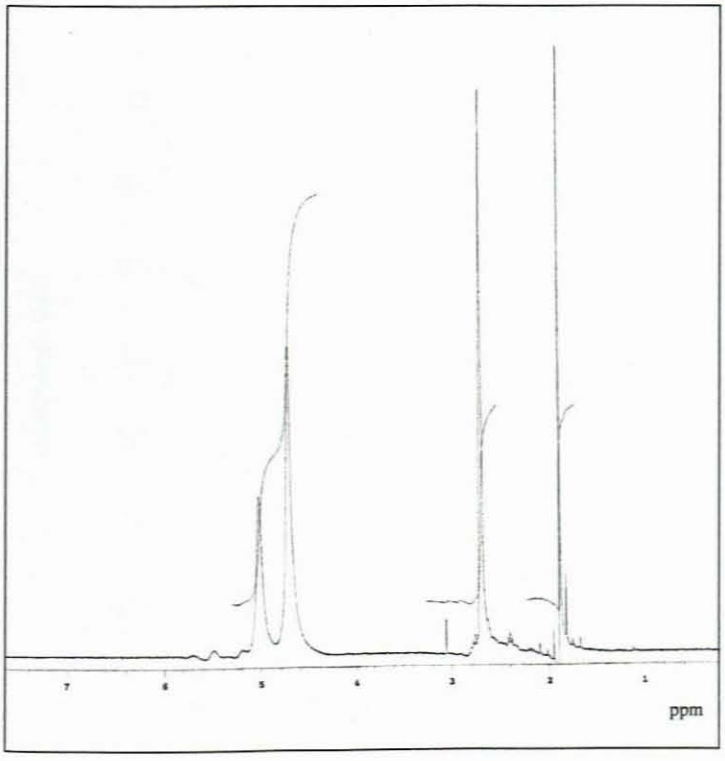

Figure 3.5: ^{1}H NMR Spectrum of *trans*-$[Co(en)_2Cl_2]Cl$

3.1.3 Electronic (UV-Visible) Spectroscopy

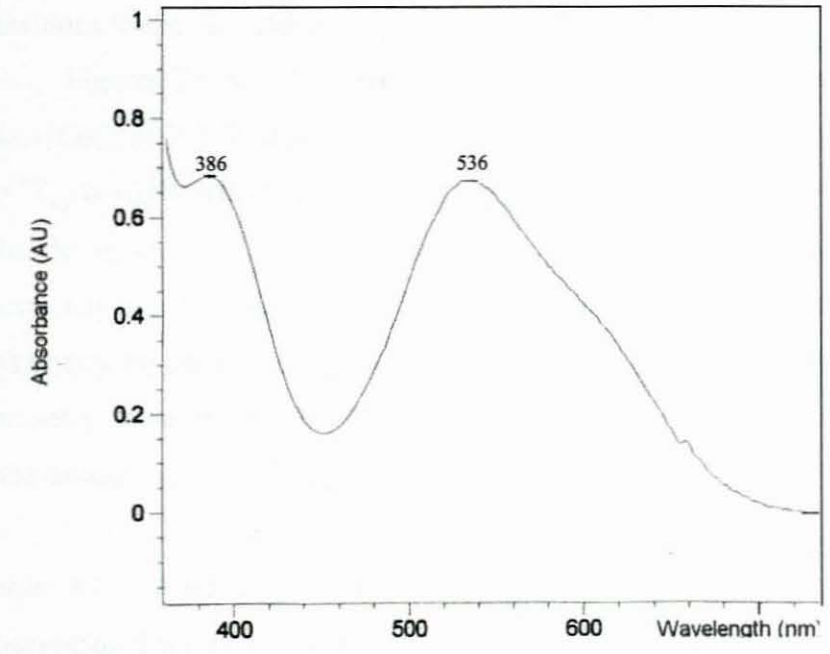

Figure 3.6: UV/Visible Absorption Spectrum of *cis*-$[Co(en)_2Cl_2]Cl$

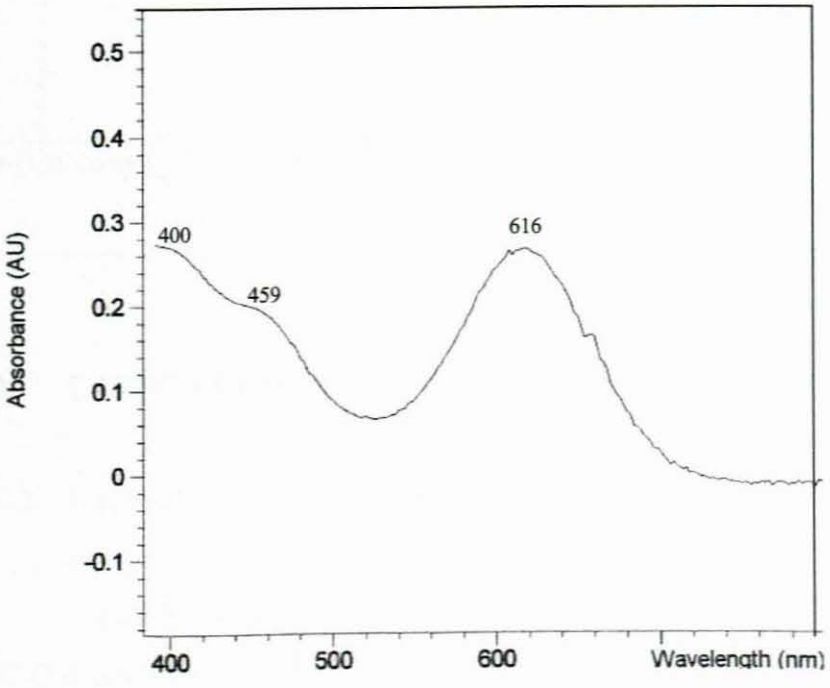

Figure 3.7: UV/Visible Absorption Spectrum of *trans*-$[Co(en)_2Cl_2]Cl$

The visible absorption spectra of Co^{III} complexes are expected to be consistent with transitions from the $^1A_{1g}$ ground state to other singlet states. In Co^{III} octahedral complexes the two absorption bands found in the visible spectrum represent transitions to the $^1T_{1g}$ and $^1T_{2g}$ upper states.

Figures 3.6 and 3.7 illustrate the UV/visible absorption spectra for *cis*- and *trans*-$[Co(en)_2Cl_2]Cl$ respectively. In the spectrum of the *trans* isomer, the splitting of the $^1T_{2g}$ is slight whereas that of the $^1T_{1g}$ is marked. Since the ethylenediamine and chloride ligands are far apart in the spectrochemical series, the ν_1 band splits completely giving rise to three bands whereas the *cis* isomer merely shows slight asymmetry in the lower region band. In addition, the *cis* isomer lacks a centre of symmetry therefore its spectrum is more intense than that of the centrosymmetric *trans* isomer.

Table 3.1: Absorption bands and Extinction Coefficients (ε) of UV/Visible Absorption Spectra of *trans*-$[Co(en)_2Cl_2]Cl$ and *cis*-$[Co(en)_2Cl_2]Cl$

	λ_{max}/nm	ε/mol^{-1}dm^{3}cm^{-1}
trans-$[Co(en)_2Cl_2]Cl$	400	29.2
	459	21.8
	616	27.8
cis-$[Co(en)_2Cl_2]Cl$	386	65.8
	536	64.9

3.2 CARBONATOBIS(ETHYLENEDIAMINE)COBALT(III) CHLORIDE

3.1.2 Infrared Spectroscopy

Figure 3.8 illustrates the IR spectrum of $[Co(en)_2CO_3]Cl$. The $\nu(C\text{-}O_I)$ and $\nu(C\text{-}O_{II})$ bands occur at 1580 cm^{-1}and 1059 cm^{-1} respectively. The bidentate mode of coordination of the carbonate group gives rise to strong bands at 1580 cm^{-1} and 1273 cm^{-1}, whereas, if the carbonate group was bonded in a unidentate fashion, one would expect to observe bands at ~1600 cm^{-1}, 1495 cm^{-1} and 1335 cm^{-1} [70]. The NH

stretching vibration is indicated by the presence of a peak between 3100-3200 cm^{-1}, whilst the Co-O stretching vibration is observed at ~395 cm^{-1}.

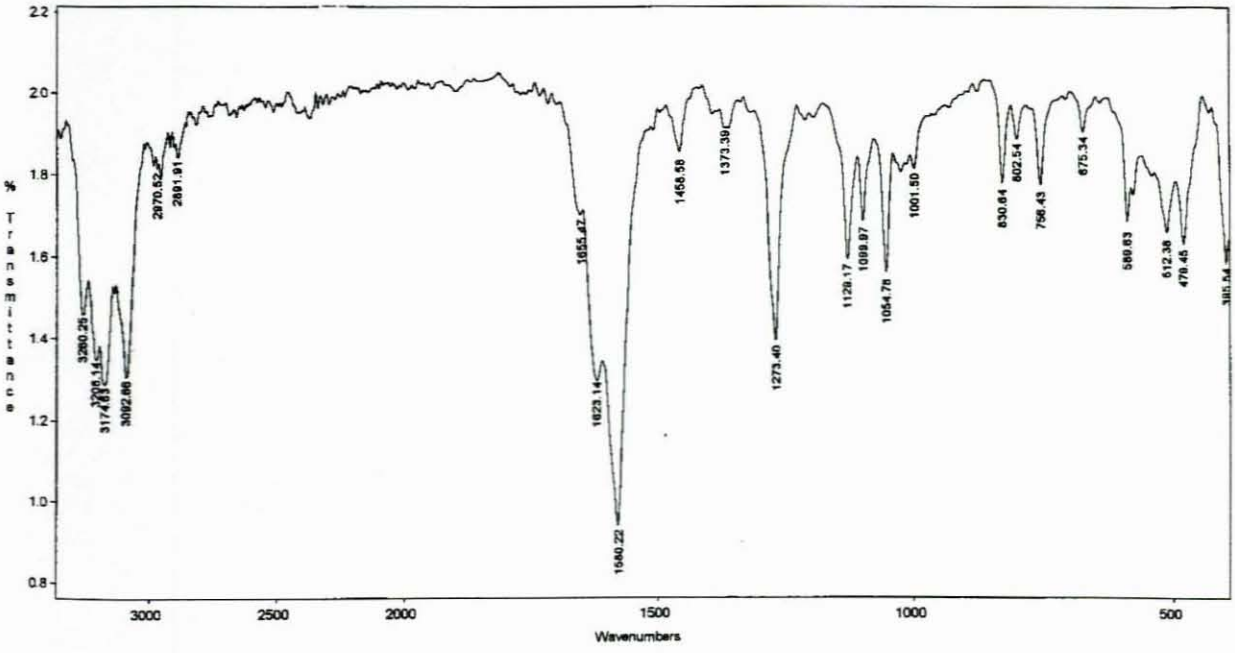

Figure 3.8: IR Spectrum of *cis*-$[Co(en)_2CO_3]Cl$

3.2.2 NMR Spectroscopy

The ^1H NMR spectrum (Figure 3.9) shows a multiplet between δ 2.49 ppm and δ 2.72 ppm. This corresponds to the overlap of triplets, attributable to the splitting of the methylene protons on the ethylenediamine ring of *cis*-$[Co(en)_2CO_3]Cl$. The ^{13}C NMR spectrum (Figure 3.10) shows two peaks at ~δ 46 ppm, which represent the methylene carbons of ethylenediamine, and the presence of the carbon of the carbonate group appears to be confirmed by the peak at ~δ 170 ppm.

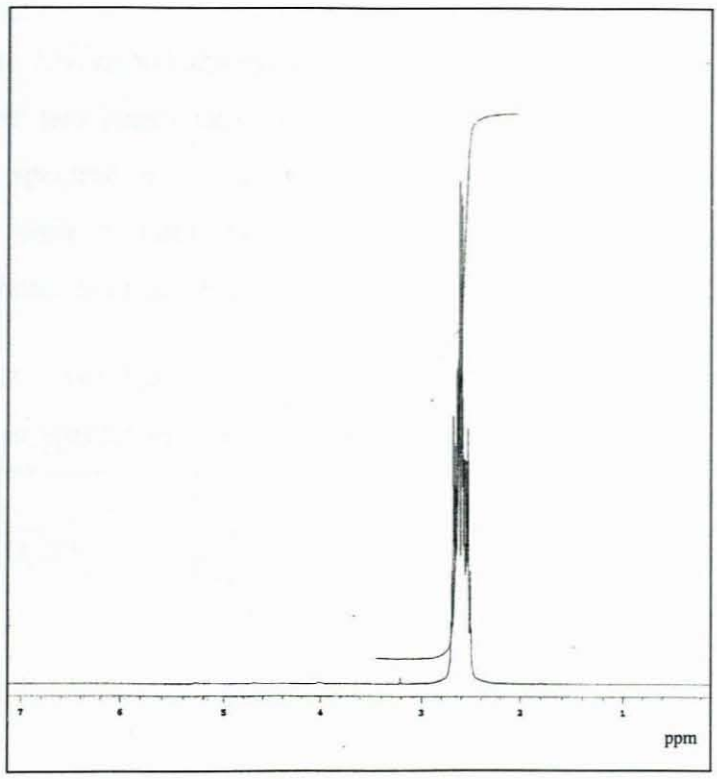

Figure 3.9: ^{1}H NMR spectrum of *cis*-[Co(en)$_2$CO$_3$]Cl

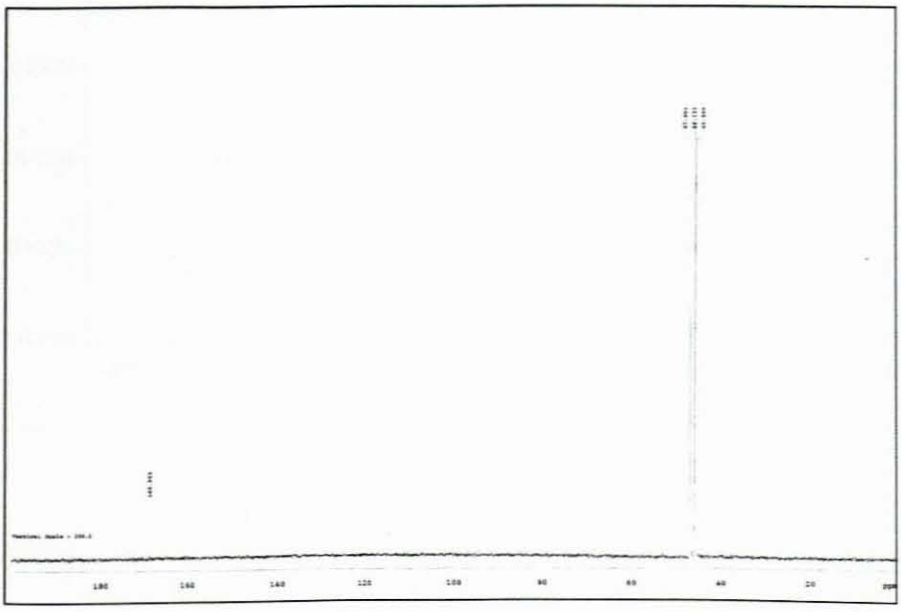

Figure 3.10: ^{13}C NMR spectrum of *cis*-[Co(en)$_2$CO$_3$]Cl

3.2.3 Electronic (UV-Visible) Spectroscopy

The UV/visible absorption spectrum of $[Co(en)_2CO_3]Cl$ is shown in Figure 3.11. The two peaks may be attributed to d-d absorptions. Comparison of the electronic spectrum of *cis*-$[Co(en)_2Cl_2]Cl$ (Figure 3.6) with that of $[Co(en)_2CO_3]Cl$, reveals a shift in both the $^1A_{1g} \rightarrow {}^1T_{1g}$ and $^1A_{1g} \rightarrow {}^1T_{2g}$ transitions to a lower wavenumbers. Such an observance is in accordance with the spectrochemical series.

Table 3.2: Absorption bands and Extinction Coefficients (ε) of UV/Visible Absorption Spectra of $[Co(en)_2CO_3]Cl$

	λ_{max}/nm	ε/mol^{-1}dm^{3}cm^{-1}
$[Co(en)_2CO_3]Cl$	360	115
	510	129

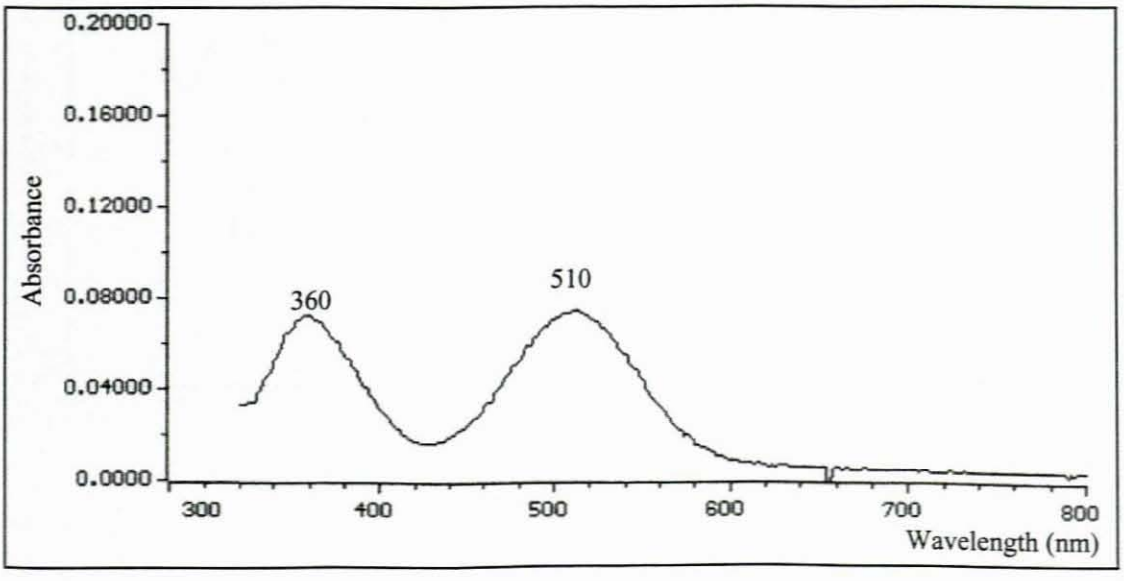

Figure 3.11: The UV/Visible Absorption Spectrum of *cis*-$[Co(en)_2CO_3]Cl$

3.3 REACTION OF *cis*-$[Co(en)_2Cl_2]Cl$ WITH L-LYSINE MONOHYDROCHLORIDE

3.3.1 Complex 1 - $[Co(en)_2(lys)]I_2$

3.3.1.1 IR Spectroscopy

The infrared spectrum (Figure 3.12) provides evidence as to which groups within the structure of lysine are coordinated in the $[Co(en)_2(lys)]I_2$ complex. A sharp C=O stretching band at 1657 cm^{-1} in the infrared spectrum of $[Co(en)_2(lys)]I_2$, indicates that the carboxylate group is coordinated[70]. In the infrared spectrum of lysine, the free COOH group is indicated by the peak at ~1627 cm^{-1} (Figure 3.13). The two distinct bands at 3100-3200 cm^{-1} (NH_2 stretching region) may be attributable to the coordinated and uncoordinated amino groups. Thus it is suggested that the glycinate portion is involved in chelation with the ω amino group free.

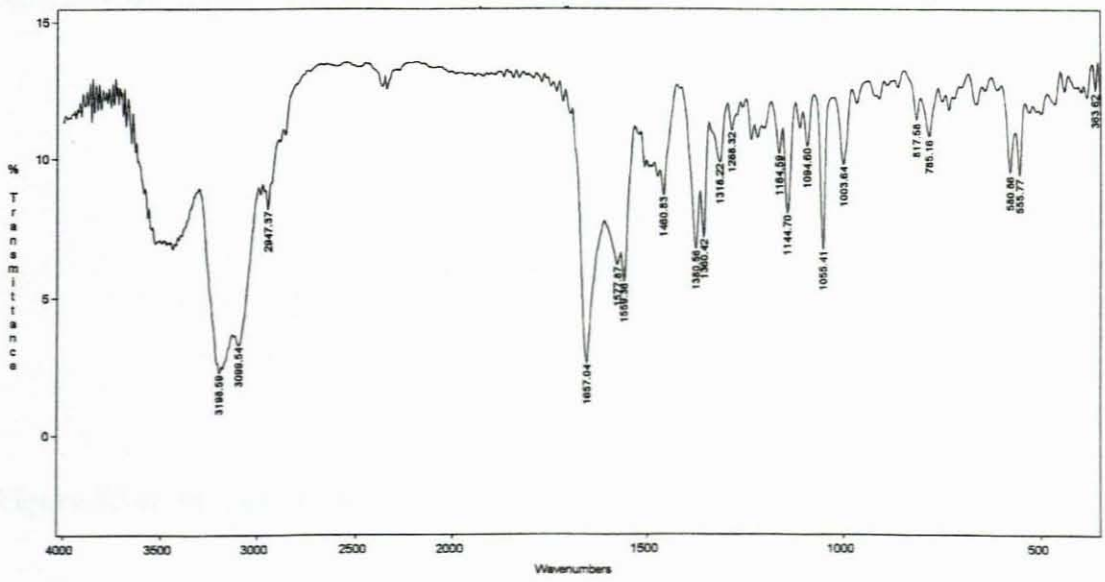

Figure 3.12: IR Spectrum of $[Co(en)_2(lys)]I_2$

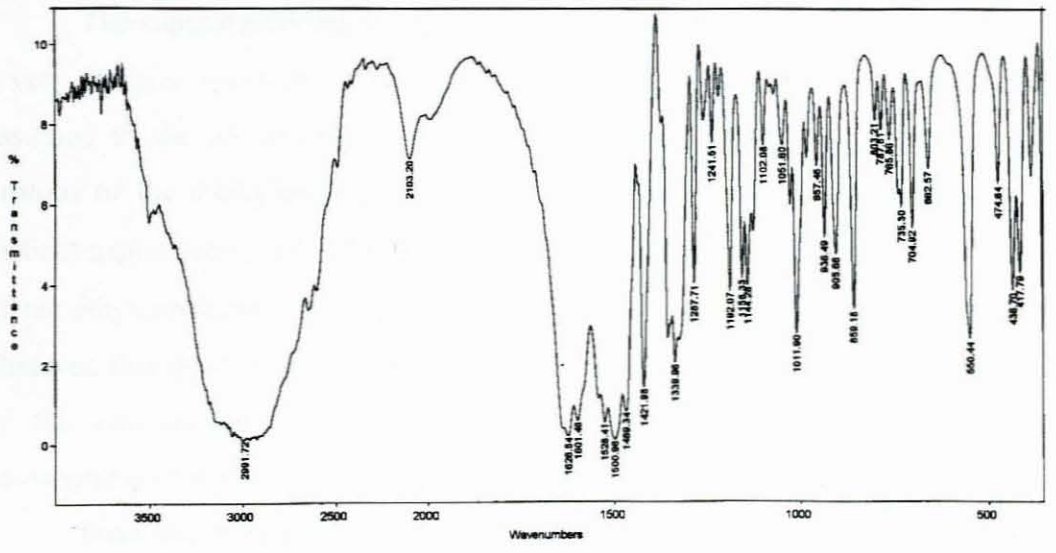

Figure 3.13: IR Spectrum of L-Lysine monohydrochloride

3.3.1.2 NMR Spectroscopy

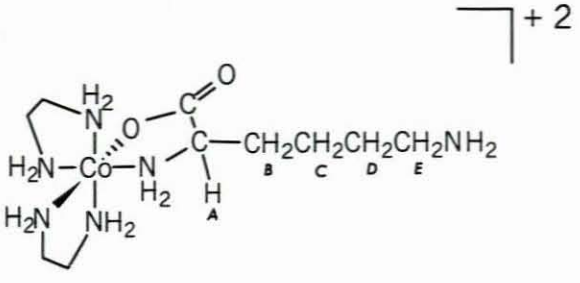

Figure 3.14: Proposed Structure for $[Co(en)_2(lys)_2]I_2$

The ^1H NMR spectrum of $[Co(en)_2(lys)_2]I_2$ (Figure 3.15) yields a complex pattern due to the different chemical shifts of the diastereoisomeric racemic pairs [(+)(-)(+)(-)(+)] and [(+)(+)(+)(-)(-)].

The asymmetric CH (A) proton of the coordinated lysine gives two sets of doublet of doublets at δ 3.51 ppm and δ 3.65 ppm. This arises from splitting by the two adjacent methylene protons. Each doublet of doublets has the same integrated intensity therefore it appears reasonable to suggest the presence of equal proportions of each within the racemate.

The superimposition of the quartets (B), quintets(C,D) and triplet (E) leads to a very complex spectrum. The pattern between δ 1.4 ppm and δ 1.95 ppm may be assigned to the protons of the first three methylene groups of lysine, whilst the protons of the methylene group attached to the free terminal amino group give a distinct triplet between δ 2.93 and δ 3.05 ppm. The protons of the $-CH_2CH_2-$ group of the ethylenediamine ring occur between δ 2.58 and δ 2.88 ppm. Moreover, it is observed that the distinct triplet appears close to the peaks for the $-CH_2CH_2-$ protons of the ethylenediamine ring. This fact suggest similarities in the chemical environment of the $-CH_2$ groups, notably adjacent to amino groups.

From the integration of the value of 8 units for the ethylenediamine protons, 2 units for the methylene group attached to the terminal amino group, 6 units for the remaining methylene groups and 1 unit for the methine proton (each diastereoisomer contributing ½ H), it appears possible to confirm the proposed structure. From the ^{13}C spectrum (Figure 3.16), it is seen that there is a pair of peaks for each carbon atom, thus confirming the presence of a racemic mixture.

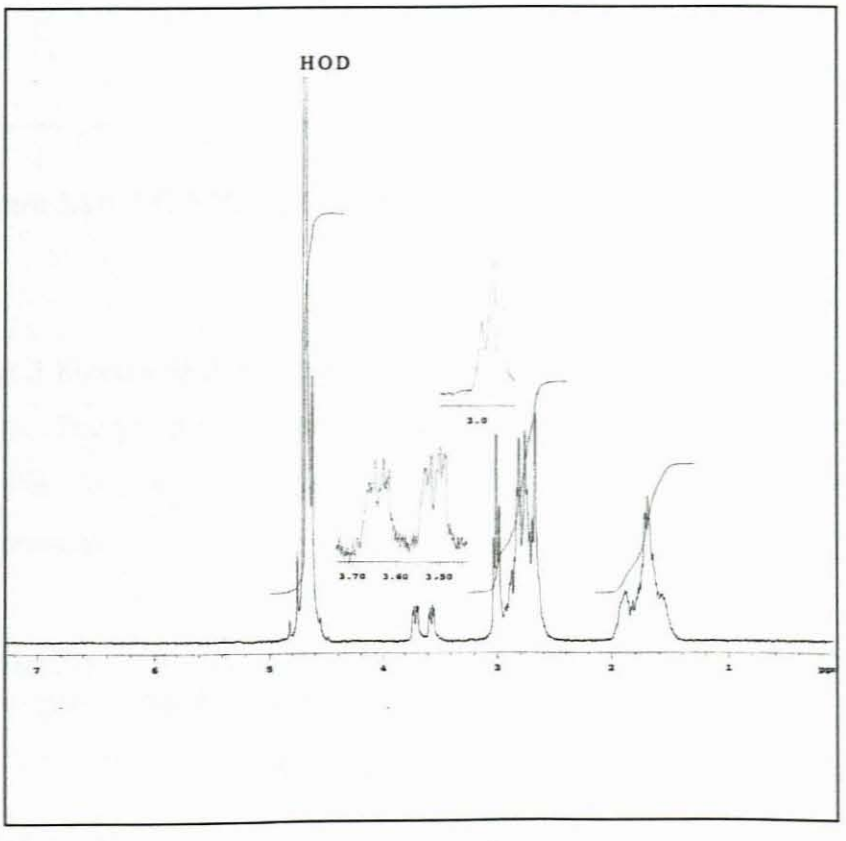

Figure 3.15: ^1H NMR spectrum of$[Co(en)_2(lys)]I_2$

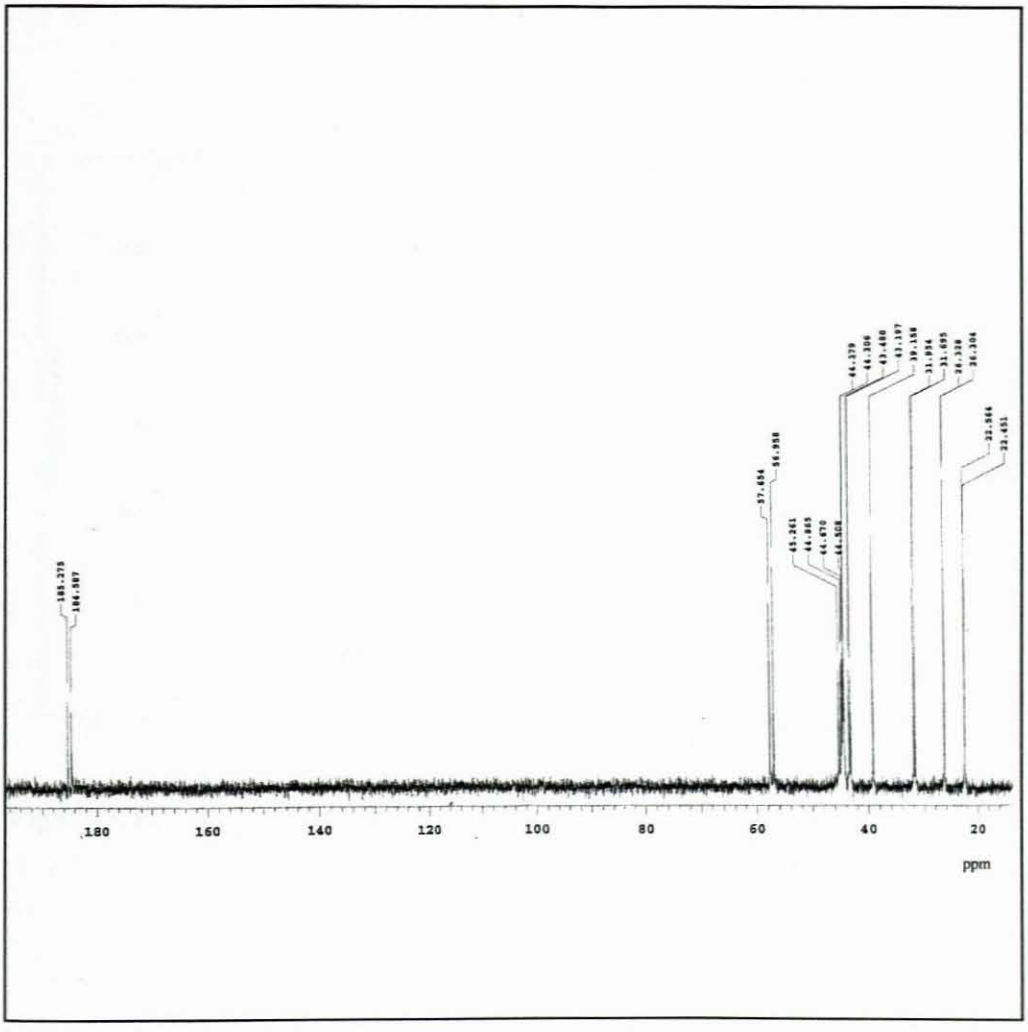

Figure 3.16: ^{13}C NMR spectrum of $[Co(en)_2(lys)]I_2$

3.3.1.3 Electronic (UV-Visible) Spectroscopy

The two bands observed (Figure 3.17) are due to d-d transitions corresponding to the $^1A_{1g} \rightarrow {}^1T_{1g}$ (longer wavelength) and $^1A_{1g} \rightarrow {}^1T_{2g}$ (shorter wavelength) absorptions.

Table 3.3: Absorption bands and Extinction Coefficients (ε) of UV/Visible Absorption Spectra of $Co(en)_2(lys)]I_2$

	λ_{max}/nm	ε/mol^{-1}dm^{3}cm^{-1}
$Co(en)_2(lys)]I_2$	348	105.6
	488	69.0

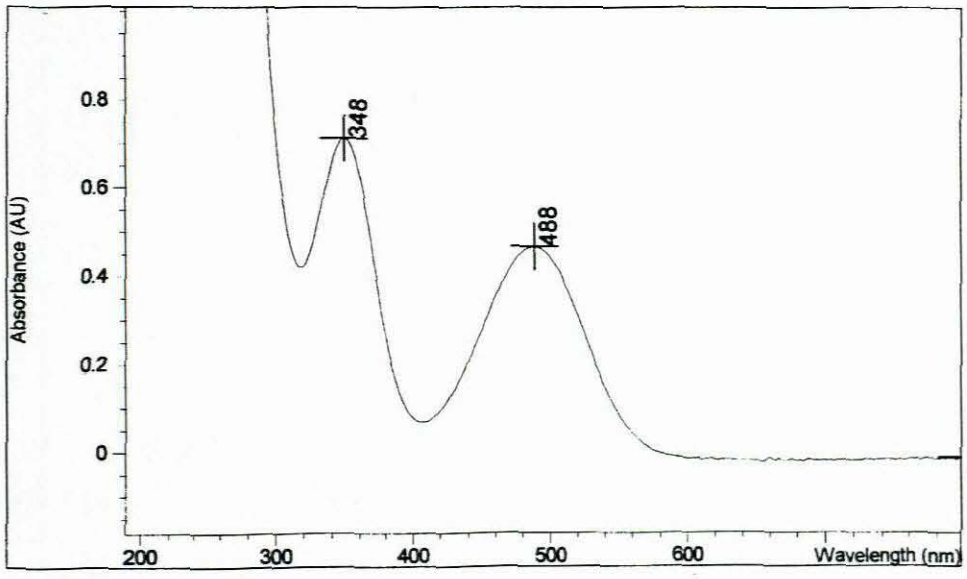

Figure 3.17: UV/Visible Absorption Spectrum of $[Co(en)_2(lys)]I_2$

3.3.1.4 Mass Spectrometry

The mass spectrum of $[Co(en)_2(lys)]I_2$ is represented in Figure 3.18. The base peak, at m/z = 264, corresponds to the $[Co(en)(lys)]^+$ ion. The complex shows a splitting pattern corresponding to the loss of one iodine atom (m/z = 451), followed by the loss of one molecule of ethylenediamine (m/z = 392) and subsequently the second iodine atom (m/z = 264).

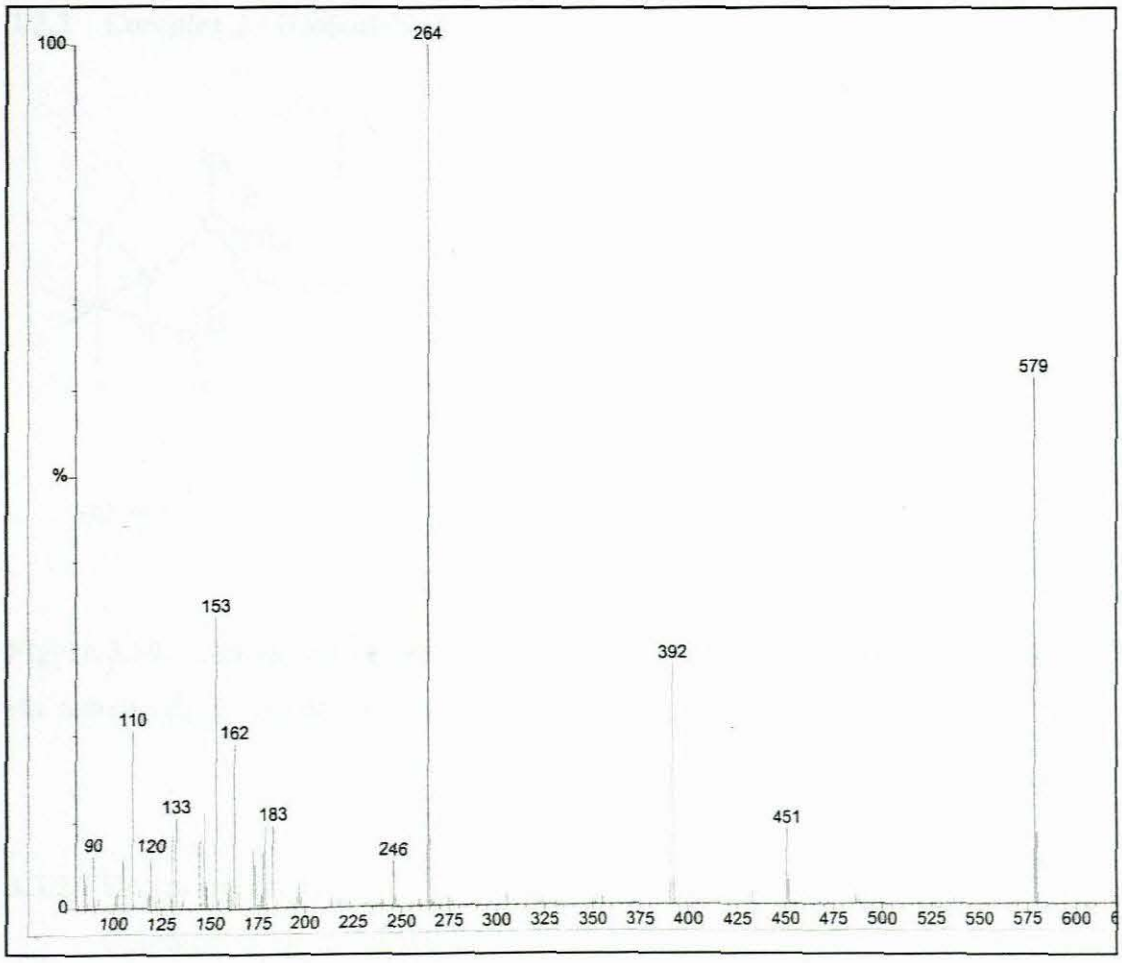

Figure 3.18: Mass Spectrum of $[Co(en)_2(lys)]I_2$

3.3.2 Complex 2 - $[Co(en)_3]Cl_3$

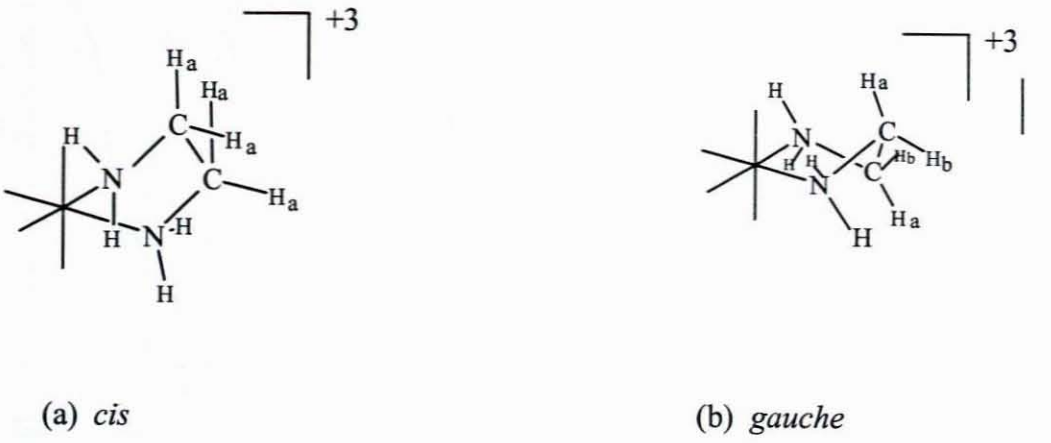

(a) *cis* (b) *gauche*

Figure 3.19: The (a) *cis* or 'envelope' structure and (b) the *gauche* structure of the cobalt-ethylenediamine ring

3.3.2.1 IR Spectroscopy

Coordinated ethylenediamine molecules may adopt one of two arrangements, namely those of *cis* and *gauche,* of the carbon and nitrogen skeleton (Figure 3.19).

Infrared spectra provide a criterion for dividing the complex into the two types. The infrared spectrum of $[Co(en)_3]Cl_3$ is illustrated in Figure 3.20. The NH stretching region occurs between 3100 and 3300 cm^{-1}, whilst the bands at about 1600 cm^{-1} may be assigned to the NH_2 bending vibration. Quagliano and Mizushima[71] indicated that the cobalt-ethylenediamine ring is in the *gauche* configuration, and X-ray crystallographic data for $[Co(en)_3]Cl_3$ further supports this conclusion[72]. Sheppard and Powell[43] suggested that the general band structure in the infrared spectrum is typical of the *gauche* configuration of all metal-ethylenediamine rings. The bands that appear in the regions ~1460, ~1300, ~900 cm^{-1} may be assigned to the CH_2 bend, CH_2 wag and CH_2 rock, respectively. Moreover, the band at ~1051 cm^{-1}, which is sharp and strong, may be the result of the stretching vibration of either the C-N or C-C bond[69].

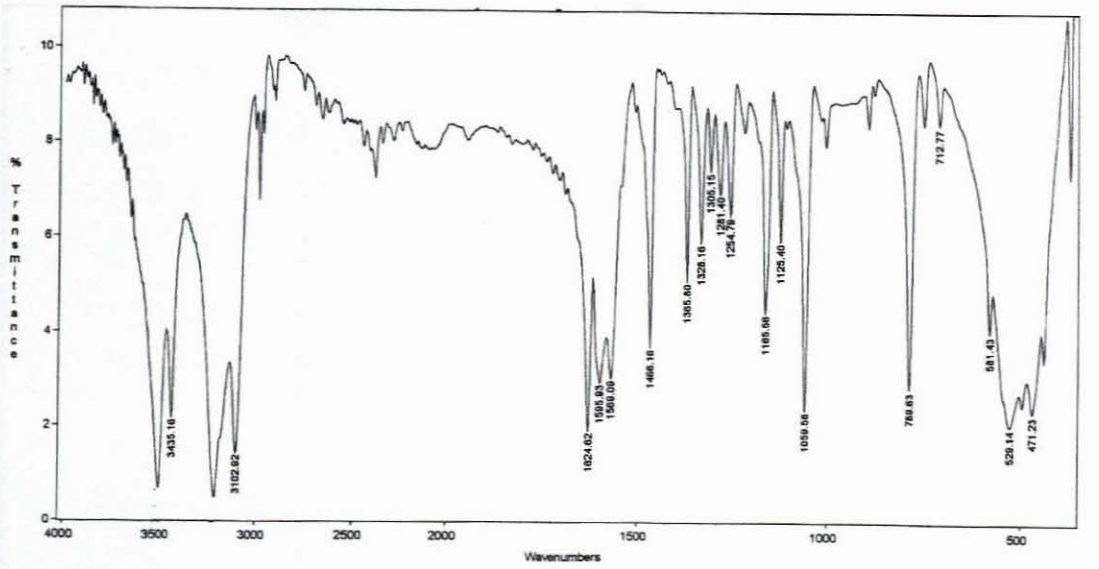

Figure 3.20: IR Spectrum of $[Co(en)_3]Cl_3$

3.3.2.2 NMR Spectroscopy

In the ^1H NMR spectrum of $[Co(en)_3]Cl_3$, it is observed that a resonance between δ 2.58 and δ 2.90 ppm (Figure 3.21), which is of considerable breadth and which exhibits unresolved fine structure. The latter feature may be caused either by electron-coupled spin-spin interaction between the two pairs of non-equivalent hydrogen atoms, as might occur with a rigid *gauche* form of the ligand but not within the *cis*, from similar spin-spin interaction between the CH_2 and NH_2 groups if the hydrogen atoms of the *cis* do not exchange sufficiently rapidly with those of the water solvent or a combination of both effects[43]. Furthermore, in the case of this complex the broad resonance band for the CH_2 groups may presumably be due to the presence of extra structure caused by interaction with the magnetic moment of the cobalt nucleus of spin 7/2.

The ^{13}C NMR spectrum of $[Co(en)_3]Cl_3$ is shown in Figure 3.22. A single peak is observed at ~δ 44 ppm since all of the carbon atoms are chemically equivalent. This appears to confirm the proposed structure of the complex.

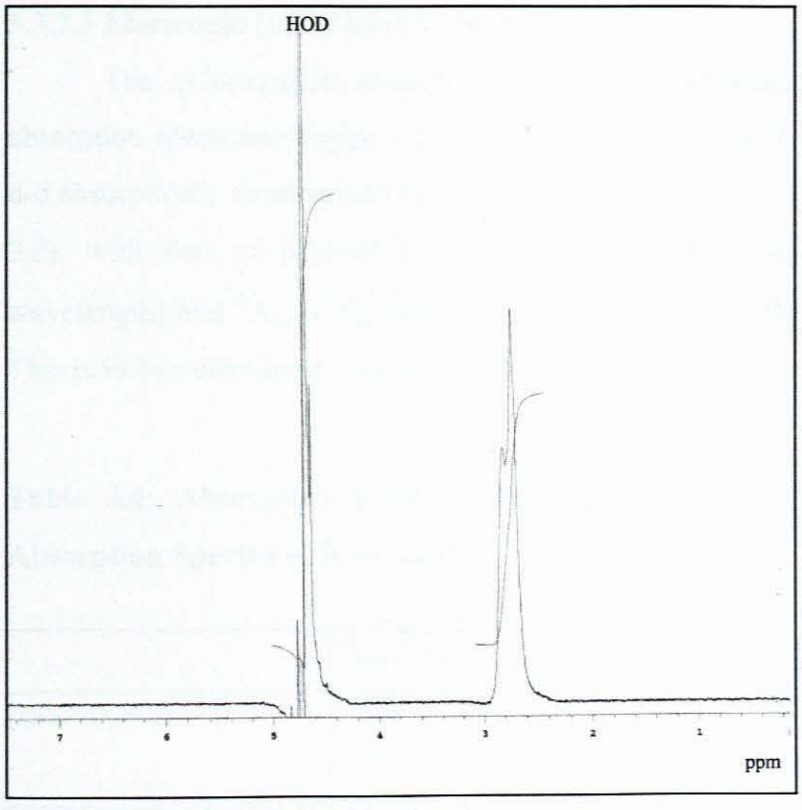

Figure 3.21: ^{1}H NMR of $[Co(en)_3]Cl_3$

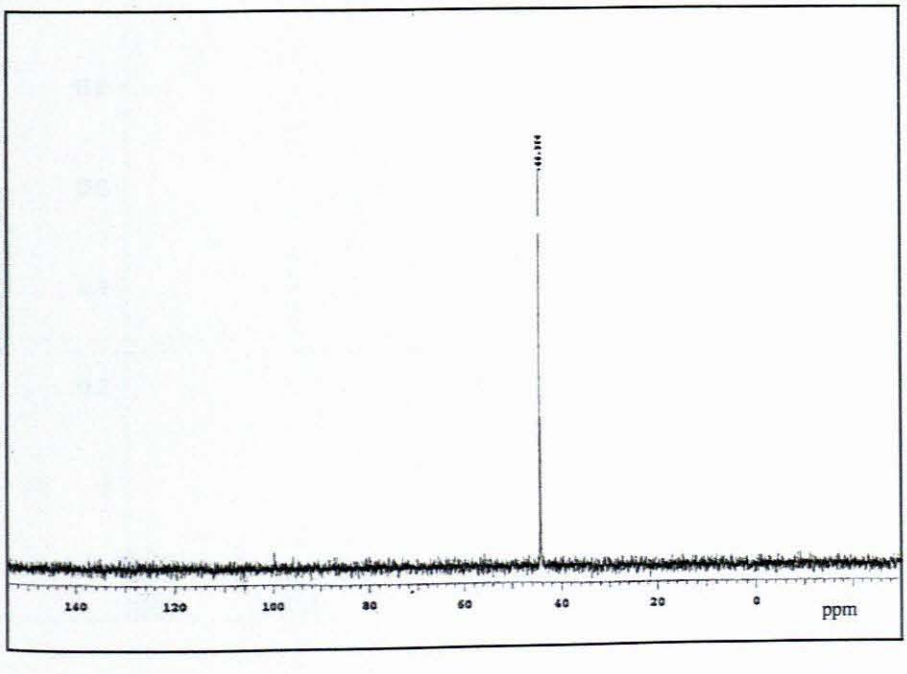

Figure 3.22: ^{13}C NMR of $[Co(en)_3]Cl_3$

3.3.2.3 Electronic (UV-Visible) Spectroscopy

The $[Co(en)_3]Cl_3$ complex exhibits D_3 symmetry. In the UV/visible absorption spectrum (Figure 3.23), two bands are observed which arise as a result of d-d absorptions. Comparison of the electronic spectrum of cis-$[Co(en)_2Cl_2]Cl$ (Figure 3.6), with that of $[Co(en)_3]Cl_3$ reveals a shift in both the $^1A_{1g} \rightarrow {}^1T_{1g}$ (longer wavelength) and $^1A_{1g} \rightarrow {}^1T_{2g}$ (shorter wavelength) transitions to lower wavenumbers. This is in fact consistent with the spectrochemical series.

Table 3.4: Absorption bands and Extinction Coefficients (ε) of UV/Visible Absorption Spectra of $[Co(en)_3]Cl_3$

	λ_{max}/nm	ε/mol^{-1}dm^{3}cm^{-1}
$[Co(en)_3]Cl_3$	338	59.7
	466	66.1

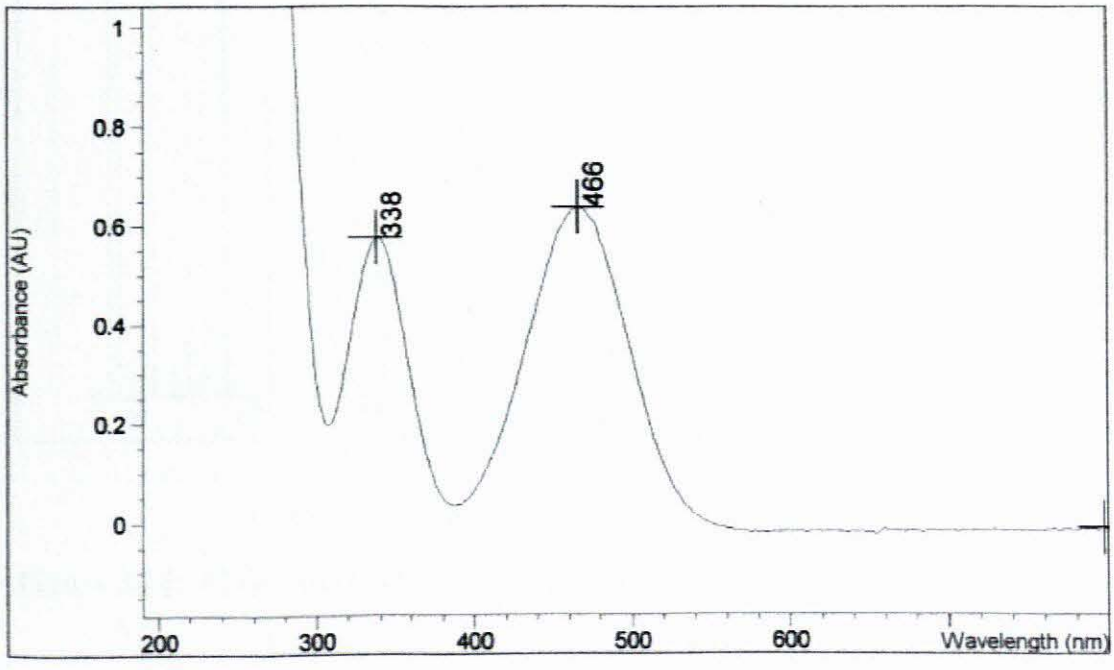

Figure 3.23: UV/Visible Absorption Spectrum of $[Co(en)_3]Cl_3$

3.3.2.4 Mass Spectrometry

Figure 3.24 shows the mass spectrum of the $Co(en)_3]Cl_3$ complex. The base peak occurs at m/z = 177 corresponding to the $[Co(en)_2]^+$ ion. The complex appears to lose two chloride ions (m/z = 309 and 273), followed by an ethylenediamine molecule (m/z = 213) and subsequently a third chloride ion (m/z = 177).

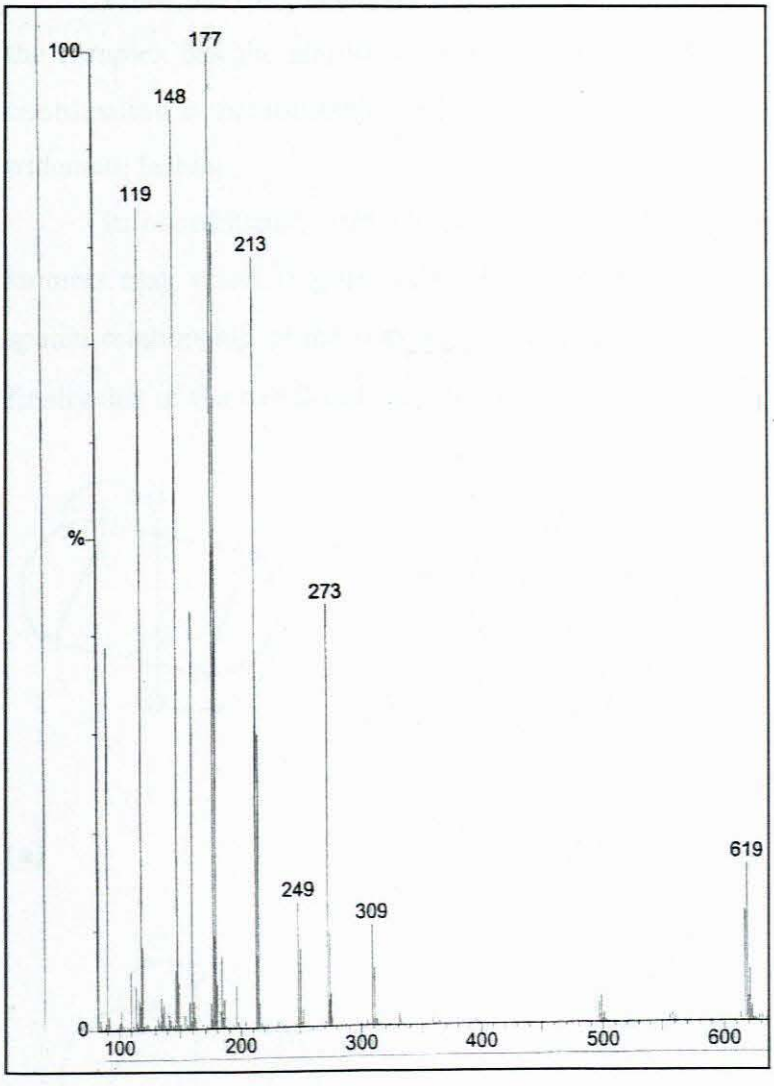

Figure 3.24: Mass Spectrum of $[Co(en)_3]Cl_3$

A summary of all data for the complexes formed from the reaction of *cis*-$[Co(en)_2Cl_2]Cl$ with lysine monohydrochloride is listed in the tables in Appendix A.

3.4 REACTION OF cis-$[Co(en)_2Cl_2]Cl$ WITH DL-2,3-DIAMINOPROPIONIC ACID MONOHYDROCHLORIDE

3.4.1 Complex 1 – $[Co(2,3\text{-}DAP)_2]I$

From the microanalysis and mass spectrometry data, it may be deduced that the complex has the empirical formula $CoC_6H_{14}N_4O_2I$. The only possible mode of coordination is that illustrated in Figure 3.25, within which the ligand coordinates in a tridentate fashion.

In coordination with DL-2,3-diaminopropionic acid, five possible geometric isomers may result (Figure 3.25). The isomers are named by considering first the spatial relationship of the two oxygen atoms, then of the two α-nitrogen atoms, and finally that of the two β-nitrogen atoms

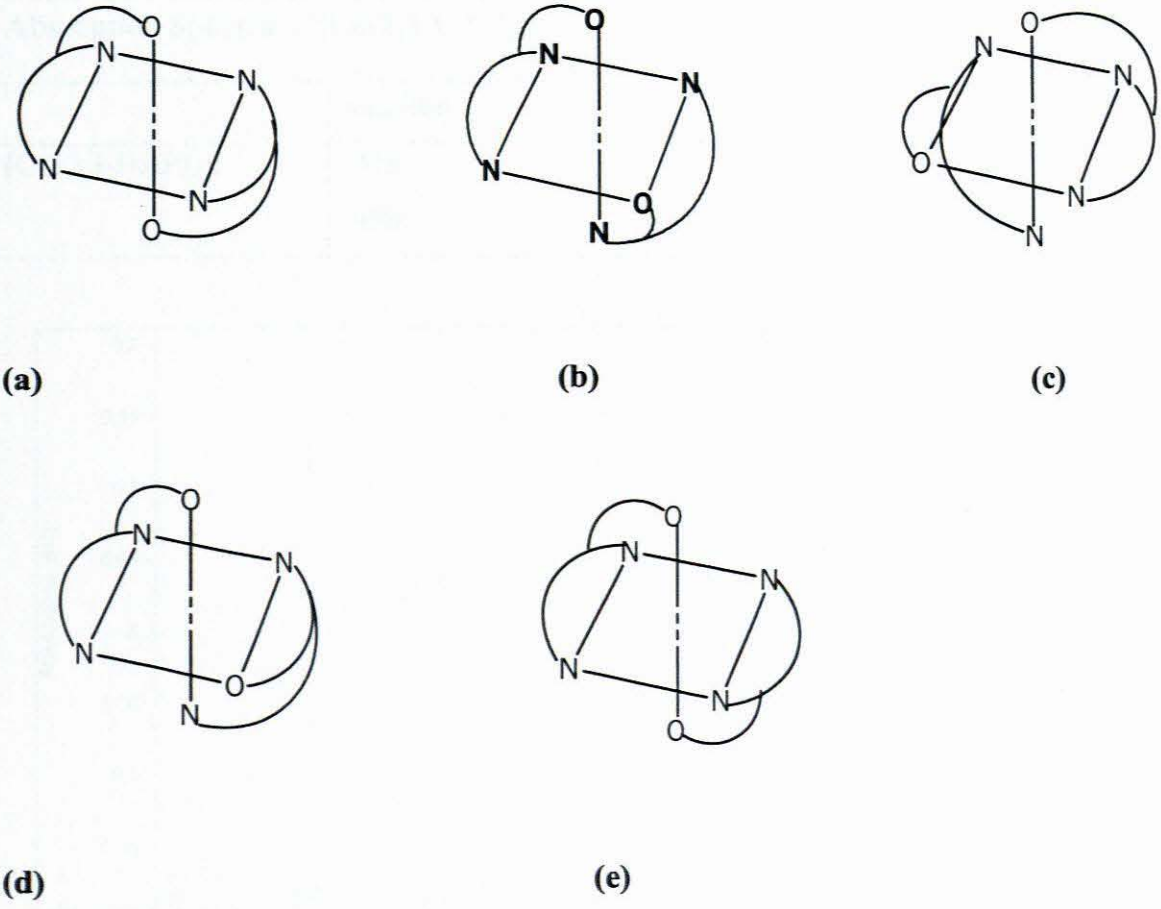

Figure 3.25: Geometrical isomers of bis(2,3-diaminopropionato)cobalt(III) ion
(a) ***trans, cis, cis*** **(b)** ***cis, cis, trans*** **(c)** ***cis, trans, cis*** **(d)** ***cis, cis, cis***
(e) ***trans, trans, trans***[35]

3.4.1.1 Electronic (UV-Visible) Spectroscopy

The UV/visible absorption spectrum of the complex $[Co(2,3\text{-}DAP)_2]I$ is shown in Figure 3.26. These isomers exhibit UV spectra that agree with crystal field considerations for *cis*- and *trans* isomers. Since the spectrum shows no shoulder on the high energy side of the long wavelength band in the visible spectrum, it can be deduced that the complex contain no *trans*-oxygens. Thus figures (a) and (e) are ruled out as possible isomers. The circular dichroism (CD) spectrum of the complex was not obtained and the complex was not resolved into optically pure isomers, therefore it was not possible to determine which of the *cis*-O isomers had been prepared. The bands in the visible spectrum are due to d-d transitions, of which the one at the longer wavelength appear to be due to the transition $^1A_{1g} \rightarrow {}^1T_{1g}(O_h)$ and the one at the shorter wavelength is due to the transition $^1A_{1g} \rightarrow {}^1T_{2g}(O_h)$.

Table 3.5: Absorption bands and Extinction Coefficients (ε) of UV/Visible Absorption Spectra of $[Co(2,3\text{-}DAP)_2]I$

	λ_{max}/nm	ε/mol^{-1}dm^{3}cm^{-1}
$[Co(2,3\text{-}DAP)_2]I$	348	41.5
	498	66.1

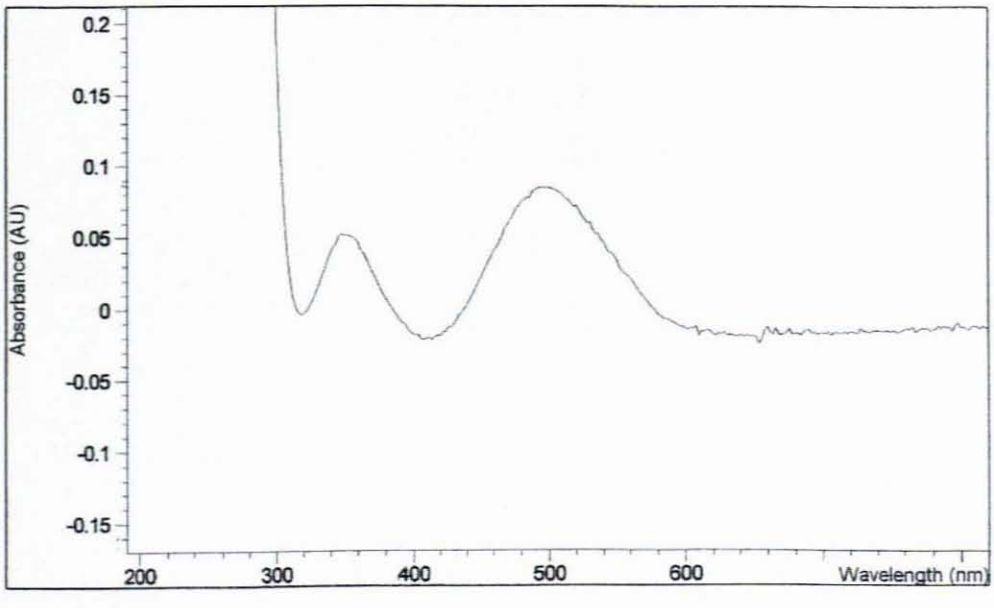

Figure 3.26: UV/Visible Absorption Spectrum of $[Co(2,3\text{-}DAP)_2]I$

3.4.1.2 Infrared Spectroscopy

Figure 3.27 depicts the IR spectrum of the complex $[Co(2,3\text{-}DAP)_2]I$. The sharp peak at 1666 cm^{-1} is indicative of the presence of coordinated carboxylate groups. The NH_2 stretching bands occur between 3100-3200 cm^{-1}. The peak at 438 cm^{-1} represents the ν(M-N) band whilst the M-O stretching mode is observed at 362 cm^{-1} [70] (Figure 3.27).

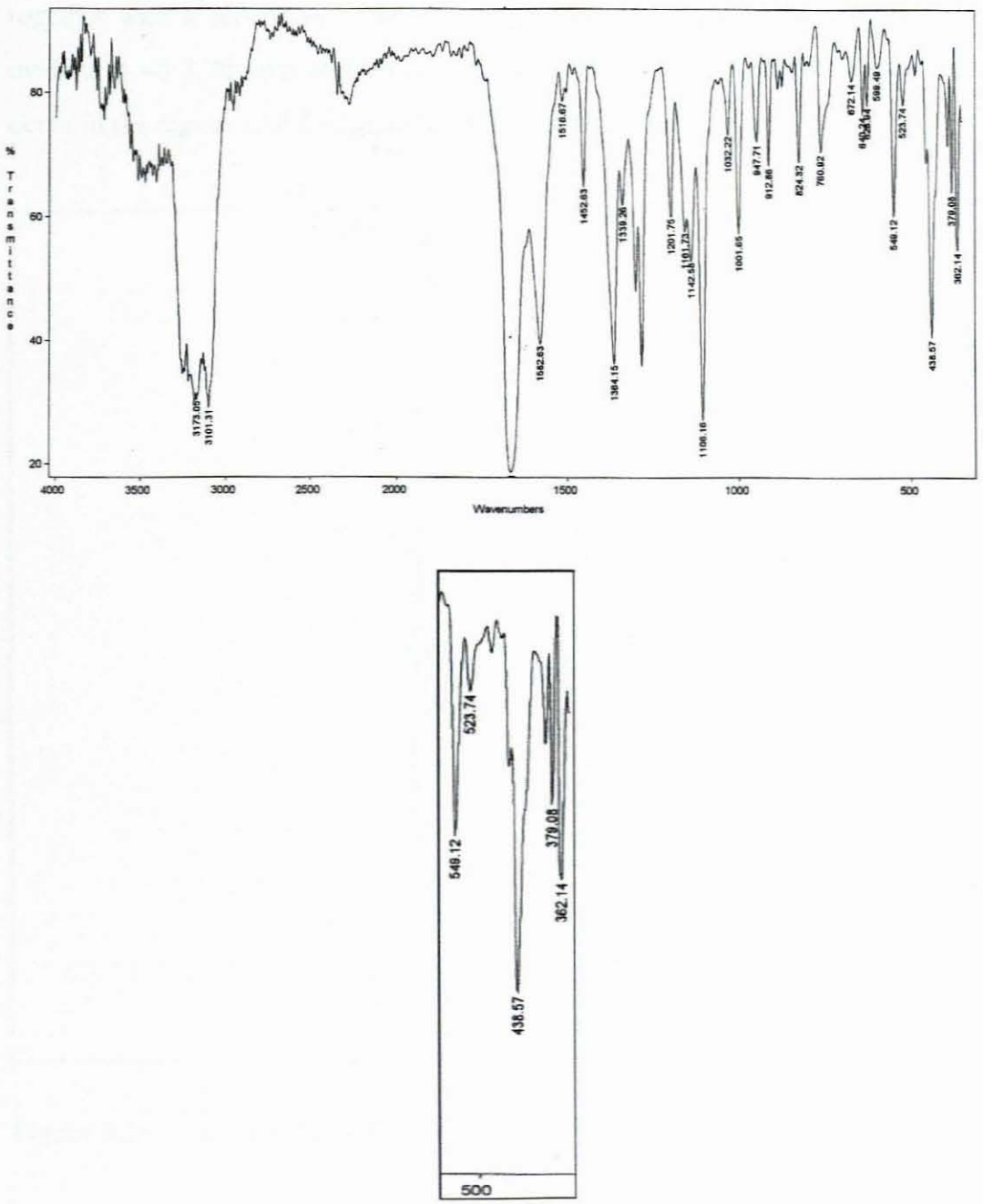

Figure 3.27: IR Spectrum of $[Co(2,3\text{-}DAP)_2]I$

3.4.1.3 NMR Spectroscopy

The ^{1}H NMR spectrum of [Co(2,3-DAP)$_2$]I is illustrated in Figure 3.28. The spectrum is very complicated since three of the *cis* isomers are possibly present. The ratio of the integration of the methylene protons to the methine protons of the amino acid are predicted to be 2:1 and a sets of doublet of doublets (splitting of the methylene protons by the methine protons) and sets of doublets (splitting of the methine protons by the methylene protons) should be present. In fact, three sets of doublet of doublets are observed, the first set between δ 2.84 ppm and δ 2.97 ppm together with a second set between δ 3.24 and δ 3.34 ppm. A set of doublets is evident at ~δ 3.70 ppm and ~δ 3.79 ppm. A further set of doublets may possibly occur in the region of δ 2.65 ppm but such a feature is poorly resolved.

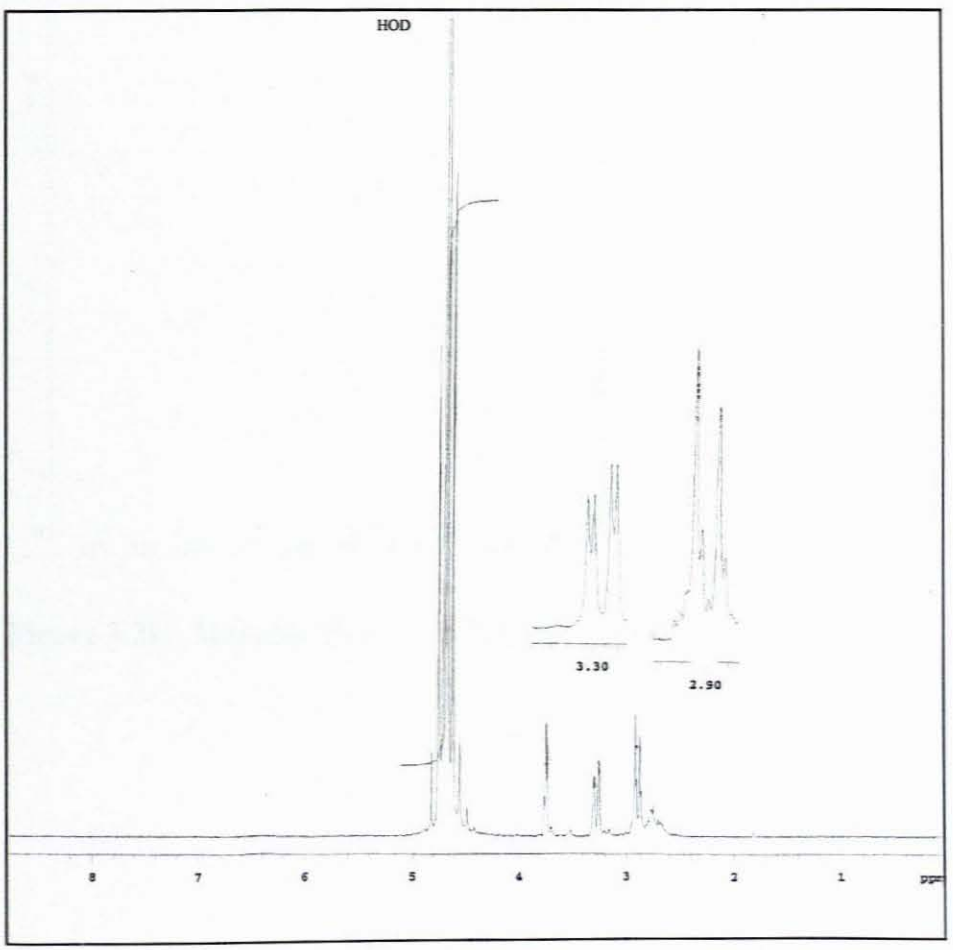

Figure 3.28: ^{1}H NMR Spectrum of [Co(2,3-DAP)$_2$]I

3.4.1.4 Mass Spectrometry

The mass spectrum of $[Co(2,3\text{-}DAP)_2]I$, as depicted in Figure 3.29, shows the base peak at m/z = 265. This appears to be due to the largest molecular ion, i.e. $[CoC_6H_{14}N_4O_2]^+$, which may confirm the proposed structure.

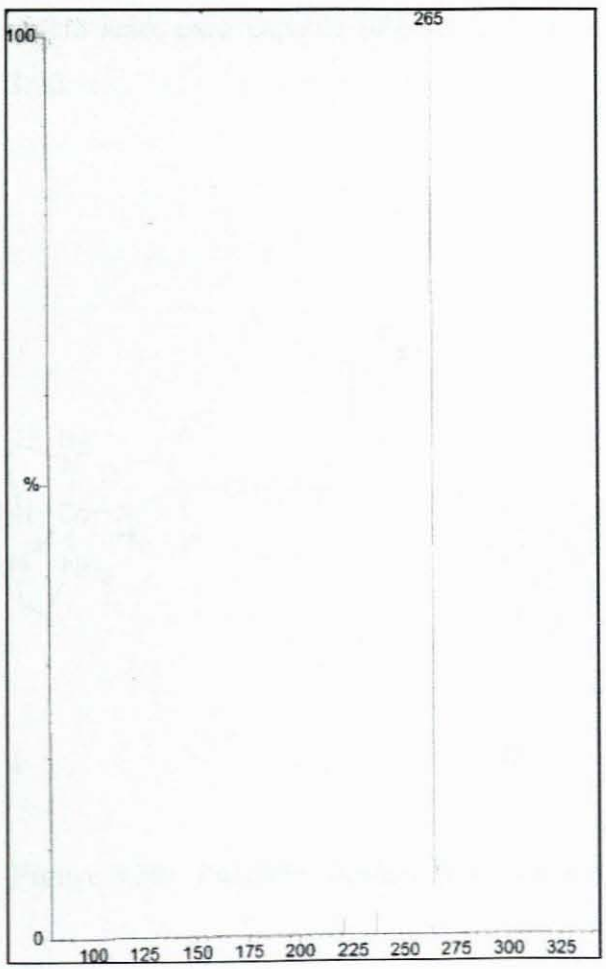

Figure 3.29: Mass Spectrum of $[Co(2,3\text{-}DAP)_2]I$

3.4.2 Complex 2 - $[Co(en)_2(2,3\text{-DAP})]I_2$

3.4.2.1 Stereochemistry of the System

Within the chelate system $[Co(en)_2(2,3\text{-DAP})]I_2$ there are three geometric isomers that could result from the different possible modes of coordination of the amino acid, each capable of existing in diastereoisomeric pairs as shown in Figure 3.30.

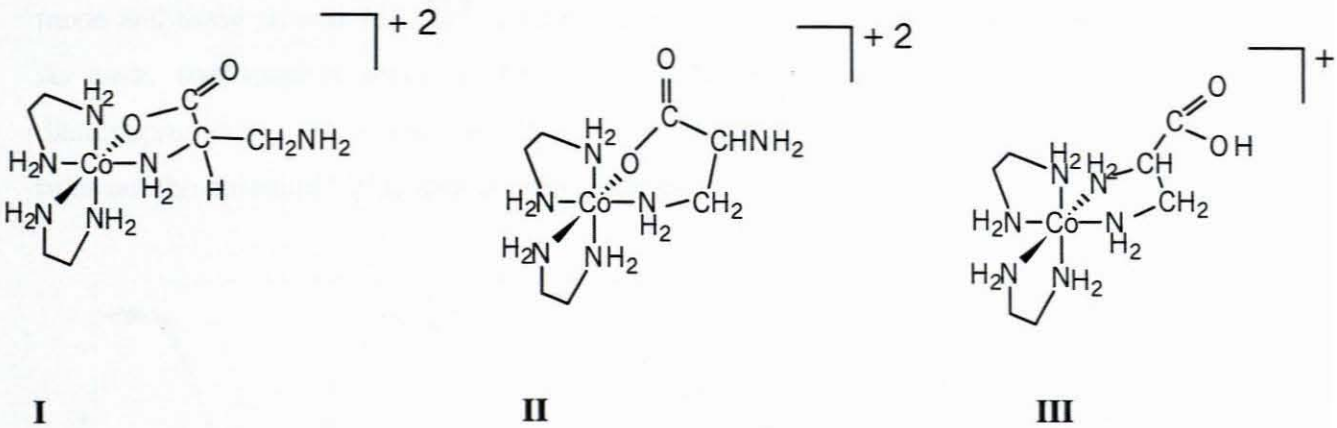

I **II** **III**

Figure 3.30: Possible Geometric Isomers of $[Co(en)_2(2,3\text{-DAP})]^{n+}$

Isomer I involves the formation of a five-membered chelate ring formed by the amino and α-carboxylate groups, thus rendering the ω-amino group uncoordinated. In the case of isomer II the six-membered ring is formed by the α-carboxylate group and the ω-amino group, leaving the α-amino group free. Within the structure of isomer III the ring is formed by both amino groups leaving the carboxylate groups free.

3.4.2.2 IR Spectroscopy

An intense C=O stretching band is observed at 1638 cm^{-1} in the infrared spectrum of $[Co(en)_2(2,3\text{-}DAP)]I_2$ (Figure 3.31). Such a band is typical of the presence of coordinated carboxylate groups[70]. The infrared spectrum of the free ligand shows the C=O stretching band at 1617 cm^{-1}, whereas the bands around 3200 cm^{-1} are consistent with the NH_2 stretching region. Comparison of the NH stretching region of the free ligand (Figure 3.32) with that of the complex, shows a marked difference in the wavenumbers. For the free ligand the NH stretching mode occurs as a broad band around 3100 cm^{-1}; the complex shows bands between 3100-3200 cm^{-1}. This may be due to both coordinated and uncoordinated amino groups within the structure of the complex. The band at 385 cm^{-1} is indicative of the M-O stretching mode and those around 454 cm^{-1} appear consistent with the M-N stretching mode[70]. As such, confirmation seems to be provided that the glycinate portion of 2,3-diaminopropionic acid is coordinated in the complex $[Co(en)_2(2,3\text{-}DAP)]I_2$, which rules out the possibility of isomer III being formed.

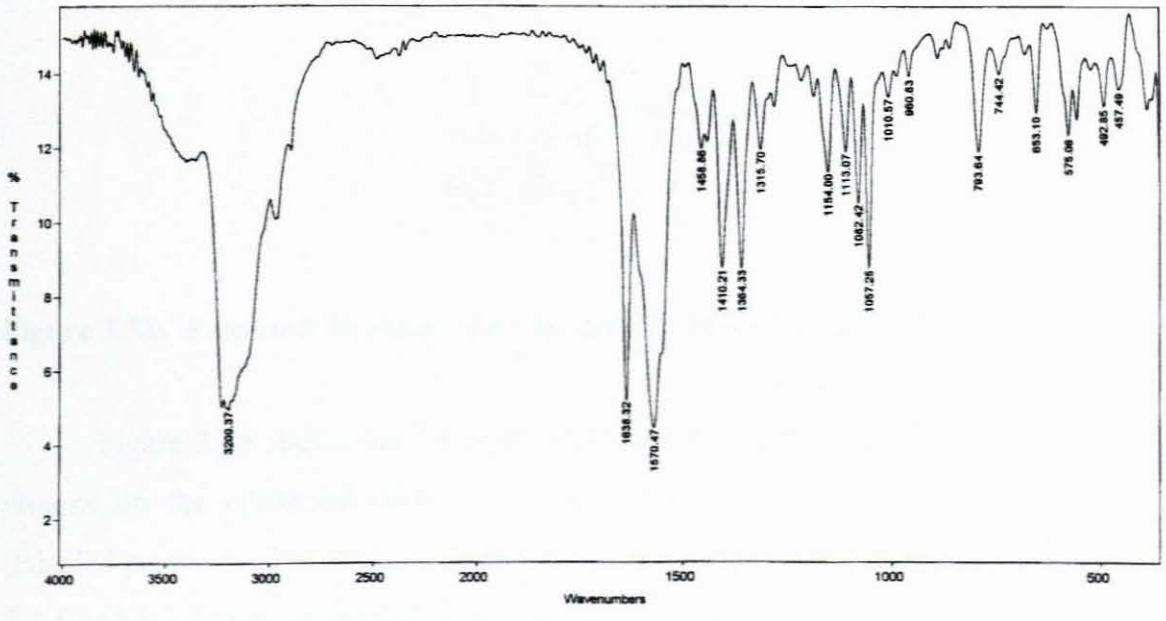

Figure 3.31: IR Spectrum of $[Co(en)_2(2,3\text{-}DAP)]I_2$

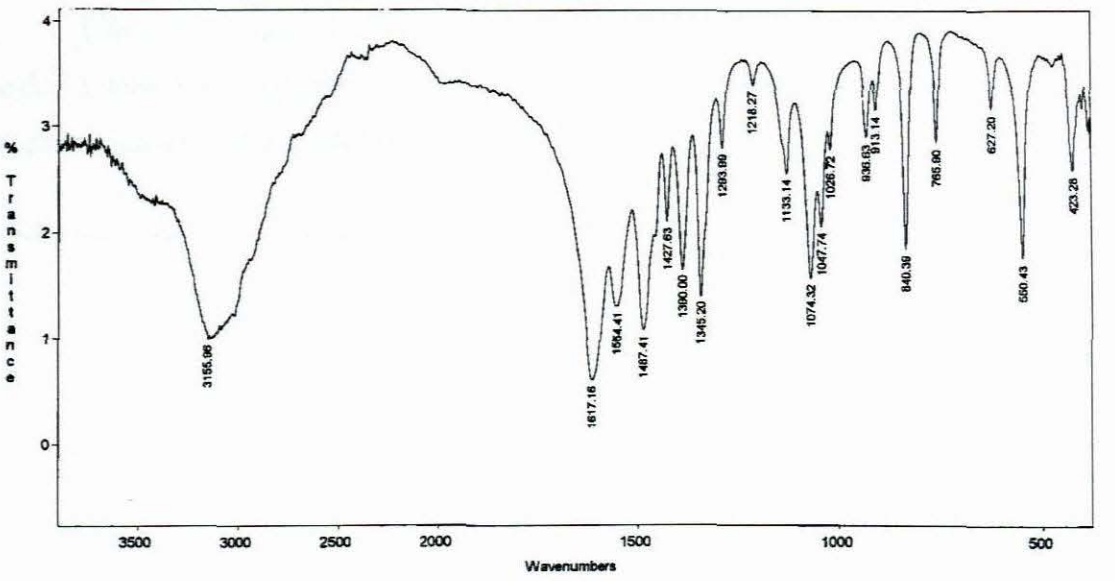

Figure 3.32: IR Spectrum of DL-2,3-Diaminopropionic Acid monohydrochloride

3.4.2.3 NMR Spectroscopy

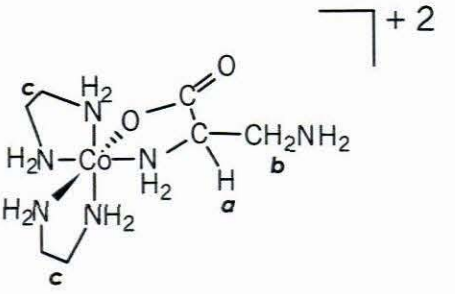

Figure 3.33: Proposed Structure for Complex 2 - $[Co(en)_2(2,3\text{-}DAP)]I_2$

Figure 3.34 shows the ^1H NMR spectrum of $[Co(en)_2(2,3\text{-}DAP)]I_2$. The 8 protons on the ethylenediamine backbone occur between δ 2.6 and δ 2.9 ppm (labelled proton c). The methine proton of an ABX system (proton a) occurs between δ 3.5 and δ 3.7 ppm, whilst the AB portion (proton b) is centred around δ 2.98 ppm. The methine proton should occur as a triplet but in this case is poorly defined. However, it has an integration of 1, enabling confirmation of the assignment. The similarity between the chemical shifts of the methylene protons in 2,3-diaminopropionic acid and those within the ethylenediamine ring, is due to the protons being in the same chemical environment, notably adjacent to the respective amino groups.

Figure 3.35 shows the ^{13}C NMR spectrum of $[Co(en)_2(2,3\text{-DAP})]I_2$. A pair of peaks is observed representing each carbon. This may indicate the presence of a racemic mixture of the complex.

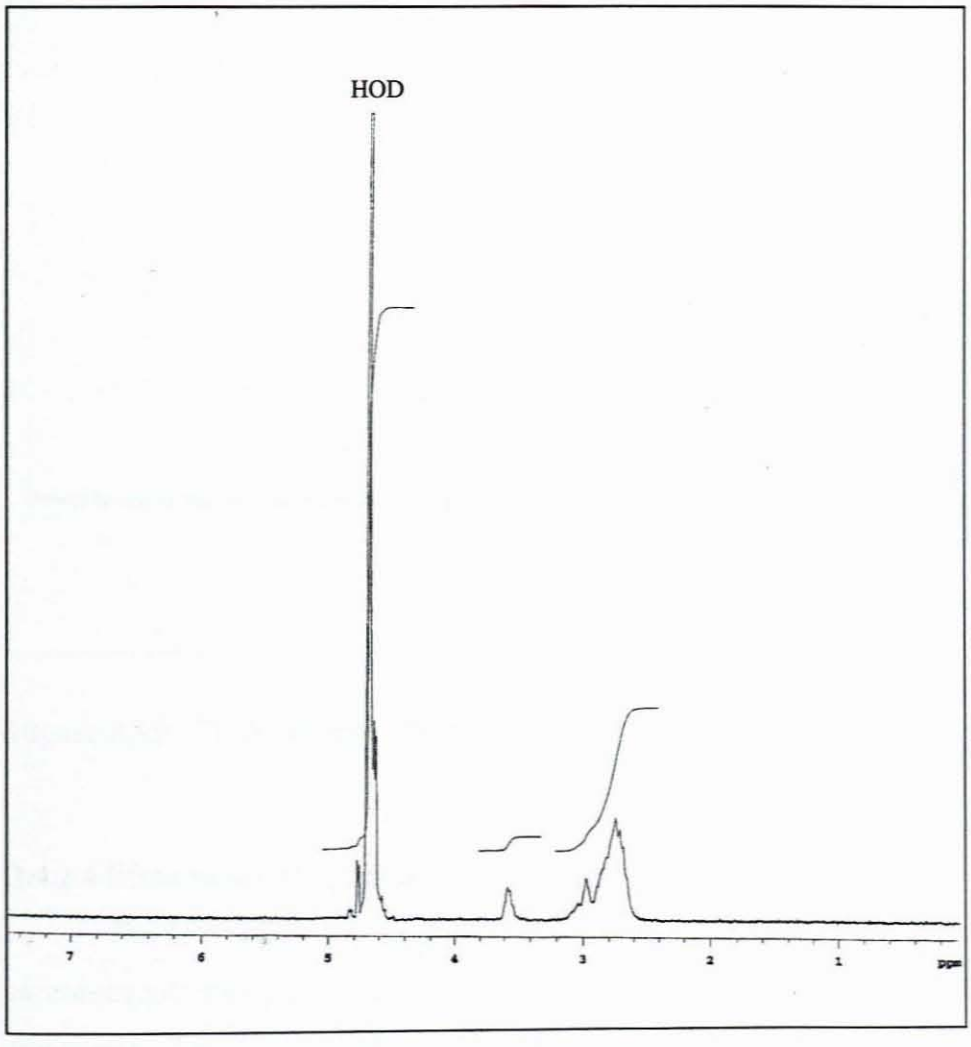

Figure 3.34: ^1H NMR Spectrum of $[Co(en)_2(2,3\text{-DAP})]I_2$

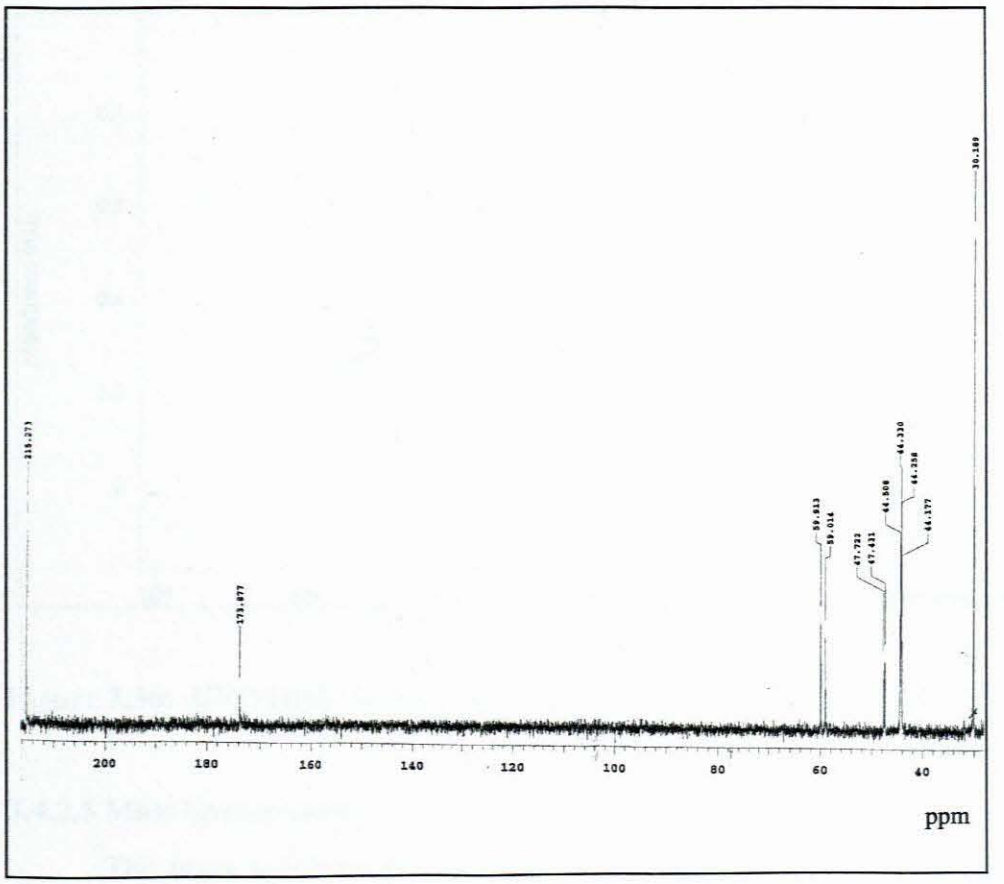

Figure 3.35: ^{13}C NMR Spectrum of $[Co(en)_2(2,3\text{-}DAP)]I_2$

3.4.2.4 Electronic (UV-Visible) Spectroscopy

The UV/visible spectrum of the $[Co(en)_2(2,3\text{-}DAP)]I_2$ complex (Figure 3.36) is consistent with the assigned structure. The pair of bands, attributable as d-d transitions, has been observed for the complex (Table 3.6). The peaks are symmetrical which indicates the absorption of the *cis* isomer. The λ_{max} in *cis*-$[Co(en)_2Cl_2]Cl$ is shifted towards shorter wavelengths as the chloride ligands are substituted for the carboxylate and amino groups, which is in accordance with the spectrochemical series.

Table 3.6: Absorption bands and Extinction Coefficients (ε) of UV/Visible Absorption Spectra of $[Co(en)_2(2,3\text{-}DAP)]I_2$

	λ_{max}/nm	ε/mol^{-1}dm^{3}cm^{-1}
$[Co(en)_2(2,3\text{-}DAP)]I_2$	338	77.3
	468	77.0

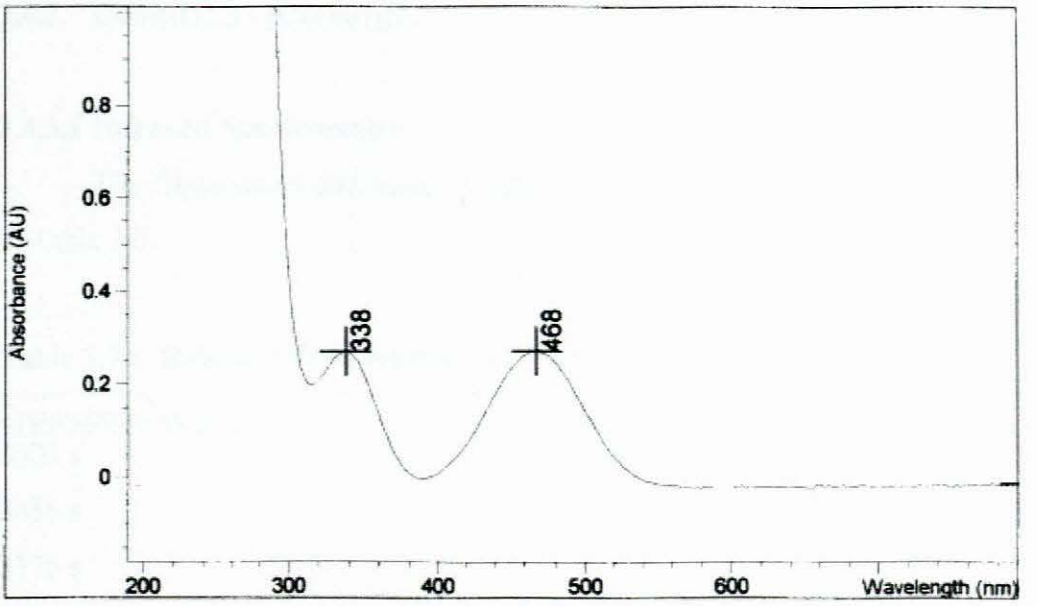

Figure 3.36: UV/Visible Absorption Spectrum of $[Co(en)_2(2,3\text{-DAP})]I_2$

3.4.2.5 Mass Spectrometry

The mass spectrum of $[Co(en)_2(2,3\text{-DAP})]I_2$ is represented in Figure 3.37. The base peak, unlike in the $[Co(en)_2(lys)]I_2$ complex, occurs at m/z = 177, corresponding to the $[Co(en)_2]^+$ ion. The peaks at m/z = 409 corresponds to the loss of one iodine atom, at m/z = 349 to a further loss of an ethylenediamine molecule, whilst the signal at m/z = 281 represents the $[Co(en)_2(2,3\text{-DAP})]^+$ ion and at that at m/z = 222 is consistent with the $[Co(en)(2,3\text{-DAP})]^+$ ion.

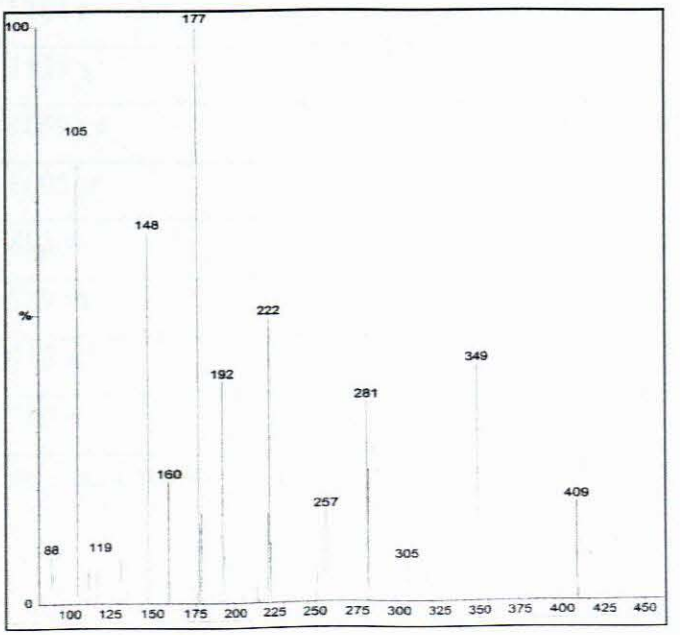

Figure 3.37: Mass Spectrum of $[Co(en)_2(2,3\text{-DAP})]I_2$

3.4.3 Complex 3 - $[Co(en)_3]I_3$

3.4.3.1 Infrared Spectroscopy

The frequencies and band assignments for the $[Co(en)_3]I_3$ complex are listed in Table 3.7.

Table 3.7 : Relevant Frequencies (cm^{-1}) of $[Co(en)_3]I_3$

Frequencies (cm^{-1})	Assignments
3503 **s** 3456 **s** 3175 **s** 3103 **s**	N-H stretching
1624 **vs**	N-H asymmetric deformation
1595 **m**	
1538 **m**	
1465 **s**	CH_2 bending
1364 **s**	
1327 **s**	CH_2 wagging
1281 **m**	
1254 **m** 1164 **s**	N-H asymmetric deformation
1125 **s**	
1059 **vs**	C-C / C-N stretching
1005 **w**	
895 **w**	CH_2 rocking
789 **vs**	N-H symmetric deformation
712 **w**	
580 **w**	

vs = very strong **s** = strong **m** = medium **w** = weak

3.4.3.2 NMR Spectroscopy

The ^{1}H NMR spectrum of $[Co(en)_3]I_3$ (Figure 3.38) reveals a characteristic single broad resonance band between δ 2.58 and δ 2.98 ppm, indicative of the protons of the CH_2 groups within the ethylenediamine ring. The ^{13}C NMR spectrum (Fig. 3.39) appears to confirm the proposed structure with a single peak at ~δ 44 ppm representing the chemically equivalent carbon atoms.

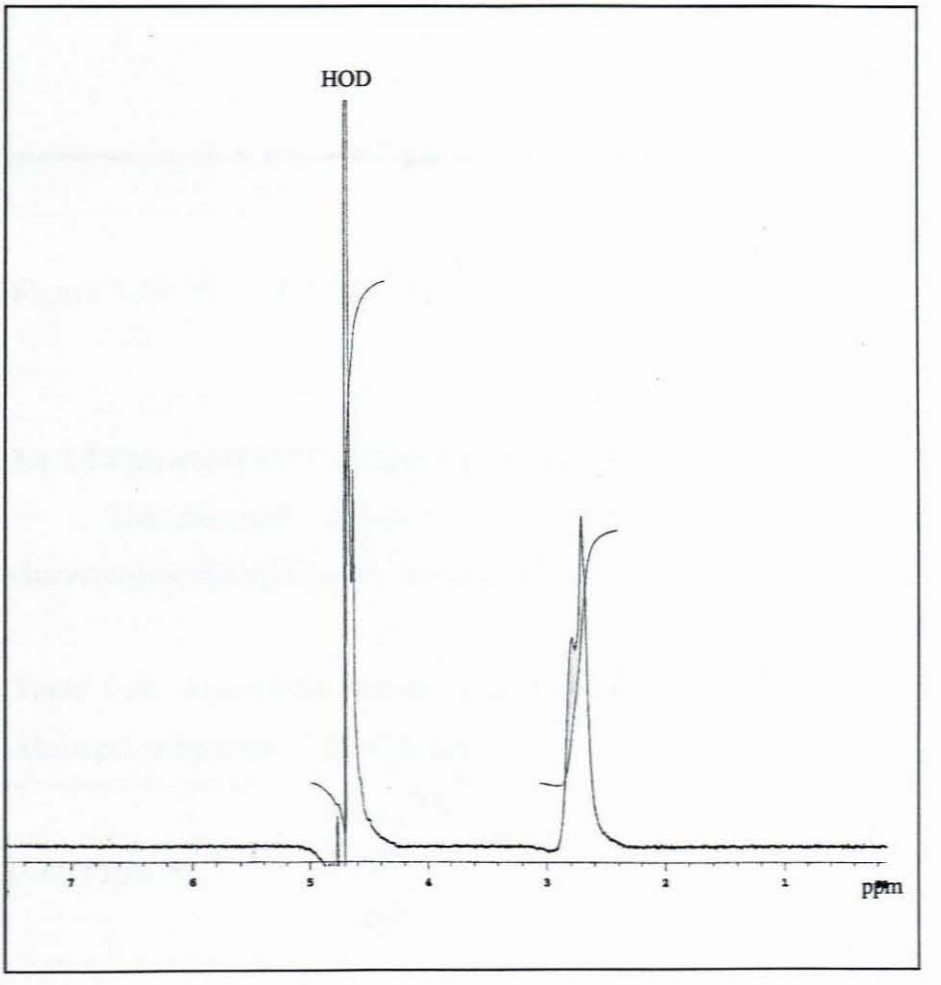

Figure 3.38: ^{1}H NMR Spectrum of $[Co(en)_3]I_3$

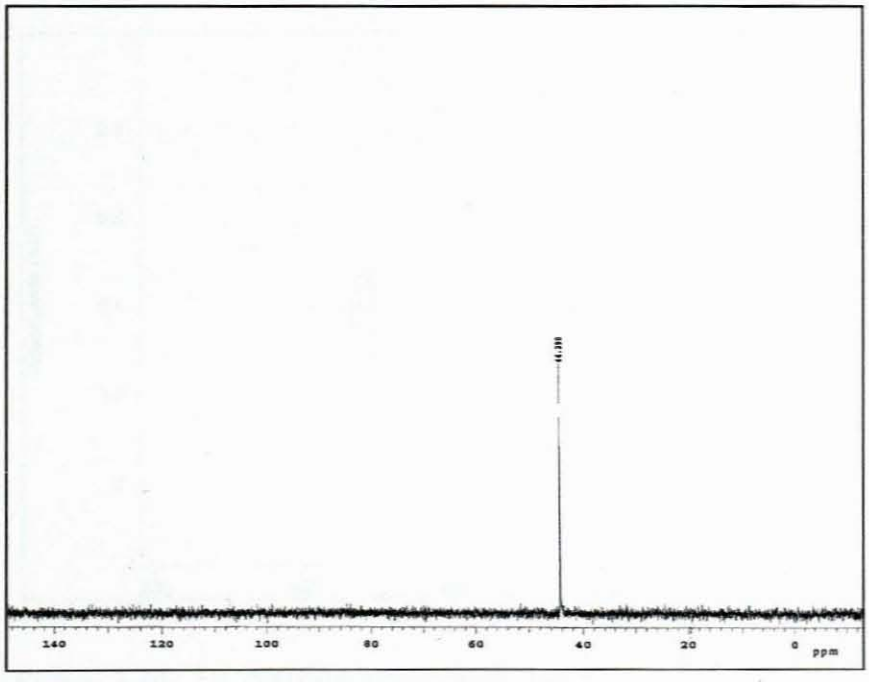

Figure 3.39: ^{13}C NMR Spectrum of $[Co(en)_3]I_3$

3.4.3.3 Electronic (UV-Visible) Spectroscopy

The electronic spectrum of $[Co(en)_3]I_3$ is shown in Figure 3.40. The characteristic absorptions are listed below.

Table 3.8: Absorption bands and Extinction Coefficients (ε) of UV/Visible Absorption Spectra of $[Co(en)_3]I_3$

	λ_{max}/nm	ε/mol^{-1}dm^{3}cm^{-1}
$[Co(en)_3]I_3$	334	89.6
	466	79.1

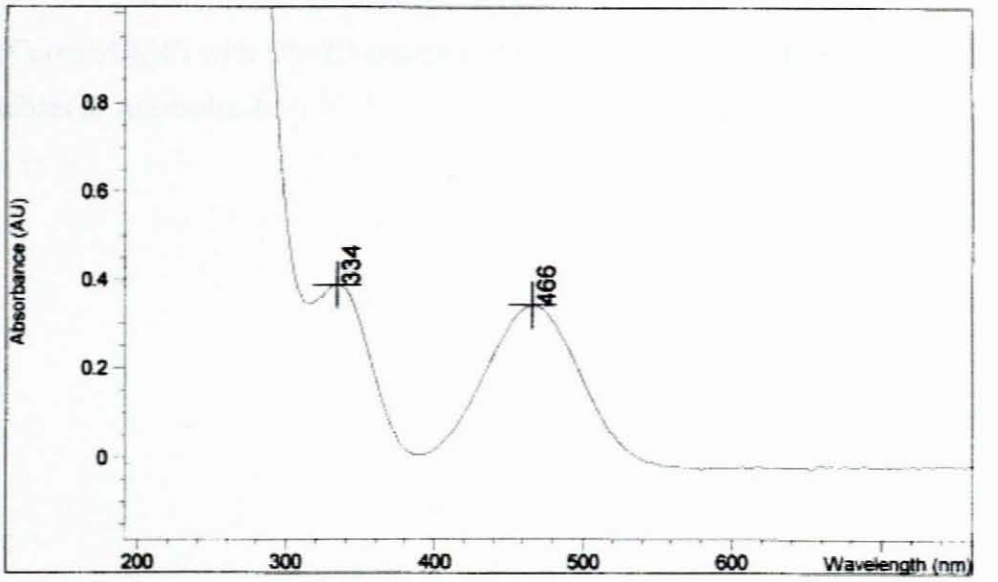

Figure 3.40: UV/Visible Absorption Spectrum of $[Co(en)_3]I_3$

3.4.3.3 Mass Spectrometry

Figure 3.41 depicts the mass spectrum of $[Co(en)_3]I_3$, with the base peak appearing at m/z = 179, corresponding to the $[Co(en)_2]^+$ ion.

The splitting pattern indicates the loss of one iodine atom (m/z = 493), followed by the loss of an ethylenediamine molecule (m/z = 432), then the remaining two iodine atoms (m/z = 305 and m/z = 178). Furthermore, the loss of a second molecule of ethylenediamine appears to corresponds to a peak at m/z = 119.

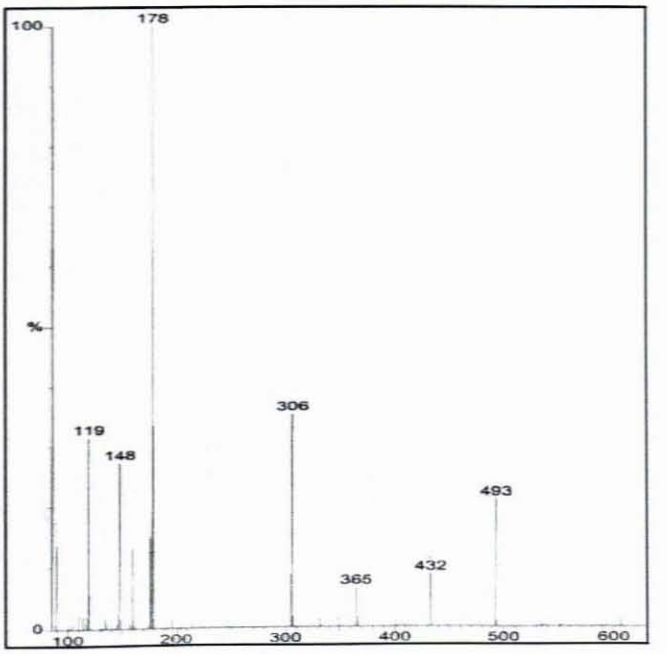

Figure 3.41: Mass Spectrum of $[Co(en)_3]I_3$

A summary of all data for the complexes formed from the reaction of *cis*-$[Co(en)_2Cl_2]Cl$ with DL-2,3-diaminopropionic acid monohydrochloride is listed in the tables in Appendix A.

3.5 THE PREPARATION OF THE [Co(2,3-DAP)$_2$]Cl COMPLEX

From the electronic spectra, which is discussed in section 3.5.3, it was deduced that the complex, [Co(2,3-DAP)$_2$]Cl, has no trans oxgens. Figure 3.42 illustrates the possible isomers that may have been isolated.

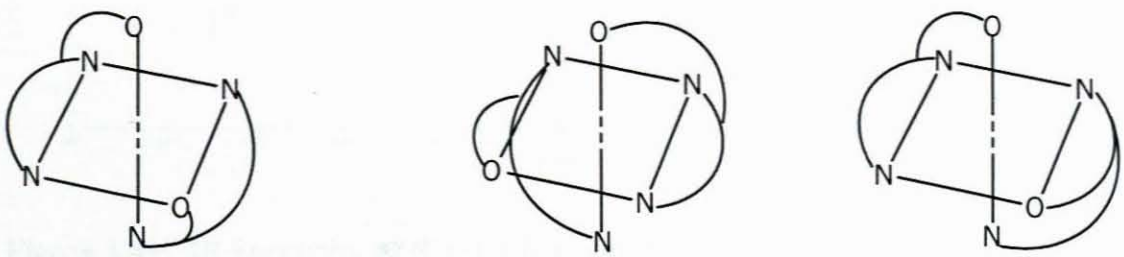

Fig 3.42: Possible Isomers of [Co(2,3-DAP)$_2$]Cl

3.5.1 Infrared Spectroscopy

Figure 3.43 shows the IR spectrum of [Co(2,3-DAP)$_2$]Cl. At 1669 cm^{-1}, a C-O stretching band is observed, a feature which is typical of coordinated carboxylate groups. The ν(C-O) band occurs at ~1620 cm^{-1} in the free ligand (Figure 3.32). The N-H stretching region occurs between 3100 and 3300 cm^{-1}, whilst the strong band at 441 cm^{-1} represents the M-N stretching mode.

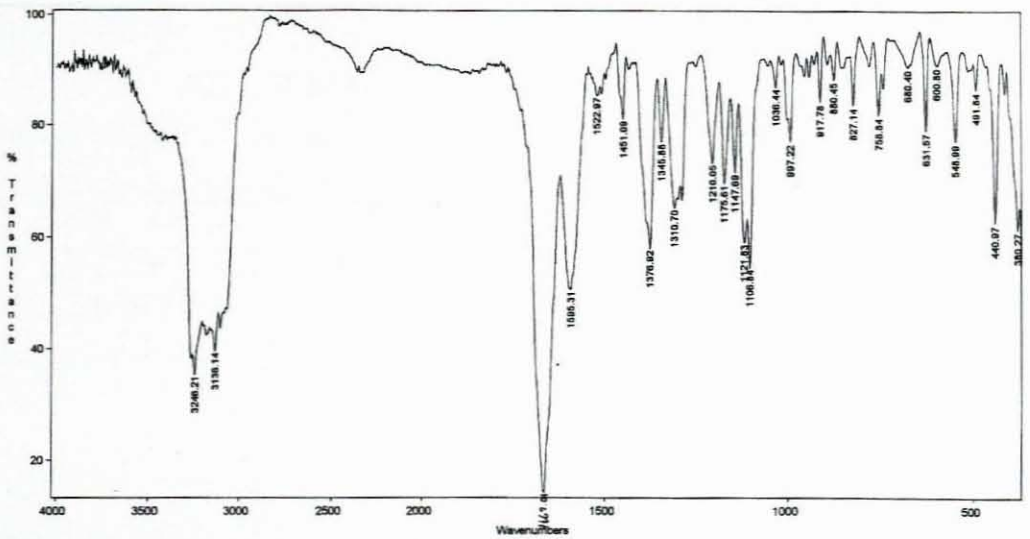

Figure 3.43: IR Spectrum of [Co(2,3-DAP)$_2$]Cl

3.5.2 NMR Spectroscopy

From the ^{13}C spectrum of [Co(2,3-DAP)$_2$]Cl (Figure 3.44), it may be deduced three isomers are present. Three peaks are observed at ~δ 180 ppm representing the carboxylate groups, whilst two sets of three peaks, representing the methylene and methine carbons, are present at ~δ 44 ppm and ~δ 62 ppm, respectively. From the ^{1}H NMR spectrum (Figure 3.45), three sets of doublets are seen at δ 3.75 ppm, δ 3.52 ppm and δ 2.69 ppm together with one well defined doublet of doublets at δ 2.90 ppm. A further doublet of doublets occurs at δ 3.27 ppm, but is only apparent in the expanded spectrum.

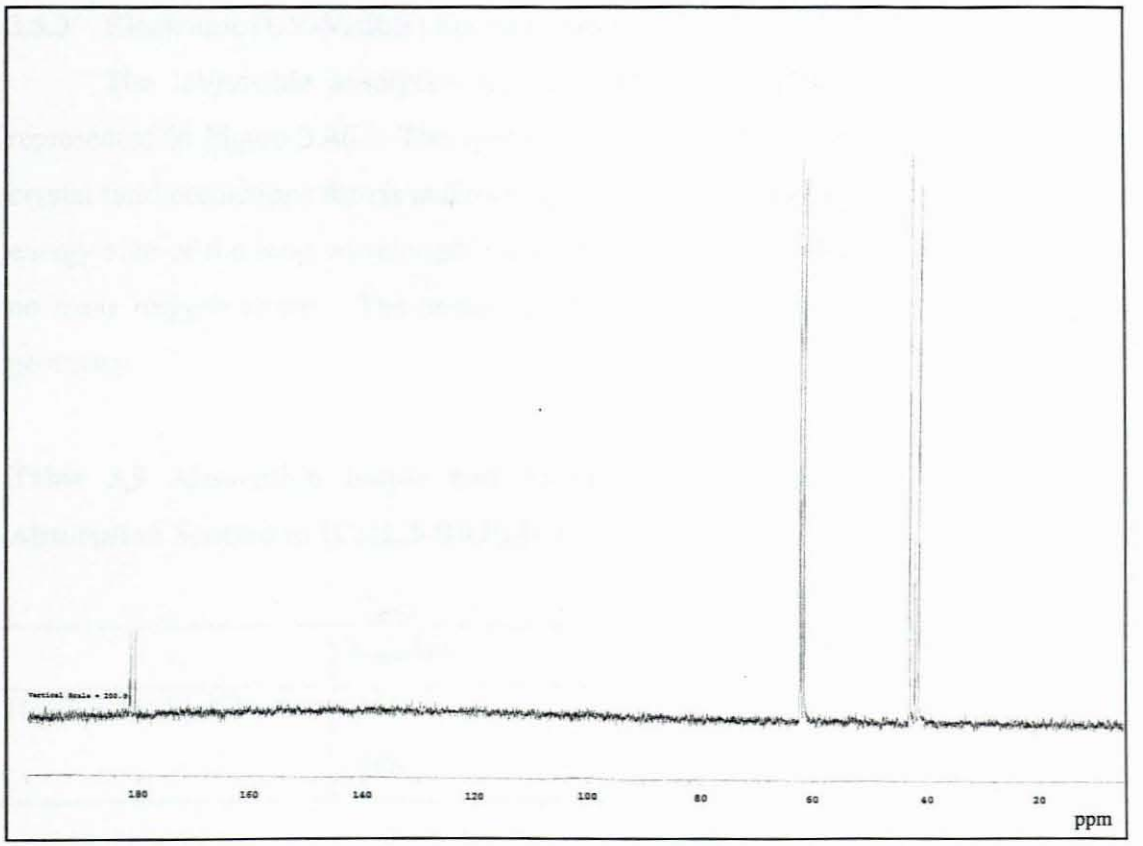

Figure 3.44: ^{13}C NMR Spectrum of [Co(2,3-DAP)$_2$]Cl

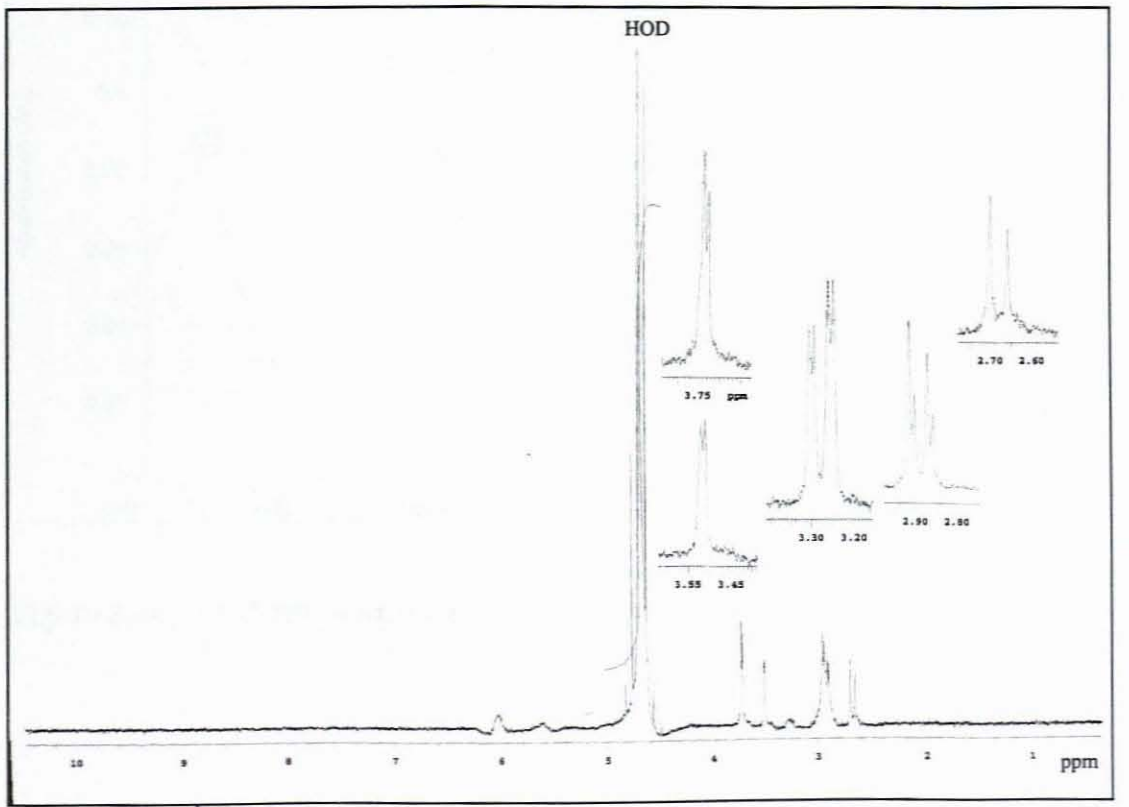

Figure 3.45: ^{1}NMR Spectrum of [Co(2,3-DAP)$_2$]Cl

3.5.3 Electronic (UV-Visible) Spectroscopy

The UV/visible absorption spectrum of the complex $[Co(2,3\text{-}DAP)_2]Cl$ is represented in Figure 3.46 . The spectrum is in agreement with that expected from crystal field predictions for *cis* and *trans* isomers. No shoulder is observed on the high energy side of the long wavelength band, thus it is deduced that the isomer contains no *trans* oxygen atoms. The peaks are, however, symmetrical confirming the *cis* geometry.

Table 3.9 Absorption bands and Extinction Coefficients (ε) of UV/Visible Absorption Spectra of $[Co(2,3\text{-}DAP)_2]Cl$

	λ_{max}/nm	ε/mol^{-1}dm^{3}cm^{-1}
$[Co(2,3\text{-}DAP)_2]Cl$	348	42.9
	498	67.3

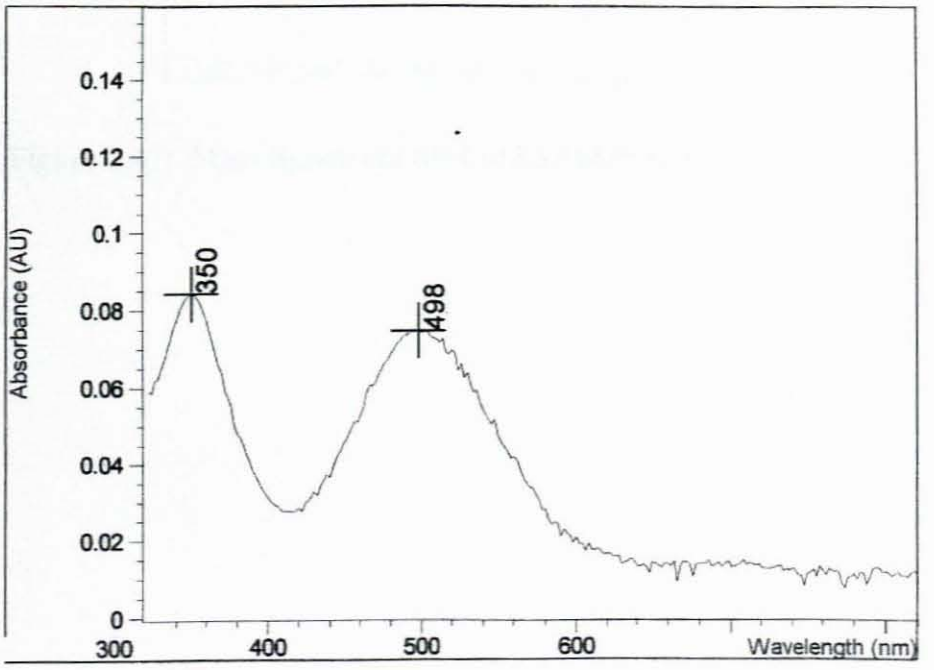

Figure 3.46: UV/Visible Absorption Spectrum of $[Co(2,3\text{-}DAP)_2]Cl$

3.5.4 Mass Spectrometry

The largest molecular ion in the complex $[Co(2,3\text{-}DAP)_2]Cl$ corresponds to $[CoC_6H_{14}N_4O_2]^+$. The mass spectrum of $[Co(2,3\text{-}DAP)_2]Cl$, as depicted in Figure 3.47, shows the most intense peak at m/z = 265. This seems to confirm the proposed structure (Figure 3.42).

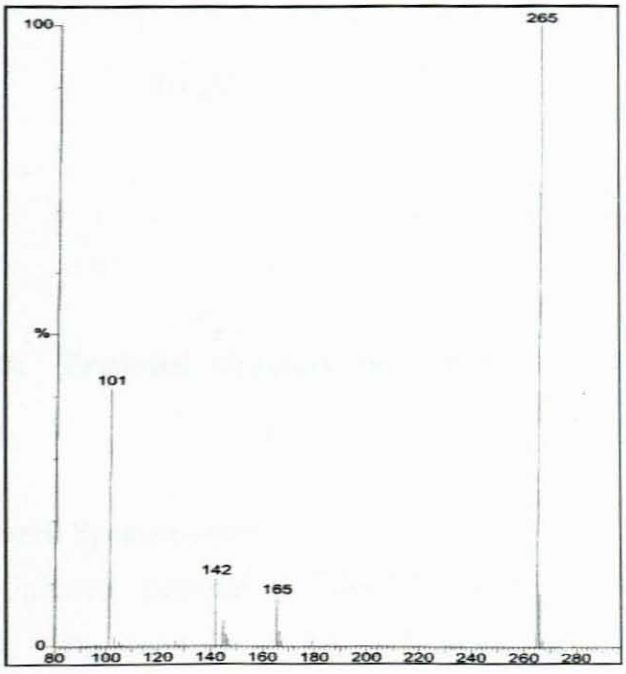

Figure 3.47: Mass Spectrum of $[Co(2,3\text{-}DAP)_2]Cl$

3.6 THE PREPARATION OF THE *trans*- [Co(2,3-DAP)(2,3-DAPH)Cl_2] COMPLEX

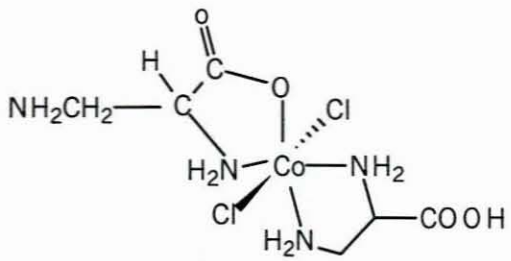

Figure 3.48: Proposed structure for the *trans*-[Co(2,3-DAP)(2,3-DAPH)Cl_2] complex

3.6.1 Infrared Spectroscopy

The infrared spectrum of *trans*-[Co(2,3-DAP)(2,3-DAPH)Cl_2] is shown in Figure 3.49. The band at ~1707 cm^{-1} represents the stretching mode of the uncoordinated and unionised C=O group[70]. There is also a peak at 1655 cm^{-1}, which is typical of coordinated carboxylate groups. Thus it may be deduced that one of the ligands bond to the cobalt via the glycinate portion and the other ligand coordinates through both amino groups. The two bands of approximately equal intensity around 3200 cm^{-1} represent the N-H stretching mode. The band at 1584 cm^{-1} is characteristic of the N-H bending vibration. The band at 1426 cm^{-1} represents the CH_2 bend, the band at 1354 cm^{-1} the CH_2 wag, and at 944 cm^{-1} the CH_2 rock. The sharp band at 1080 cm^{-1} represents the C-N stretching vibration.

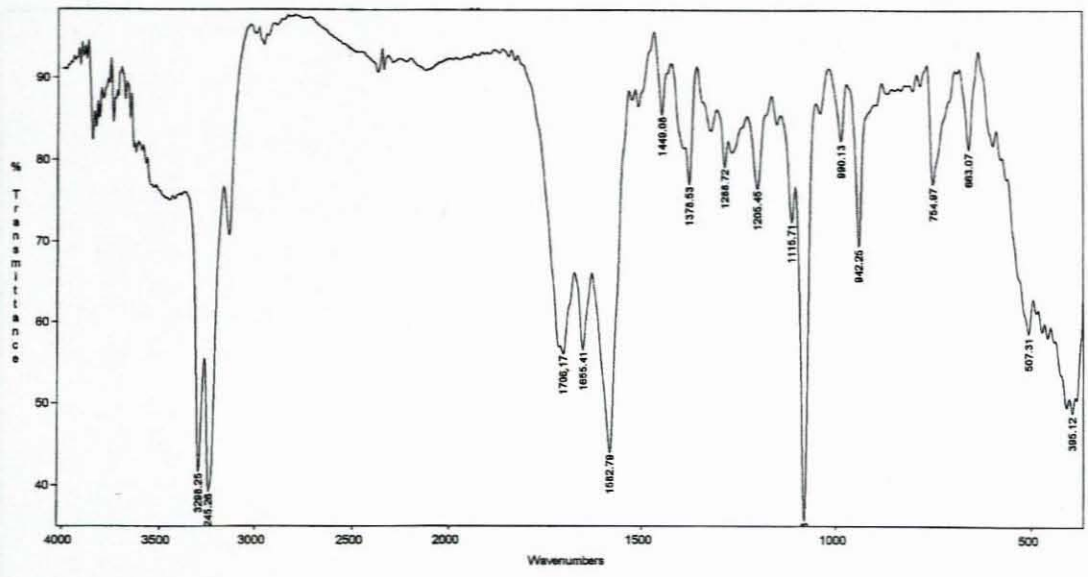

Figure 3.49: IR Spectrum of *trans*- [Co(2,3-DAP)(2,3-DAPH)Cl_2]

3.6.2 NMR Spectroscopy

From the ^{13}C NMR spectrum, illustrated in Figure 3.50, we observe pairs of peaks at ~δ 170 ppm , ~δ 59 ppm and ~δ 54 ppm. These represent the carbon atoms of the carboxylate groups, the methylene groups and the methine groups of each ligand, respectively. The solid state ^{13}C NMR spectrum is shown in Figure 3.51. Again, signals are observed at ~δ170 ppm , ~δ 59 ppm and ~δ 54 ppm.

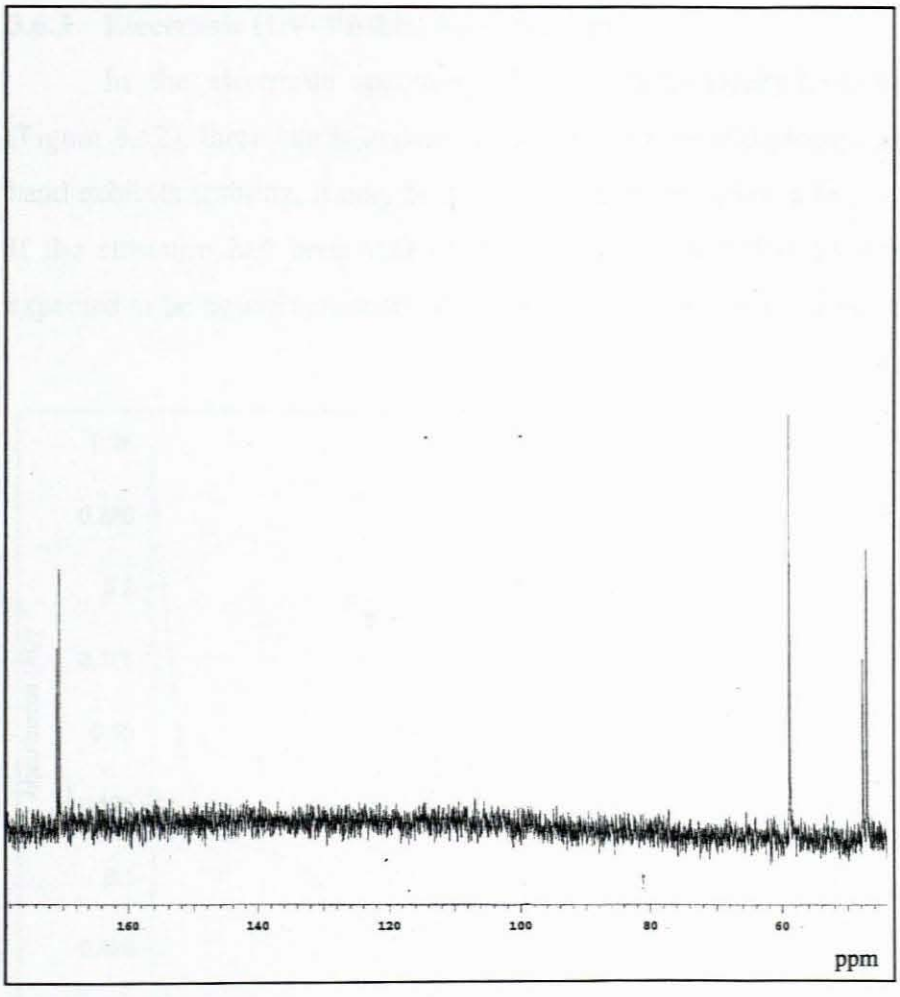

Figure 3.50: ^{13}C NMR Spectrum of *trans*- [Co(2,3-DAP)(2,3-DAPH)Cl_2]

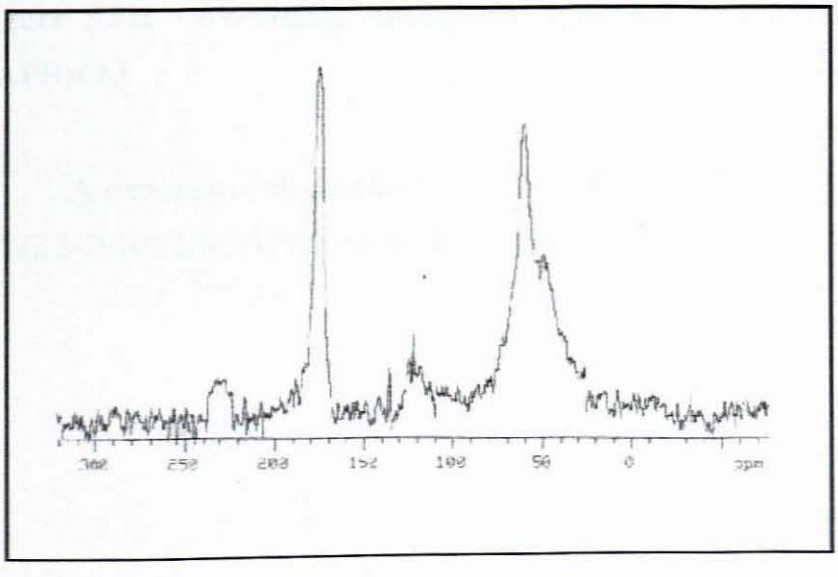

Figure 3.51: Solid State ^{13}C NMR Spectrum of *trans*- [Co(2,3-DAP)(2,3-DAPH)Cl_2]

3.6.3 Electronic (UV-Visible) Spectroscopy

In the electronic spectrum of the [Co(2,3-DAP)(2,3-DAPH)Cl_2] complex (Figure 3.52), three bands appear, attributable to the d-d absorption. Since the $^1T_{1g}$ band exhibits splitting, it may be deduced that the complex is in fact the *trans* isomer. If the structure had been that of the *cis* isomer, the first band would have been expected to be nearly symmetrical, and the second band around 600 nm, very intense.

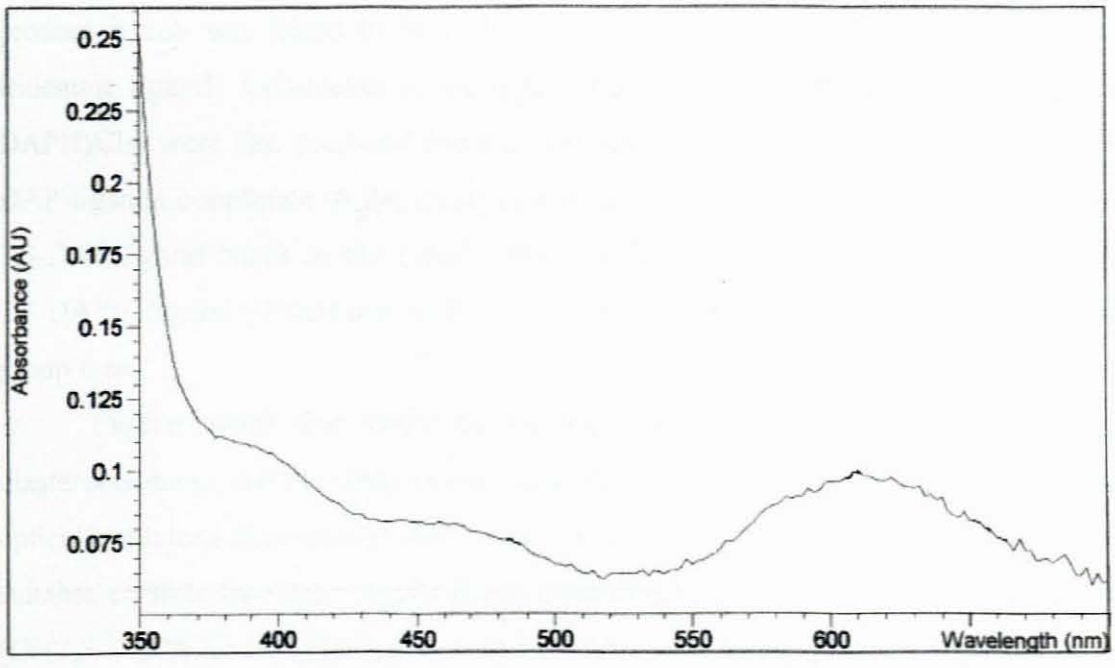

Figure 3.52: UV/Visible Absorption Spectrum of *trans*- [Co(2,3-DAP)(2,3-DAPH)Cl_2]

A summary of all data for the complexes [Co(2,3-$DAP)_2$]Cl and [Co(2,3-DAP)(2,3-DAPH)Cl_2] is listed in the tables in Appendix A.

CONCLUSION

It was found that in complexes of the type $[Co(en)_2AA]^+$, where AA = lysine and DL-2,3-DAPH, the amino acid coordinated in a bidentate fashion with the α-amino and carboxylate groups, leaving the ω- amino group uncoordinated. The byproduct formed in the reaction of $[Co(en)_2Cl_2]Cl$ with the amino acids, is $[Co(en)_3]^+$. Reaction of $[Co(en)_2Cl_2]Cl$ with DL-2,3-DAPH yielded an additional product which was found to be $[Co(2,3\text{-}DAP)_2]^+$, where DL-2,3-DAP bonds as a tridentate ligand. Complexes of the type $[Co(2,3\text{-}DAP)_2]Cl$ and $[Co(2,3\text{-}DAP)(2,3\text{-}DAPH)Cl_2]$ were also prepared and characterised. In the former case, the two 2,3-DAP ligands coordinate to the metal in a tridentate fashion whilst in the latter, one 2,3-DAP ligand bonds to the metal centre via the glycinate portion and the second 2,3-DAPH ligand coordinates with both amino groups leaving the carboxylic acid group free.

Further work that could be carried out, includes the resolution of the diastereoisomers, and the study of the stereochemistry by circular dichroism (CD) and optically rotatory dispersion (ORD). Also, additional attempts could be made to grow suitable crystals for single crystal X-ray crystallography. For complexes of the type $[Co(2,3\text{-}DAP)(2,3\text{-}DAPH)Cl_2]$, one could endeavour to synthesise the complex to achieve CoN4 coordination or CoN_2O_2 coordination. One could also attempt synthesis of complexes of the trichlorodiethylenetriaminecobalt(III) ion with α-ω-diaminocarboxylic acids. It would be interesting to note, in the latter instance, whether all three available coordination sites will be utilised in chelation.

REFERENCES

1. S.T Chow and C.A. McAuliffe, Transition Metal Complexes Containing Tridentate Amino Acids: In Progresses in Inorganic Chemistry, Vol. 19; S.J Lippard (Ed.) (1975) and therein.
2. E. K. Chong, J.M Harrowfield, W.G. Jackson, A.M. Sargeson and J. Springborg, J., *J. Am. Chem. Soc.*, 1985, **107**, 2015.
3. C.J. Boreham, D.A. Buckingham and F.R. Keene, *J. Am. Chem. Soc.*,1979, **101**, 1409.
4. J.I. Legg and J. Steele, *J. Inorg. Chem.,* 1971, **10**,2177
5. D.A. Buckingham and J.P. Collman, *Inorg. Chem.*, 1967, **6**, 1803.
6. S.K. Hall and B.E. Douglas, *Inorg. Chem.*,1969, **8**, 372.
7. J. Meisenheimer, *Ann.,* 1924, **438**, 217.
8. C.T. Liu and B.E. Douglas, *Inorg. Chem.*,1964, **3**,10, 372.
9. D.A. Buckingham, L. Durham and A.M. Sargeson, *Aust. J. Chem*, 1967, **20**, 257.
10. M. Saburi, M. Homma and S.Yoshikawa, *Inorg. Chem.*,1960, **8**, 36.
11. D.A. Alexander and D.H. Busch, *Inorg. Chem.*,1966, **5**, 9,1590.
12. E. Dreschel, *J.Prakt. Chem*, 1889, **39**, 425.
13. E. Schulze and E. Winterstein, *Chem. Ber.*, 1899, **32**, 3191.
14. V.Dessaignes, *Compt. Rend.*, 1850, 30,324.
15. L.N. Vanquelin and P.J. Robiquet, *Ann. Chim*, 1806, 57,88.
16. H. Ritthausan, *J.Prakt. Chem*, 1866, **99**, 454.
17. L. Wolff, *Ann. Chem.*, 1890, **260**, 79.
18. K.M. Wellman, S. Bogdansky, W.Mungall, T.G. Mecca and C.R. Hare, *Tetrahedron Lett.*, 1967, **37**, 3607.
19. E.Dreschel, *Chem. Ber.*, 1890, **23**, 3090.
20. E. Fischer and F. Weigert, *Chem. Ber.*, 1902, **35**, 3776.
21. A.I. Virtanen and P. Linko, Acta Chem. Scand., 1955, **9**, 531.
22. E. Fischer, *Chem. Ber.*, 1901, **34**, 454.
23. E. Cramer, *J.Prakt. Chem*, 1865, **96**, 76.
24. E. Erlenmeyer, *Chem. Ber.*, 1902, **35**, 3769.
25. E. Fischer and H. Leuchs, *Chem. Ber.*, 1902, **35**, 3787.
26. W.J.N Burch, *J. Chem. Soc.*, 1930, 310
27. F.G Hopkins and S.W. Cole, *J. Physio.*,1902, **27**, 418

28. A. Ellinger and C. Flamand, *Chem. Ber.*, 1907, **40**, 3029.
29. T.H. Haskell, S.A. Fusari, R.P. Frohardt, and O.R. Bartz, *J. Am. Chem Soc*, 1952, **74**, 599
30. E. Klebs, *Z. Physio. Chem.*, 1894, **19**, 301.
31. E. Fischer, *Chem. Ber.*, 1901, **34**, 2900.
32. V.M. Kothar and D.H. Busch, *Inorg. Chem.*,1969, **8**, 11,2276.
33. R.D. Gillard, N.C. Payne and G.B. Robertson, *J. Chem Soc*, 1970, 2580.
34. Academic Software and IUPAC Stability Constants Database, 1992-9, copyright.
35. W.A. Freeman and C.T. Liu, *Inorg. Chem.*,1968, **7**, 4,764.
36. C.T. Liu and J.A. Ibers, *Inorg. Chem.*,1969, **8**, 1911.
37. A. Louie and T. Meade, *PNAS*, 1997, unpublished.
38. N.N. Saha, S.K. Majumdar, S.C. Bhattacharya, P.N. Roy, R. Handa and S. Guha, *Indian J. Phys.*, 1966, **40**, 681
39. E.W. Wilson, Jr., M.H. Kasperian and R.B. Martin, *J. Am. Chem. Soc.*,1970, **92**, 5365.
40. K.A. Mesce, T.M. Amos and S.M. Clough, *Biotech. Histochem*, 68,222.
41. G. Székely, *Brain Res.*, 1976, **103**, 275.
42. G. Lázár, *Neurosci.*, 1978, **3**, 725.
43. D.B. Powell and N. Sheppard, *J. Am. Chem. Soc.*,1959,791.
44. K. Kustin, R.F. Pasternack and E.M. Weinstock, *J. Am. Chem. Soc.*,1968, **88**, 4610.
45. L.E. Erickson, J.W. McDonald, J.K. Howie and R.P. Clow, *J. Am. Chem. Soc.*,1968, **90**, 6371.
46. K. Swaminathan and D.H. Busch, *J. Inorg. Nucl. Chem.*,1961, **20,**159.
47. D.H. Busch and J.C. Bailar, Jr., *J. Am. Chem. Soc.*,1953, **75**, 4574; 1956, 7**8**,716.
48. M.L. Morris and D.H. Busch, *J. Am. Chem. Soc.*,1956, **78**, 5178
49. N.N. Greenwood and A. Earnshaw, Chemistry of the Elements, 1984, Pergamon Press, Cambridge.
50. P. Pfeiffer, W. Christeleit, Th. Hesse, H. Pfitzner and H. Thielert, *J. Prakt. Chem.*, 1938, **150**, 261.
51. K.A. Fraser, H.A. Long, R. Candlin and M.M. Harding, *Chem. Comm*, 1965, 344.
52. K.A. Fraser and M.M. Harding, *J. Am. Chem. Soc.*,1967, **A**, 415.
53. M.M. Harding and H.A. Long, *J. Am. Chem. Soc.*,1968, **A**, 2554.
54. T.J. Kistenmacher, *Acta Cryst.*, 1972, **28B**, 1302.

55. R.H Kretsinger, F. A. Cotton and R.F. Bryan, *Acta Cryst.*, 1963, **16**, 65

56. M.M. Harding and S.J. Cole, *Acta Cryst.*, 1963, **16**, 643.

57. B. Evertsson and G. Lundgren, *Acta Chem. Scand.*, 1966, **15**, 1544.

58. H.C. Freeman, J.M. Guss, M.J. Healy, R.P. Martin and C.E. Nockolds, *Chem. Comm*, 1969, 225.

59. C.M. Grammacioti and R.E. Marsh, *Acta Cryst.*, 1966, **21**, 594.

60. T. Boyne, R. Pepinsky and T. Watanabe, *Acta Cryst.*, 1957, **10**, 438.

61. D. van der Helm and W.A. Franks. *Acta Cryst.*, 1966, **25B**, 451.

62. D. van der Helm and M.B. Hassain. *Acta Cryst.*, 1969, **25B**, 457.

63. D. van der Helm, A.F. Nicholas and C.G. Fischer, *Acta Cryst.*, 1970, **26B**, 1172.

64. D. van der Helm and C.E. Tatsch,. *Acta Cryst.*, 1972, **28B**, 2307.

65. P.N. Roy, H. Hnada and S. Guha, *Indian J. Physio.*, 1966, **40**, 68

66. J.C. Bailar, *Inorganic Syntheses*, 1946, **2**,222,

67. J. Springborg and C.E. Schaeffer, *Inorganic Syntheses*, 1973,**14**, 64.

68. M.M. Chamberlain and J.C. Bailar, *J. Am. Chem. Soc.*, 1959, **81**, 6412.

69. M.E. Baldwin, *J. Chem. Soc.*, 1960, 4369.

70. K. Nakamoto, Infrared and Raman Spectra of Inorganic and Coordination Compounds, 1978, 3rd Ed., John Wiley and Sons, Inc., USA.

71. Mizushima and Quaglino, *J. Am. Chem. Soc.*, 1953, **75**, 6084.

72. Nakatsu, Shiro, Saito and Kuroya, *Bull. Chem. Soc. Japan*, 1957,**30**, 158; Saito, Nakatsu, Shiro and Kuroya, *Acta. Cryst.*, 1955, **25**, 731.

APPENDIX A

REACTION OF *cis*-$[Co(en)_2Cl_2]Cl$ WITH LYSINE MONOHYDROCHLORIDE

Table A1: Elemental Analysis Data of Complexes formed from the Reaction of *cis*-$[Co(en)_2Cl_2]Cl$ with Lysine Monohydrochloride

	Found (Calc)/ %			
	C	**H**	**N**	**I**
Complex 1 –$[Co(en)_2(lys)]I_2$	20.01 (20.78)	4.98 (5.06)	14.21 (14.54)	43.43 (43.90)
Complex 2 – $[Co(en)_3]Cl_3$	20.85 (20.65)	7.00 (6.98)	24.32 (24.03)	30.78 (29.99)

Table A2: Important IR Spectral Bands of Complexes formed from the Reaction of *cis*-$[Co(en)_2Cl_2]Cl$ with Lysine Monohydrochloride

	Frequencies (cm^{-1})	**Assignments**
Complex 1 -$[Co(en)_2(lys)]I_2$	3100-3200	NH_2 stretching
	1657	C=O stretching
Complex 2 – $[Co(en)_3]Cl_3$	3100-3330	NH stretching
	1624	NH bending
	1466	CH_2 bend
	1365	CH_2 wag
	~900	CH_2 rock

Table A3: ^{1}H NMR Chemical Shift Data of Complexes formed from the Reaction of *cis*-$[Co(en)_2Cl_2]Cl$ with Lysine Monohydrochloride

	Chemical Shift /ppm	Assignments
Complex 1 - $[Co(en)_2(lys)]I_2$	3.51 and 3.65	dd, 1H, J = 3.75 and 3.86, J = 3.71 and J = 3.85 respectively, CH of lys
	2.93 - 3.05	t, 2H, J = 7.15 and 7.32, CH_2 attached to the ω-NH_2 group of lys
	2.58 – 2.88	m, 8H, CH_2 of en
	1.44 – 1.98	m, 6H, 3 X CH_2 of lysine adjacent to CH
Complex 2 – $[Co(en)_3]Cl_3$	2.58 – 2.98	1 broad peak, 12H, CH_2 of en

Table A4: ^{13}C NMR Chemical Shift Data of Complexes formed from the Reaction of *cis*-$[Co(en)_2Cl_2]Cl$ with Lysine Monohydrochloride

	Chemical Shift /ppm
Complex 1 -$[Co(en)_2(lys)]I_2$	~185 (1 pair)
	~ 45-43 (4 pairs)
	~39 (1 pair)
	~31 (1 pair)
	~26 (1 pair)
	~22 (1 pair)
Complex 2 – $[Co(en)_3]Cl_3$	44

Table A5: UV-Visible Spectroscopic Data of Complexes formed from the Reaction of *cis*-$[Co(en)_2Cl_2]Cl$ with Lysine Monohydrochloride

	λ_{max}/nm	ε/ $mol^{-1}dm^3cm^{-1}$
Complex 1 -$[Co(en)_2(lys)]I_2$	348	105.59
	488	68.97
Complex 2 – $[Co(en)_3]Cl_3$	338	66.06
	466	59.71

Table A6: Fragmentation Patterns of Complexes formed from the Reaction of *cis*-$[Co(en)_2Cl_2]Cl$ with Lysine Monohydrochloride

	m/z	Fragment
Complex 1 -$[Co(en)_2(lys)]I_2$	264	$[Co(en)lys]^+$
Complex 2 – $[Co(en)_3]Cl_3$	177	$[Co(en)_2]^+$

REACTION OF *cis*-$[Co(en)_2Cl_2]Cl$ with DL-2,3-DIAMINOPROPIONIC ACID MONOHYDROCHLORIDE

Table A7: Elemental Analysis Data of Complexes formed from the Reaction of *cis*-$[Co(en)_2Cl_2]Cl$ with DL-2,3-Diaminopropionic acid Monohydrochloride

	Found (Calc)/ %			
	C	**H**	**N**	**I**
Complex 1 – $[Co(2,3\text{-}DAP)_2]I$	18.39 (18.38)	3.81 (3.60)	14.00 (14.29)	31.69 (32.37)
Complex 2 – $[Co(en)_2(2.3\text{-}DAP)]I_2$	15.69 (15.68)	4.14 (4.32)	15.14 (15.68)	47.27 (47.35)
Complex 3 - $[Co(en)_3]I_3$	11.56 (11.62)	3.97 (3.90)	12.98 (13.56)	60.27 (61.41)

Table A8: Important IR Spectral Bands of Complexes formed from the Reaction of *cis*-$[Co(en)_2Cl_2]Cl$ with DL-2,3-Diaminopropionic acid Monohydrochloride

	Frequencies (cm^{-1})	**Assignments**
Complex 1 – $[Co(2,3\text{-}DAP)_2]I$	3100-3200	NH_2 stretching
	1666	C=O stretching
	362	Co-O stretching
Complex 2 – $[Co(en)_2(2.3\text{-}DAP)]I_2$	3100-3200	NH stretching
	1638	C=O stretching
	454	Co-N stretching
	385	Co-O stretching
Complex 3 - $[Co(en)_3]I_3$	3100-3400	NH stretching
	1624	NH bending
	1465	CH_2 bend
	1327	CH_2 wag
	895	CH_2 rock

Table A9: ^{1}H NMR Chemical Shift Data of Complexes formed from the Reaction of *cis*-$[Co(en)_2Cl_2]Cl$ with DL-2,3-Diaminopropionic acid Monohydrochloride

	Chemical Shift /ppm	Assignments
Complex 1 – $[Co(2,3\text{-}DAP)_2]I$	2.84 - 2.97	dd, 1H, J = 3.28 and 4.12 , CH of 2,3-DAP
	3.15 - 3.24	dd, 1H, J = 3.57, CH of 2,3-DAP
	3.24 - 3.34	dd, 1H, J = 3.57, CH of 2,3-DAP
	3.70	d, 2H, J = 3.43, CH_2 of 2,3-DAP
	3.79	d, 2H, J = 3.43, CH_2 of 2,3-DAP
Complex 2 – $[Co(en)_2(2.3\text{-}DAP)]I_2$	2.6-2.9	m, 8H, CH_2 of en
	3.5-3.7	m, 1H, CH of 2,3-DAP
	2.98	m, 2H, CH2 of 2,3-DAP
Complex 3 – $[Co(en)_3]I_3$	2.58 – 2.98	1 broad peak, 12H, CH_2 of en

Table A10: ^{13}C NMR Chemical Shift Data of Complexes formed from the Reaction of *cis*-$[Co(en)_2Cl_2]Cl$ with DL-2,3-Diaminopropionic acid Monohydrochloride

	Chemical Shift /ppm
Complex 1 -$[Co(2,3\text{-}DAP)_2]I$	-
Complex 2 -$[Co(en)_2(2,3\text{-}DAP)]I_2$	215
	173
	59 (1 pair)
	47 (1 pair)
	44 (2 pairs)
Complex 3 – $[Co(en)_3]I_3$	44

Table A11: UV-Visible Spectroscopic Data of Complexes formed from the Reaction of *cis*-$[Co(en)_2Cl_2]Cl$ with DL-2,3-Diaminopropionic acid Monohydrochloride

	λ_{max}/nm	ε/ $mol^{-1}dm^3cm^{-1}$
Complex 1 -$[Co(2,3\text{-}DAP)_2]I$	348	41.50
	498	66.01
Complex 2 -$[Co(en)_2(lys)]I_2$	338	77.30
	468	77.00
Complex 3 – $[Co(en)_3]Cl_3$	334	89.60
	466	79.13

Table A12: Fragmentation Patterns for Complexes formed from the Reaction of *cis*-$[Co(en)_2Cl_2]Cl$ with DL-2,3-Diaminopropionic acid Monohydrochloride

	m/z	Fragment
Complex 1 -$[Co(2,3\text{-}DAP)_2]I$	265	$[Co(2,3\text{-}DAP)_2]^+$
Complex 2 -$[Co(en)_2(lys)]I_2$	177	$[Co(en)_2]^+$
	222	$[Co(en)(2,3\text{-}DAP)]^+$
	281	$[Co(en)_2(2,3\text{-}DAP)]^+$
Complex 3 – $[Co(en)_3]Cl_3$	179	$[Co(en)_2]^+$

PREPARATION OF $[Co(2,3\text{-}DAP)_2]Cl$ and $[Co(2,3\text{-}DAP)(2,3\text{-}DAPH)Cl_2]$

Table A13: Elemental Analysis Data for $[Co(2,3\text{-}DAP)_2]Cl$ and $[Co(2,3\text{-}DAP)(2,3\text{-}DAPH)Cl_2]$

	Found (Calc)/ %			
	C	**H**	**N**	**Cl**
$[Co(2,3\text{-}DAP)_2]Cl$	24.02 (23.98)	4.81 (4.69)	18.01 (18.64)	12.03 (11.79)
$[Co(2,3\text{-}DAP)(2,3\text{-}DAPH)Cl_2]$	20.38 (21.38)	4.49 (4.48)	15.69 (16.62)	20.98 (21.03)

Table A14: Important IR Spectral Bands for $[Co(2,3\text{-}DAP)_2]Cl$ and $[Co(2,3\text{-}DAP)(2,3\text{-}DAPH)Cl_2]$

	Frequencies (cm^{-1})	**Assignments**
$[Co(2,3\text{-}DAP)_2]Cl$	3100-3200	NH_2 stretching
	1666	C=O stretching
	362	Co-O stretching
$[Co(2,3\text{-}DAP)(2,3\text{-}DAPH)Cl_2]$	3200	NH_2 stretching
	~1720-1707	C=O stretching – uncoordinated and non-ionised COOH
	1655	C=O stretching – coordinated COO^-
	1584	NH bending
	1426	CH_2 bend
	1354	CH_2 wag
	944	CH_2 rock
	1080	C-N stretching

Table A15: ^{1}H NMR Chemical Shift Data of $[Co(2,3\text{-}DAP)_2]Cl$

	Chemical Shift /ppm	Assignments
$[Co(2,3\text{-}DAP)_2]Cl$	2.69	d, 2H, J = 3.04, CH_2 of 2,3-DAP
	2.90	dd, 1H, J = 3.99 and 4.12 , CH of 2,3-DAP
	3.27	dd, 1H, J = 3.44, CH of 2,3-DAP)
	3.52	d, 2H, J = 3.30, CH_2 of 2,3-DAP
	3.75	d, 2H, J = 3.02, CH_2 of 2,3-DAP

Table A16: ^{13}C NMR Chemical Shift Data for $[Co(2,3\text{-}DAP)_2]Cl$ and $[Co(2,3\text{-}DAP)(2,3\text{-}DAPH)Cl_2]$

	Chemical Shift /ppm
$[Co(2,3\text{-}DAP)_2]Cl$	180 (3 peaks)
	62 (3 peaks)
	44 (3 peaks)
$[Co(2,3\text{-}DAP)(2,3\text{-}DAPH)Cl_2]$	170
	59
	54

Table A17: UV-Visible Spectroscopic Data for $[Co(2,3\text{-}DAP)_2]Cl$ and $[Co(2,3\text{-}DAP)(2,3\text{-}DAPH)Cl_2]$

	λ_{max}/nm	ε/ $mol^{-1}dm^3cm^{-1}$
$[Co(2,3\text{-}DAP)_2]Cl$	348	42.90
	498	67.03
$[Co(2,3\text{-}DAP)(2,3\text{-}DAPH)Cl_2]$	400	
	460	*
	610	

* Complex was only partially soluble in DMSO

Table A18: Fragmentation Patterns for $[Co(2,3\text{-}DAP)_2]Cl$

	m/z	Fragment
$[Co(2,3\text{-}DAP)_2]Cl$	265	$[Co(2,3\text{-}DAP)_2]^+$

SECTION B

Cobalt(III) Complex of Chloroquine as Potential Antimalarial Agent

CHAPTER FOUR

ABSTRACT

The modification of chloroquine by coordination to metal centres, has previously been shown to lead to enhanced activity against the malaria parasite, *Plasmodium falciparum*. In continuing the efforts for the search for novel drugs against the chloroquine-resistant parasites, in this investigation a cobalt complex of chloroquine, $[Co(en)_2(CQ)Cl]Cl_2$, has been synthesised. The compound was characterised by elemental analysis, IR, NMR and UV-Visible spectroscopy and mass spectrometry. The cobalt ion was found to coordinate to chloroquine at the endocyclic N_1 position.

4.1 INTRODUCTION

Malaria is one of the world's most devastating infectious diseases, afflicting several hundred million people and killing close to two million each year, of which 90 % are children under the age of five in Africa[1]. Figure 4.1 illustrates the geographical distribution of malaria.

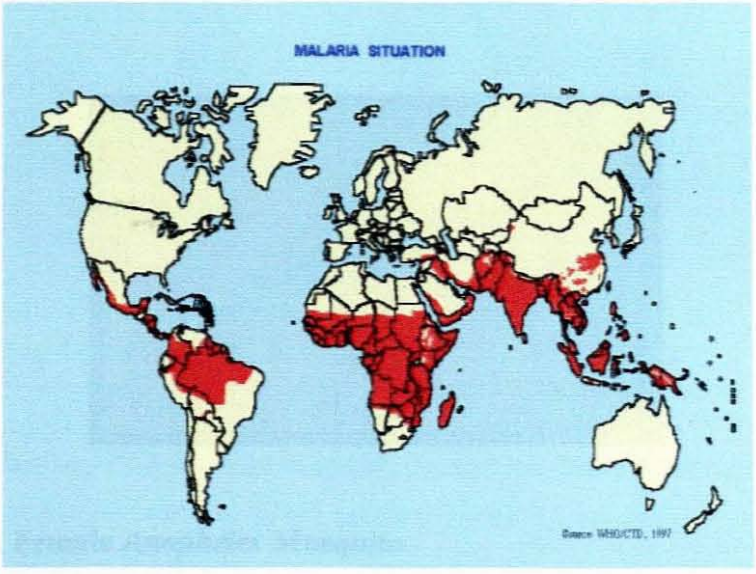

Figure 4.1: Map Showing Geographical Distribution of Malaria

A number of factors are considered to exacerbate the malaria problem:

1. Rapid spread of drug resistance.
2. Population movements to areas of high malaria transmission as a result of civil unrest.
3. Migration of non-immune populations from non-malarious areas to geographically lower regions where transmission is generally high.
4. Variable rainfall patterns and water development projects, leading to the establishment of new mosquito breeding sites.
5. Adverse socio-economic conditions leading to a reduced health budget, and thus to an inadequacy of funds for antimalarial drugs.
6. High birth rates leading to a rapid increase in the susceptible population under the ages of five[2].

Malaria is caused by the protozoal parasites of the genus *Plasmodium*. Four species of *Plasmodium* can survive in the blood of humans and effect the onset of malaria, namely, *falciparum, vivax, malariae* and *ovale*. In most cases, however, only *Plasmodium falciparum* causes death during an acute attack of malaria. The disease is transmitted to humans by the female mosquitoes of the genus *Anopheles*, of which the *Anopheles gambiae* complex is responsible for the transmission of the disease in Africa.

Figure 4.2: A Female *Anopheles* Mosquito

The disease is characterised, in clinical terms, by attacks of fever combined with the onset of rigours, headaches and joint aches together with anaemia, haemolytic jaundice and splenomegaly[3]. In endemic regions, where transmission is high, people experience continuous affliction thus inducing the development of immunity to the disease. However, until such immunity is acquired, children remain highly vulnerable. Pregnant women are also extremely susceptible to the disease since pregnancy reduces the natural defence mechanisms of the body.

Various drugs have been developed for the treatment of malaria, of which chloroquine and sulfadoxine-pyrimethamine have proved most effective. However, parasites resistant to these drugs, are now widespread in South America, Asia and Africa (Fig. 4.3).

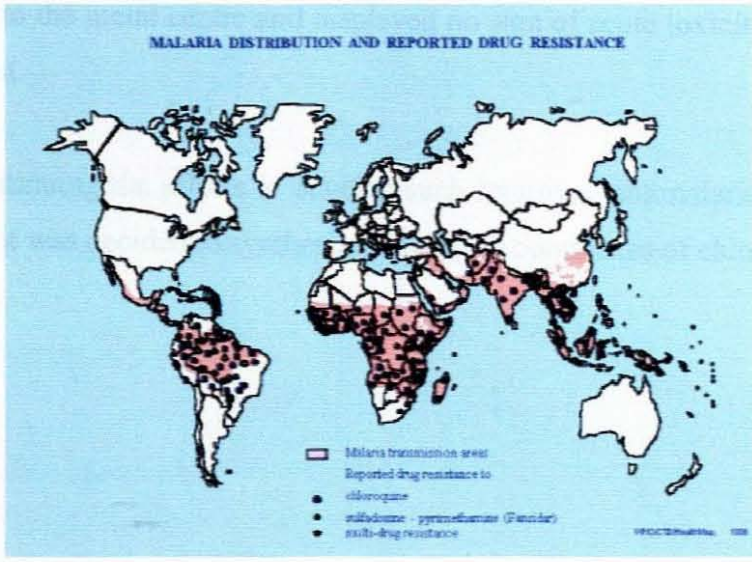

Figure 4.3: Map Showing Areas of Reported Drug-Resistance

In particular, chloroquine-resistant strains of *Plasmodium falciparum* have become a major health concern in all tropical areas around the world. As such, the search for new antimalarial therapies has become a high-priority task in the fight for the control of the disease.

4.2 APPLICATIONS OF METAL-BASED THERAPEUTIC AGENTS

Further to the remarkable success of *cis*-dichlorodiammineplatinum(II), commonly known as cisplatin, as an antitumour drug, there has been renewed interest in the use of metal-based chemotherapies for the treatment of various diseases. The efficacy of a therapeutic agent is known to be enhanced upon coordination with a suitable metal ion. Gold drugs have been used since the 1930s for the treatment of rheumatoid arthritis[4] whilst lithium is widely employed in the treatment of manic depression[5]. More recently, bismuth complexes of anti-ulcer drugs have gained popularity.

In the search for novel drugs against chloroquine-resistant malaria parasites, the modification of chloroquine by coordination to a metal centre, has attracted considerable attention in recent years[6,7]. In particular, the chloroquine complexes of Ru[6], Rh[6] and Au[7] have been synthesised. The complexes have all shown an enhanced

activity against chloroquine-resistant strains of *Plasmodium falciparum* upon coordination to the metal centre and displayed no sign of acute toxicity up to 30 days after treatment.

In continuing the efforts to develop such improved antimalarial drugs, in this investigation it was decided to synthesise cobalt(III) complexes of chloroquine

4.3 EXPERIMENTAL

4.3.1 MATERIALS

The antimalarial drug, chloroquine diphosphate (CQDP), was purchased from the Aldrich Chemical Company, UK and converted to the free base according to published procedures[8].

4.3.2 INSTRUMENTATION

4.3.2.1 Elemental Analysis

Elemental analysis of *trans*- and *cis*- dichlorobis(ethylenediamine)cobalt(III) chloride was carried out at the microanalytical laboratory of South African Bureau of Standards (SABS) in Richards Bay, South Africa. Elemental analysis of the product was performed at the Chemistry Department at the University of Manchester, United Kingdom.

4.3.2.2 NMR Spectroscopy

One dimensional and two dimensional (COSY) ^{1}H spectra and ^{13}C NMR spectra were obtained using a Varian Inova 300 MHz NMR spectrometer .

4.3.2.3 IR Spectroscopy

Infrared spectroscopy was carried out using potassium bromide (KBr) discs on an ATI Mattson Genesis Series FTIR spectrometer.

4.3.2.4 Electronic(UV-Visible) Spectroscopy

Electronic (UV-visible) spectra were measured, using water as a solvent, with a Hewlett Packard 8452A Diode Array Spectrophotometer.

4.3.2.5 Mass Spectrometry

Mass spectra were obtained using an Electrospray instrument at the University of Manchester,UK

4.3.3 METHODS

4.3.3.1 The Reaction of *cis*-$[Co(en)_2Cl_2]Cl$ with Chloroquine

Trans-$[Co(en)_2Cl_2]Cl$ (2.86 g; 10mmol) was carefully added to a solution of chloroquine (3.19 g; 10 mmol) in ethanol (30 ml). The solution was stirred for 16 hours. The unreacted starting material was removed by filtration. The ethanolic solution was evaporated to a small volume and cooled. The green precipitate was filtered and subsequently washed with ethanol and diethyl ether.

Yield: 11 %

Calculated: 43.65 % C, 6.99 % H, 16.20 % N

Found: 43.01 % C, 6.31 % H, 16.50 % N

4.4 RESULTS AND DISCUSSION

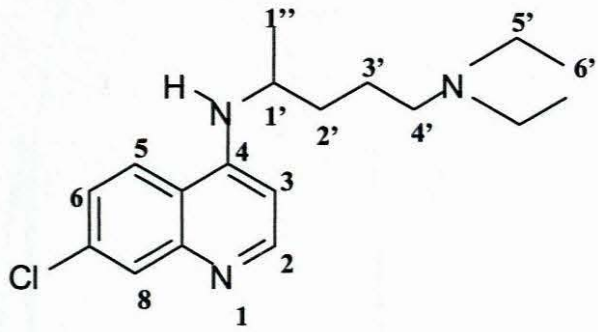

Figure 4.4: Structure of Chloroquine

4.4.1 Infrared Spectroscopy

Chloroquine possesses three potential donor sites, notably the quinoline ring nitrogen, the secondary amino nitrogen and the tertiary amino nitrogen. A comparison of the IR spectral bands of the free ligand, chloroquine (Figure 4.5), and that of the complex (Figure 4.6) shows that the sp^2 ν(C-N) mode, observed around 1330 cm^{-1} for the secondary amino group in the ligand, is not shifted in the spectrum of the complex. If a shift to a higher wavenumber was observed, it would indicate bonding of the secondary amino nitrogen to the cobalt ion within the structure of the complex. The inertness of the side chain tertiary amino nitrogen in chloroquine is revealed by the fact that there occurs no significant change in the sp^3 ν(C-N) frequency upon complexation. However, splitting of the ν(C=N) band, which occurs around 1575 cm^{-1} in the spectrum of the free ligand, is observed giving rise to two bands at 1575 cm^{-1} and 1591 cm^{-1}. Such an observation is indicative of the coordination of chloroquine through the ring nitrogen.

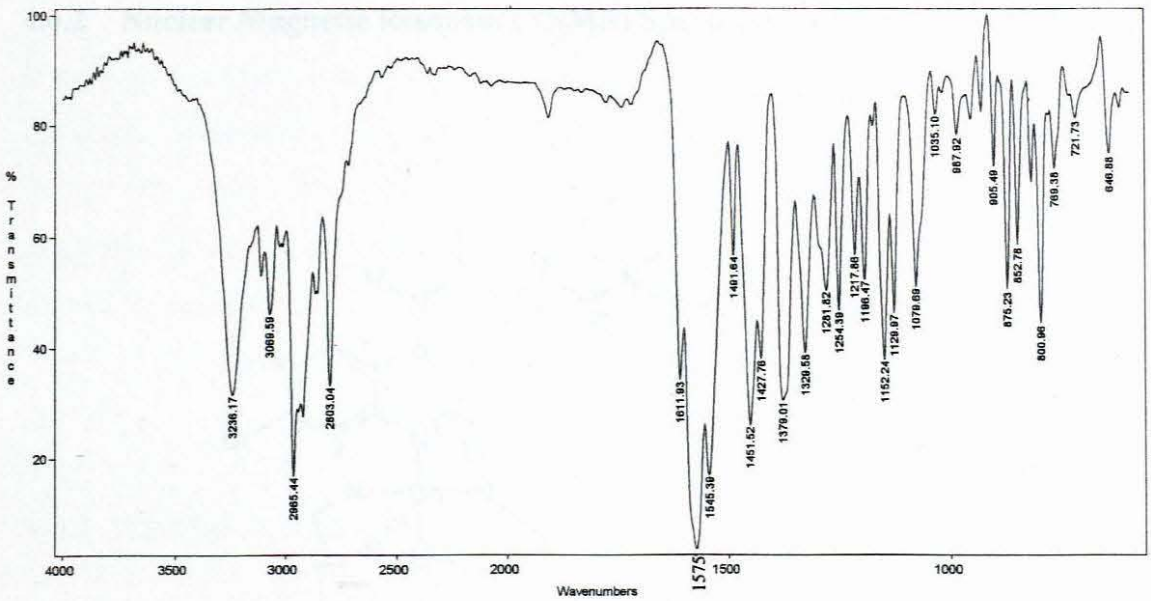

Figure 4.5: Infrared Spectrum of Chloroquine

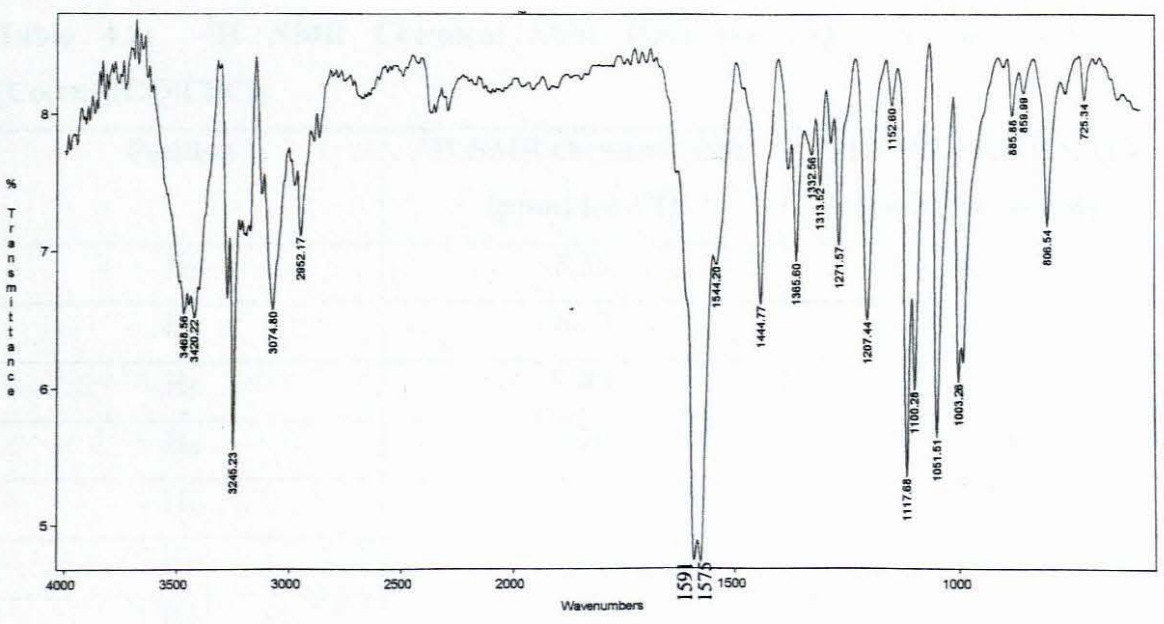

Figure 4.6: Infrared Spectrum of $[Co(en)_2(CQ)Cl]Cl_2$

4.4.2 Nuclear Magnetic Resonance (NMR) Spectroscopy

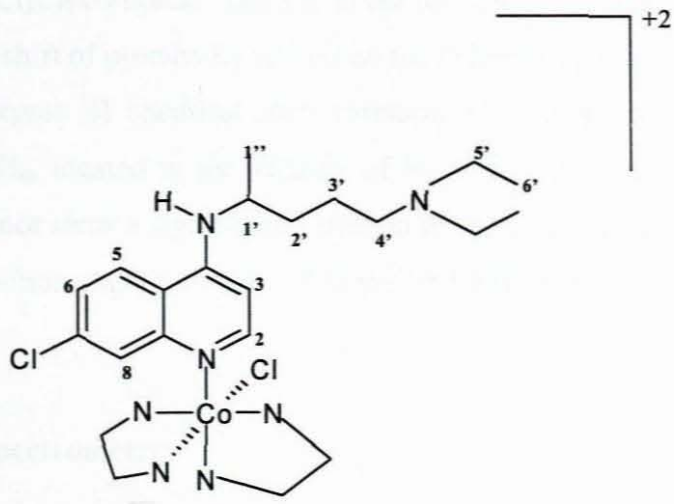

Figure 4.7: The Proposed Bonding Mode of Chloroquine in $[Co(en)_2(CQ)Cl]Cl_2$

The variation of the chemical shift in the ^1H NMR spectrum of the complex with respect to that of the free ligand is shown in Table 4.1

Table 4.1: ^1H NMR Chemical Shift Data for CQ and the complex $[Co(en)_2(CQ)Cl]Cl_2$

Position	^1H NMR chemical shift (ppm) for CQ	^1H NMR chemical shift (ppm) for complex
H_2	8.35	8.40
H_3	6.57	6.77
H_5	7.40	7.52
H_6	8.20	8.40
H_8	7.80	9.20
$H_{1'}$	3.82	3.82
$H_{2'}$	1.74	~1.7
$H_{3'}$	1.62	~1.7
$H_{4'}$	2.52	2.20-
$H_{5'}$	3.34	3.34
$H_{6'}$	1.05	1.30
$H_{1''}$	1.33	1.42

Cobalt preferentially coordinates at the endocyclic N_1 to form the $[Co(en)_2(CQ)Cl]Cl_2$ complex. The site of coordination was determined by monitoring the downfield shift of protons H_2 and H_8 on the chloroquine ring.

The largest ^1H chemical shift variation with respect to the free ligand was observed for H_8, located in the vicinity of N_1 whilst all other chloroquine protons, except H_2, do not show a significant variation in chemical shift. There is a shift of NH proton to a position slightly downfield in the ^1H NMR spectrum of the complex.

4.4.3 Mass Spectrometry

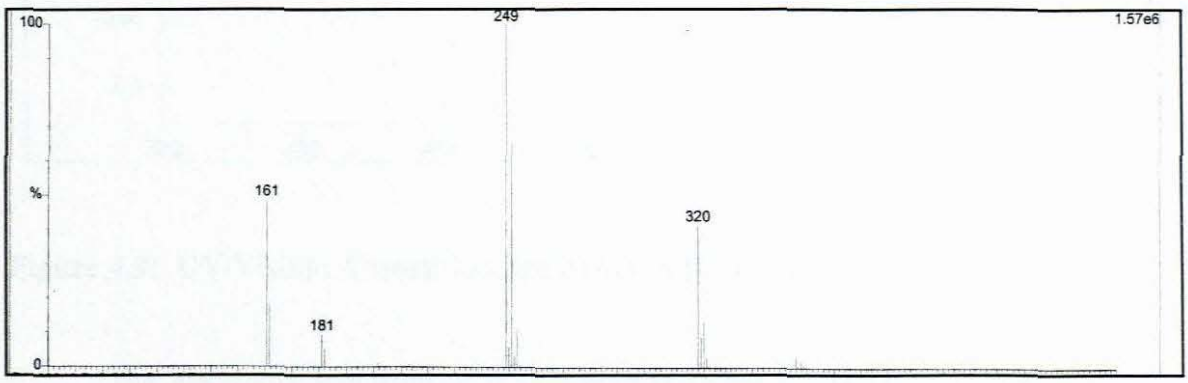

Figure 4.8: Mass Spectrum of $[Co(en)_2(CQ)Cl]Cl_2$

In the mass spectrum of $[Co(en)_2(CQ)Cl]Cl_2$ (Figure 4.8), a peak is observed at m/z = 320 which corresponds to the loss of $[Co(en)_2Cl]$ from the molecule. The base peak occurs at m/z = 249, which is due to further fragmentation at the tertiary amine nitrogen of chloroquine. The peak at m/z = 161 may be attributed to the aromatic portion of the chloroquine molecule. The results confirm the proposed structure.

4.4.4 Electronic (UV-Visible) Spectroscopy

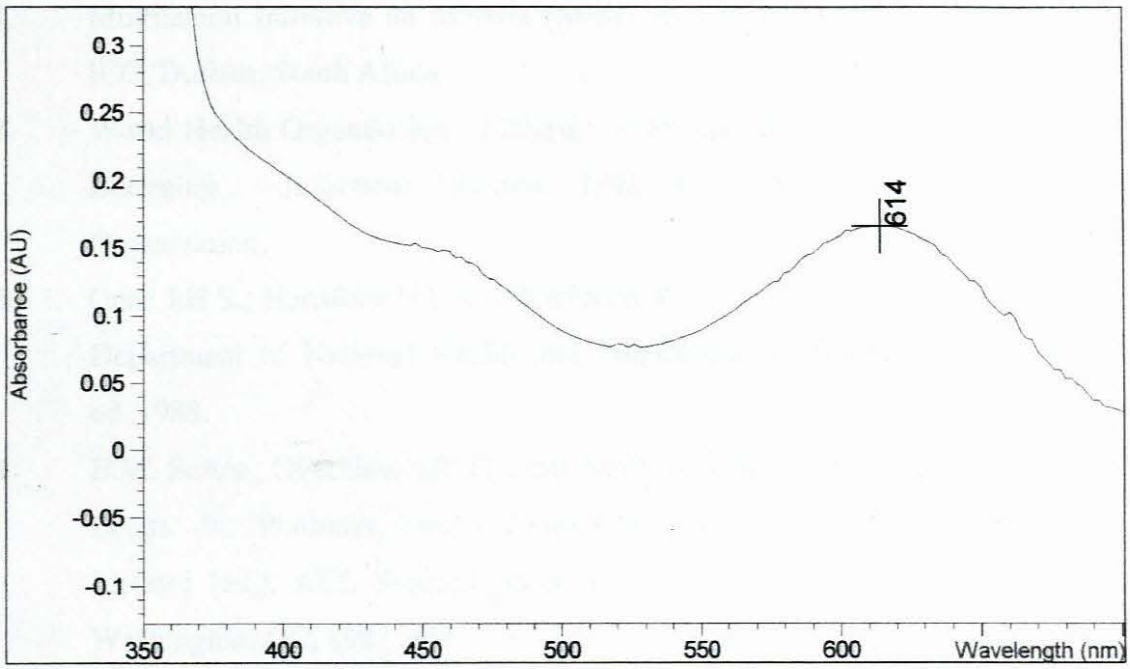

Figure 4.9: UV/Visible Absorption Spectrum of $[Co(en)_2(CQ)Cl]Cl_2$

The electronic spectrum of $[Co(en)_2(CQ)Cl]Cl_2$, as displayed in Figure 4.9, shows two peaks at 450 nm and 614 nm. These bands may be due to d-d transitions, an assignment that is consistent with the proposed octahedral geometry around the central metal ion.

4.5 CONCLUSION

A novel chloroquine complex of cobalt, $[Co(en)_2(CQ)Cl]Cl_2$, has been synthesised by direct reactions of the free base with an appropriate metal precursor. As anticipated, the cobalt appears to coordinate to chloroquine at the endocylic N_1 position.

Further experiments that might be carried out, include the *in vitro* tests for potential antimalarial activity of the complex against chloroquine-resistant malaria parasites, as well as toxicity studies of the complex. If the complex was proven to exhibit relatively low levels of toxicity, *in vivo* testing might also be attempted.

REFERENCES

1. Multilateral Initiative on Malaria (MIM) African Malaria Conference, 1999, ICC, Durban, South Africa.
2. World Health Organisation. Malaria: A Re-emerging Disease in Africa. In: Emerging Infectious Diseases, 1998, **4**, 3, 398-403. Geneva: The Organization.
3. Gear J.H.S., Hansford G.F and Pitchford R.J. 'Malaria in Southern Africa'. Department of National Health and Population Development, Pretoria, 2nd ed.,1988.
4. B.M. Sutton, Overview and Current Status of Gold-Containing Anti-Arthritis Drugs. In: 'Platinum, Gold and Other Metal Chemotherapeutic Agents', S.J. Lippard (ed.), ACS Symposium Series 209, American Chemical Society , Washington, DC, 1983, 355.
5. N.J. Birch, 'Lithium in Psychiatry'. In: H. Sigel (ed.), 'Metal Ions in Biological Systems', Dekker, New York, 1979-1983, Vol 9-16.
6. R.A. Sanchez-Delgado, M. Navarro, H. Perez and J. A. Urbina, *J. Med. Chem.*, 1996, **39**, 1095.
7. M. Navarro, H. Perez and R.A. Sanchez-Delgado, *J. Med. Chem.*, 1997, **40**, 1937.

APPENDIX B

THE REACTION OF *cis*-$[Co(en)_2Cl_2]Cl$ WITH CHLOROQUINE

Table B1: Elemental Analysis Data of $[Co(en)_2(CQ)Cl]Cl_2$

	Found (Calc)/ %		
	C	**H**	**N**
$[Co(en)_2(CQ)Cl]Cl_2$	43.01 (43.65)	6.31 (6.99)	16.50 (16.20)

Table B2: Important IR Spectral Bands of Chloroquine and $[Co(en)_2(CQ)Cl]Cl_2$

	Frequencies (cm^1)	**Assignments**
CQ	1330 1575	C-N stretching of secondary amino group C=N stretching
$[Co(en)_2(CQ)Cl]Cl_2$	1330 1575 + 1591	C-N stretching of secondary amino group C=N stretching

Table B3: ^1H NMR Chemical Shift Data for CQ and the complex $[Co(en)_2(CQ)Cl]Cl_2$

Position	**^1H NMR chemical shift (ppm) for CQ**	**^1H NMR chemical shift (ppm) for complex**
H_2	8.35	8.40
H_3	6.57	6.77
H_5	7.40	7.52
H_6	8.20	8.40
H_8	7.80	9.20
$H_{1'}$	3.82	3.82
$H_{2'}$	1.74	~1.7
$H_{3'}$	1.62	~1.7
$H_{4'}$	2.52	2.20
$H_{5'}$	3.34	3.34
$H_{6'}$	1.05	1.30
$H_{1''}$	1.33	1.42

Table B4: UV-Visible Spectroscopic Data of $[Co(en)_2(CQ)Cl]Cl_2$

	λ_{max}/nm
$[Co(en)_2(CQ)Cl]Cl_2$	450 614

Table B5: Fragmentation Patterns of $[Co(en)_2(CQ)Cl]Cl_2$

	m/z	Fragment
$[Co(en)_2(CQ)Cl]Cl_2$	320	CQ^+
	249	loss of tertiary amino group of CQ
	161	quinoline portion of CQ